

UNIVERSITY OF MINNESOTA  
**ST. ANTHONY FALLS LABORATORY**  
Engineering, Environmental and Geophysical Fluid Dynamics

Project Report No. 440

## **Dissolved Oxygen Dynamics in Holland Lake, MN**

by

O. Mohseni and Heinz G. Stefan



Prepared for

**MINNESOTA DEPARTMENT OF NATURAL RESOURCES**  
**Metro Region Fisheries, St. Paul, Minnesota**

March 2000  
(revised January 2001)  
**Minneapolis, Minnesota**

UNIVERSITY OF MINNESOTA  
**ST. ANTHONY FALLS LABORATORY**  
Engineering, Environmental and Geophysical Fluid Dynamics

Project Report No. 440

## **Dissolved Oxygen Dynamics in Holland Lake, MN**

by

O. Mohseni and Heinz G. Stefan

Prepared for

**MINNESOTA DEPARTMENT OF NATURAL RESOURCES**  
**Metro Region Fisheries, St. Paul, Minnesota**

March 2000  
(revised January 2001)  
**Minneapolis, Minnesota**

The University of Minnesota is committed to the policy that all persons shall have equal access to its programs, facilities, and employment without regard to race, religion, color, sex, national origin, handicap, age or veteran status.

Prepared for: MN Dept. of Natural Resources  
Published: 4/12/00; Revised: 1/25/01  
Disk Locators: Rep440.doc; Rep440-Cov.doc;  
Rep440Fig1.doc, Rep440Fig2.doc, Rep440Fig3.doc  
(Zip Disk #15\Omid)\Stefan Reports

## Abstract

The Minnesota Department of Natural Resources, Division of Fisheries, has been considering Holland Lake for stocking with brown trout. Holland Lake, a Twin Cities Metro Area lake, with a surface area of 0.14 km<sup>2</sup> and a maximum depth of about 61 ft (18.8 m) is located in Dakota County. The lake has two shallow subbasins with a substantial amount of rooted vegetation and a deep subbasin, which is thermally suitable for brown trout. However, due to a high oxygen depletion rate in summer, the lake becomes anoxic below the surface mixed layer. A combination of high water temperatures in the surface mixed layer and low dissolved oxygen below the surface mixed layer makes it difficult for brown trout to survive in summer. For possible future aeration of the lake, the dissolved oxygen (DO) dynamics of the lake were studied.

Historical records show that DO depletes at a rate of 0.47 mg.l<sup>-1</sup>.day<sup>-1</sup> after spring overturn in the upper stratum of the metalimnion (from 10 to 20 ft depth), such that the lake develops a negative heterograde DO profile by early July. DO depletes at a lower rate (0.22 mg.l<sup>-1</sup>.day<sup>-1</sup>) in the lower stratum of the metalimnion (from 20 to 30 ft depth). By mid-August, the entire metalimnion becomes completely anoxic.

To better understand and to quantify the processes that contribute to the DO dynamics in the lake, temperature, DO, Secchi depth, photosynthetically active radiation (PAR), total suspended solids (TSS), total organic carbon (TOC), total respiration rate and chl-*a* concentrations were monitored or measured at three locations during the summer of 1999. The Secchi depth varied from 5 to 10 ft (1.5 to 3.0 m) in the deep subbasin and from 2.5 to 9 ft (0.75 to 2.7 m) in the eastern shallow subbasin. The PAR measurements showed an attenuation coefficient of about 0.25 ft<sup>-1</sup> in the deep subbasin; it varied with depth by two orders of magnitude (from 0.2 ft<sup>-1</sup> to 25 ft<sup>-1</sup>) in the shallow subbasins, indicating increasing macrophyte density with depth. In the deep subbasin, the TSS concentration varied from 1 to 3 mg/l with a maximum of 5 mg/l in the upper stratum of the metalimnion. About 76% of the TSS were volatile, which indicates that most if not all TSS is organic material. Carbonaceous biological oxygen demand (CBOD) was estimated using the TOC profiles. The average CBOD was 18.7 mg/l, with a maximum of 24 mg/l in the upper stratum of the metalimnion.

Analyzing the data made it evident that three factors contribute to the high DO depletion rates in Holland Lake: 1) lake morphometry, 2) abundance of macrophytes in the shallow subbasins, and 3) groundwater inflow. A succession of different types of macrophytes grow, flower, age and die (senescence), and settle in the shallow subbasins. A significant amount of groundwater enters the shallow subbasins. The 16 to 18 °C water at the bottom of the shallow subbasins beds (10 to 12 ft depth) matches the water temperature in the upper stratum of the metalimnion (14 to 16 ft depth) of the deep subbasin. It is most likely that the two layers are connected by density current-type exchange flow. The density currents carry oxygen-depleted water and detritus from the shallow subbasin sediment beds into the deep subbasin. High concentrations of organic matter in the upper stratum of the metalimnion and associated high DO depletion rates can be explained by this process.

## **Acknowledgements**

The work reported herein was supported by the Minnesota Department of Natural Resources, Metro Region Fisheries. Mr. Gerald Johnson was the project officer. We would like to thank him for assistance in the fieldwork. Mark Briggs and David Wright from Ecological Services arranged for the analysis of some water samples at the Minnesota Department of Agriculture Laboratory. David Wright also had many helpful suggestions for the conduct of this study. Miao Zhang, advised by Raymond M. Hozalski in the Department of Civil Engineering, University of Minnesota, did the TOC analyses, Chris Ellis, Dragoslav Stefanovic and other St. Anthony Falls Laboratory personnel facilitated the collection of temperature and dissolved oxygen data in Holland Lake, and Travis Bogan helped with preparing some of the figures. Randy Anhorn of MCES made available his data collected in Holland Lake in the summer of 1999.

## Table of Contents

Abstract.....	i
Acknowledgements.....	ii
List of Figures.....	v
List of Tables.....	ix
I. Introduction.....	1
II. Lake Setting.....	2
III. Analysis of the Historical Records.....	4
IV. Field Work/Data Collection.....	9
IV.1. Water Temperature.....	9
IV.2. Dissolved Oxygen.....	10
IV.3. Light.....	10
IV.4. Water Sampling.....	10
V. Dissolved Oxygen Profiles.....	13
V.1. Seasonal Trends in DO Concentrations.....	13
V.2. Diurnal Changes in DO Concentrations.....	23
VI. Processes Affecting Dissolved Oxygen.....	25
VI.1. Photosynthesis.....	25
VI.2. Respiration.....	34
VI.2.1. Total Suspended Solids (TSS).....	34
VI.2.2. Total Volatile Suspended Solids (TVSS).....	34
VI.2.3. Total Organic Carbon (TOC).....	34
VI.2.4. Phaeophytin.....	35
VI.2.5. Potential Respiration Rates.....	36
VI.2.6. Summary of Oxygen Uptake Rates.....	37
VI.3. Sedimentary Oxygen Demand (SOD).....	46
VI.4. Hydrodynamic Transport.....	47
VI.5. Advection.....	55
VI.5.1. Advection by Groundwater.....	55
VI.5.2. Advection by Internal Waves.....	62
VII. Summary and Conclusions.....	71
VIII. Recommendations.....	72

References..... 75  
Appendix A. Dissolved Oxygen and Temperature Profiles Measured by the MNDNR., 76  
Appendix B. Dissolved Oxygen and Temperature Profiles Measured by the Metropolitan  
Council..... 80  
Appendix C. Calibration of Thermistors Used in Holland Lake ..... 87  
Appendix D. Diurnal Dissolved Oxygen and Temperature Profiles ..... 89

## List of Figures

**Figure 1a.** Plan view of Holland Lake.

**Figure 1b.** A cross section of Holland Lake.

**Figure 2a.** Temperature and DO profiles in Holland Lake, August 7, 1978.

**Figure 2b.** Temperature and DO profiles in Holland Lake, July 24, 1995.

**Figure 3a and 3b.** Temperature, Dissolved Oxygen (DO) and DO Saturation Profiles in Holland Lake in 1984. Data are from the EPA/STORET database.

**Figure 4.** Locations of rafts in Holland Lake where DO and temperature profiles were measured, and locations in shallow subbasins where photosynthetically active radiation (PAR) was measured. Triangles with numerals indicate where rafts were located, and circles with italic font numerals indicate where PAR was measured in the shallow subbasins. Point 4 is where the water samples were collected in the western shallow subbasin.

**Figure 5a, 5b, 5c and 5d.** Measured temperature and dissolved oxygen profiles in Holland Lake in 1999. Data were collected by the MNDNR, the Metropolitan Council and St. Anthony Falls Laboratory.

**Figure 6.** Measured dissolved oxygen content of different strata in the deep subbasin of Holland Lake.

**Figure 7.** Dissolved oxygen content of different strata (thermal regions) in the deep subbasin of Holland Lake.

**Figure 8.** Rate of change of dissolved oxygen concentration in different strata (thermal regions) of the deep subbasin of Holland Lake.

**Figure 9.** Rate of change of dissolved oxygen concentration in the entire water column of the deep subbasin of Holland Lake.

**Figure 10.** Diurnal dissolved oxygen variation in Holland Lake, August 2 and 3, 1999. Simple average concentrations for several layers and locations are plotted versus time of day.

**Figure 11.** Seasonal trends of Secchi depth transparency  $z_s$  in Holland Lake in different years (from Metropolitan Council, MNDNR and the St. Anthony Falls Laboratory data).

**Figure 12.** Measured Secchi depth transparency  $z_s$  and estimated coefficient of attenuation  $\eta$  in subbasins of Holland Lake.

**Figure 13.** Areas (shaded) of dense macrophyte vegetation in the eastern shallow subbasin of Holland Lake in summer 1999.

**Figure 14.** Measured photosynthetically active radiation (PAR) in the deep subbasin of Holland Lake. The attenuation coefficients are estimated by fitting an exponential function to the three measurements.



- Figure 15.** Chlorophyll *a* (chl-*a*) concentration profiles measured on 8/23/1999 at three locations in Holland Lake. Point 4 was within the smaller (western) shallow subbasin (Figure 4).
- Figure 16.** Measured photosynthetically active radiation (PAR) in the shallow subbasins of Holland Lake. The locations of the measurements are shown in Figure 4.
- Figure 17.** Attenuation coefficients  $\eta$  estimated at different depths in the shallow subbasins of Holland Lake.
- Figure 18.** Total suspended solids (TSS) profiles measured at three locations in Holland Lake, 8/23/99.
- Figure 19.** Total volatile suspended solids (TVSS) profiles measured at three locations in Holland Lake, 8/23/99.
- Figure 20.** Total organic carbon (TOC) profiles measured at three locations in Holland Lake, 8/19/99.
- Figure 21.** Carbonaceous biochemical oxygen demand (CBOD) profiles estimated from TOC at three locations in Holland Lake
- Figure 22.** Phaeophytin concentration profiles measured at three locations in Holland Lake, 8/23/99.
- Figure 23.** Respiration rates measured in Holland Lake. The large filled circles identify samples with a significant content of particulate matter.
- Figure 24.** Measured and estimated respiration rates in Holland Lake. Solid line gives values measured on 9/21/99 by dark bottle incubation. Dashed lines are estimated respiration rates using the chl-*a* profile and the water temperature profiles measured on 8/23/99 and 9/19/99, respectively.
- Figure 25.** Temperature profile time series in the deep subbasin (raft # 1) of Holland Lake, summer 1999.
- Figure 26.** Temperature profile time series at the border of the deep subbasin and the eastern shallow subbasin (raft # 2) of Holland Lake, summer 1999.
- Figure 27.** Temperature profile time series in the deep subbasin (raft # 3) of Holland Lake, summer 1999.
- Figure 28.** Isotherms of the deep subbasin of Holland Lake.
- Figure 29.** Isotherms at the boundary of subbasins of Holland Lake.
- Figure 30.** Isotherms of the shallow subbasin of Holland Lake.
- Figure 31.** Daily weather parameters at the Twin Cities airport in July 1999.
- Figure 32.** Hydrogeological map of the region around Holland Lake [after *Minnesota Geological Survey*, 1990]. The lake is between the white arrows.
- Figure 33.** Piezometric groundwater surface in a cross section through Holland Lake, (Elevation data are from the Minnesota Geological Survey, 1990).

- Figure 34.** Topographical map of the vicinity of Holland Lake with lake surface elevations.
- Figure 35.** The Holland Lake capture zone of the aquifer. Approximate groundwater streamlines and equal piezometric head lines around Holland Lake showing the capture zone of groundwater.
- Figure 36.** Maximum daily amplitude of temperature changes in the deep subbasin of Holland Lake (Raft 1).
- Figure 37.** Maximum daily amplitude of temperature changes between the deep subbasin and the eastern shallow subbasin of Holland Lake (Raft 2).
- Figure 38.** Maximum daily amplitude of temperature changes in the shallow subbasin of Holland Lake (Raft 3).
- Figure 39.** Monthly averages of maximum diurnal temperature changes in the deep subbasin of Holland Lake (Raft 1).
- Figure 40.** Monthly averages of maximum diurnal temperature changes at the border of the deep subbasin and the eastern shallow subbasin of Holland Lake (Raft 2).
- Figure 41.** Monthly averages of maximum diurnal temperature changes in the shallow subbasin of Holland Lake (Raft 3).
- Figure 42.** Ten minute averaged water temperature and instantaneous wind speed time series for July 25-28, 1999, in Holland Lake. Wind speed data were measured over Lake MaCarrons, MN, by the Metropolitan Council.
- Figure 43.** Maximum diurnal changes in temperature and the corresponding potential vertical water movements in Holland Lake during the storm event of July 26, 1999.
- Figure 44.** Temperature and DO threshold isotherms for Brown Trout survival in Holland Lake. The figure is plotted using the monthly, biweekly and weekly temperature profiles measured by the MNDNR, the Met Council and the St. Anthony Falls Laboratory.
- Figure 45.** Temperature and DO threshold lines (22 °C and 3 mg/l, respectively) for a more severe brown trout habitat in Holland Lake. The figure is plotted using the monthly, biweekly and weekly temperature profiles measured by the MNDNR, the Met Council and the St. Anthony Falls Laboratory.
- Figure A.1.** Temperature and DO profiles in Holland Lake collected by the MNDNR from 1975-1995.
- Figure A.2.** Temperature and DO profiles in Holland Lake collected by the MNDNR from 1997-1998.
- Figure A.3.** Temperature and DO profiles in Holland Lake collected by the MNDNR from 1998-1999.
- Figure B.1 and B.2.** Temperature and DO profiles in Holland Lake collected by the Metropolitan Council for 1983.

**Figure B.3 and B.4.** Temperature and DO profiles in Holland Lake collected by the Metropolitan Council in 1985.

**Figure B.5 and B.6.** Temperature and DO profiles in Holland Lake collected by the Metropolitan Council in 1993.

**Figure D.1.** Diurnal temperature and DO profiles measured in the subbasins of Holland Lake, summer 1999.

**Figure D.2.** Diurnal dissolved oxygen content in the upper 10 ft of water in Holland Lake, on August 2 and 3, 1999

## **List of Tables**

**Table 1.** Correlation coefficients between the total suspended solids (TSS), total volatile suspended solids (TVSS), chlorophyll-a (chl-*a*), phaeophytin (PYT) and total organic carbon (TOC) in different strata.

**Table 2.** Estimates of the groundwater residence times in subbasins of Holland Lake in summer.

**Table C.1.** Initial and final corrections applied to the thermistors mounted on Raft # 1.

**Table C.2.** Initial and final corrections applied to the thermistors mounted on Raft # 2.

**Table C.3.** Initial and final corrections applied to the thermistors mounted on Raft # 3.



## **I. Introduction**

Holland Lake located in Dakota County at the southern fringes of the Twin Cities Metropolitan Area is being considered for stocking with brown trout by the Division of Fisheries of the Minnesota Department of Natural Resources (MNDNR). Holland Lake is suitable for this purpose because it is exceptionally deep in comparison to other lakes in the Metro Area and has relatively good water quality because of a very limited drainage area. However, there are frequent problems with low concentrations of dissolved oxygen (DO) in the lake metalimnion and hypolimnion, which adversely affect the stocking of the lake with brown trout. In the summer, water temperature in the surface mixed layer (epilimnion) exceeds the maximum temperature tolerance of brown trout (24 °C), which forces brown trout to find suitable habitat (between 10 °C to 20 °C) in deeper layers of the lake. However, in summer, the stratum above the thermocline becomes anoxic faster than the strata below it. When brown trout travel to the surface for feeding, they have to pass through an anoxic layer, and when they enter the epilimnion, they have to tolerate high temperatures. The combination of these stresses is not conducive for brown trout survival in Holland Lake. This study was conducted to better understand the DO stratification dynamics in Holland Lake and to provide background information for a potential lake aeration system.

This report includes a review of the historical records collected by the MNDNR and the Metropolitan Council of Twin Cities, measurements conducted in the summer of 1999, and an interpretation of the data in light of the processes affecting the dissolved oxygen dynamics of the lake.

## II. Lake Setting

Holland Lake with a surface area of 0.14 km<sup>2</sup> (Figure 1a\*), and mean and maximum depths of 15 ft (5.1 m) and 61 ft (18.8 m), respectively, is located in Dakota County, MN (N44.7887° and W93.1429°). The lake basin consists of two shallow vegetated subbasins and a deep subbasin (Figure 1b). According to the MNDNR, the lake basin is 69% littoral and 31% profundal. The relative depth<sup>†</sup> of the entire lake is 4.4% and of the deep subbasin is 6.6%, which categorizes Holland Lake as a deep lake (>4%). The watershed drainage area into the lake is heavily forested (hardwood). The lake is surrounded by tall trees and therefore well sheltered from wind. Aquatic macrophytes covered about 50% of the lake based on the 1983 site observations [Osgood, 1985]. Less than 1% of the lake surface is covered by emergent vegetation. Rooted aquatic plants are primarily coontail and watermilfoil [Department of Natural Resources, 1996]. The two subbasins with maximum depths of 14.8 ft (4.5<sup>‡</sup> m) and surface areas of 0.05 and 0.02 km<sup>2</sup>, respectively, probably have more photosynthetic oxygen production than the deep subbasin because of dense macrophyte beds.

In 1970, the MNDNR described Holland Lake as a hard water lake with moderate fertility. In 1986, the MNDNR reported [Department of Natural Resources, 1986] that a major storm sewer of the City of Eagan, which had been draining into Holland Lake, had drastically reduced the water quality of the lake since the 1975 survey. Since 1988, no storm sewers have been allowed to drain into the lake.

---

\* The map is extracted from a 1985 report by R. A. Osgood for the Metropolitan Council of Twin Cities. This map implies that the lake depth must have increased by 1.5 m since the 1963 US Geological Survey map. The increase in depth, presumably due to a rise in lake stage (Holland Lake is a terminal lake without surface outflow) was also observed on July 1, 1999 by the MNDNR and the SAFL staff.

† Relative depth  $z_r$  is an expression of the maximum depth ( $z_{max}$ ) as a percentage of the lake mean diameter.  $z_r = 50 z_{max} \sqrt{\frac{\pi}{A}}$  [Wetzel, 1983].

‡ Measurements on July 1, 1999.

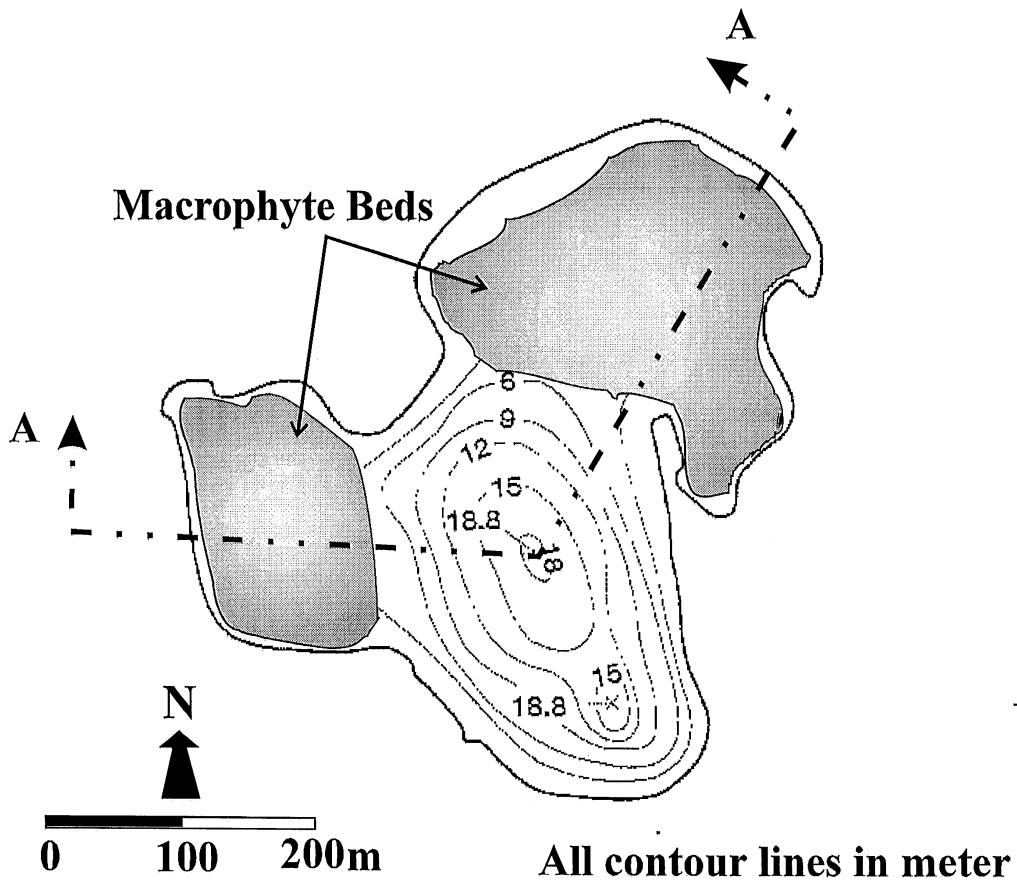
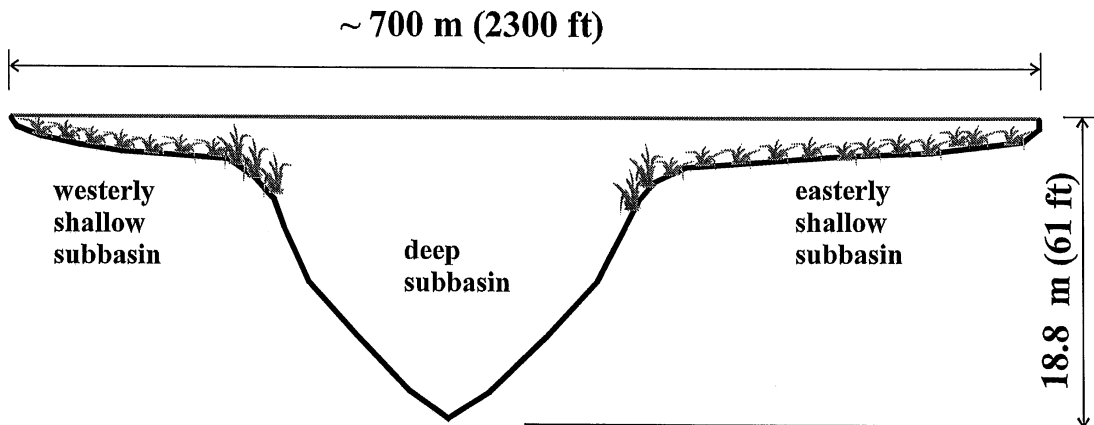


Figure 1a. Plan view of Holland Lake.



SECTION A-A

Figure 1b. A cross section of Holland Lake.



### III. Analysis of the Historical Records

Records of water temperature and dissolved oxygen concentration measured by the MNDNR, Metro Area Fisheries, since June 1970 were reviewed at the beginning of this study. These data are profiles measured several times a year near the deepest point of the lake. In addition, Secchi depth, conductivity, alkalinity and other water quality parameters (nitrate, sulfate and phosphorous) are sometimes included in the data. Water temperature and DO profiles were available for June, July or August of 1970, 1978, 1980, 1985, 1990 and 1995. Since December of 1997, water temperature and DO profiles have been measured approximately once a month. All measurements were made at one-foot intervals in the deep subbasin of Holland Lake down to a depth of about 50 ft (15 m) (Appendix A).

Water temperature and DO profiles with coarser than 1-ft (0.3 m) depth resolution were obtained in 1972, 1973 and 1974 by the U.S. Geological Survey. Water temperature and DO profiles were also measured frequently by R. A. Osgood for the Metropolitan Council in 1983, 1984, 1985 and 1993 (Appendix B).

All water temperature and DO profiles show a strong stratification in summer as is typical for deep Minnesota lakes, and oxygen deficiencies in the hypolimnion as is typical for deep metro area lakes. What is unusual is an anoxic layer in the thermocline in summer. Figure 2 displays two sets of temperature and DO profiles collected by the Minnesota Department of Natural Resources. Figure 2a shows a DO profile in August 1978 with an 8 ft layer which exhibits a significant DO deficit below the surfaced mixed layer, and Figure 2b shows a DO profile in July 1995 with an anoxic layer. The data collected by Osgood (1983-1985) give the progression of the DO profile in the deep subbasin from ice-out until the fall turnover in two-week time interval. The data collected in 1984 and reproduced in Figure 3 show that after ice-out there was more than 8 mg/l of DO in the water column. By June 6, an increase in metalimnetic DO was evident (metalimnetic oxygen maximum) at a depth of 10 to 20 ft. The DO positive heterograde profile became a negative heterograde profile by June 21. By July 24, a 4 ft thick anoxic layer developed in the thermocline. There was an 11 ft layer below it with a DO concentration of about 3 mg/l. The measurements show that this layer also became anoxic by mid August.

Other records show similar trends in the DO profile throughout summer, with some variations from one year to another. Only the DO records collected in 1984 and 1985 by Osgood at about 2 week intervals establish a coherent seasonal pattern in the DO profile clearly.

The observed changes in DO profiles with time (Figure 3) could be produced by a variety of processes. A list of potential processes is as follows:

1. A high concentration of phytoplankton can cause an increase in DO during the day if light penetration is sufficient to cause significant photosynthesis. There are times when a DO maximum has been observed in the metalimnion (metalimnetic oxygen maximum, MOM) but not in the surface layer. This would require higher phytoplankton concentrations or more efficient phytoplankton in the metalimnion.

2. Plant respiration can be a significant oxygen sink. Plant respiration can be by algae or by rooted vegetation. Algae are predominant in the deep subbasin and macrophytes are abundant in the shallow subbasins.
3. When DO depletion is observed in the metalimnion of the deep subbasin, it may also be due to a significant concentration of dead organic matter (TOC, BOD, detritus). The source of this material may be the two shallow vegetated subbasins or dead phytoplankton sinking into the deep subbasin.
4. Excessive loss of DO in certain layers of the lake can be due to exceptionally high sediment oxygen demand (SOD). Accumulations of detrital material and large amounts of inactive macrophytes in the shallow subbasins of the lake can increase DO depletion rates in layers between 5 ft and 15 ft depth substantially.
5. Any interaction between the oxygen depleted layers of the shallow subbasins and the deep subbasin can create an anoxic layer in the thermocline or the hypolimnion of the deep subbasin.
6. Groundwater intrusions can be a source of low DO water and can contribute to the water exchange between basins.

An intensive field study was conducted to quantify some of the factors affecting these processes and to determine the most likely causes and mechanism for the observed DO dynamics in Holland Lake.

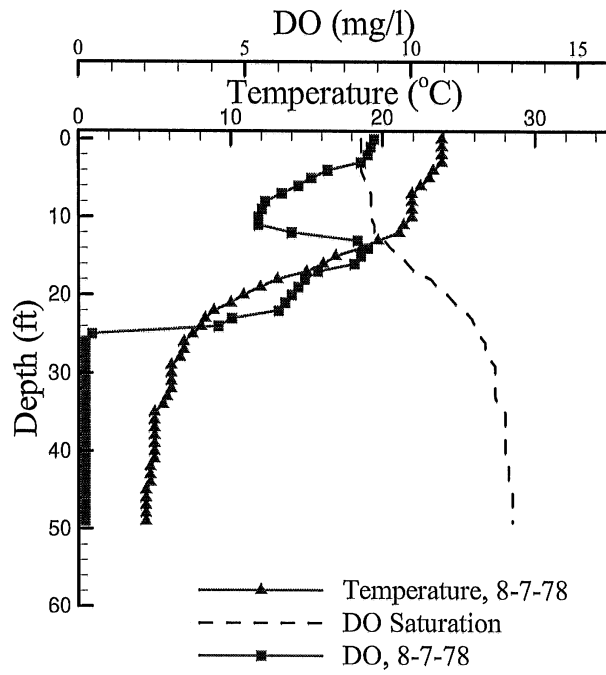


**Figure 2a.** Temperature and DO profiles in Holland Lake in August 7, 1978.

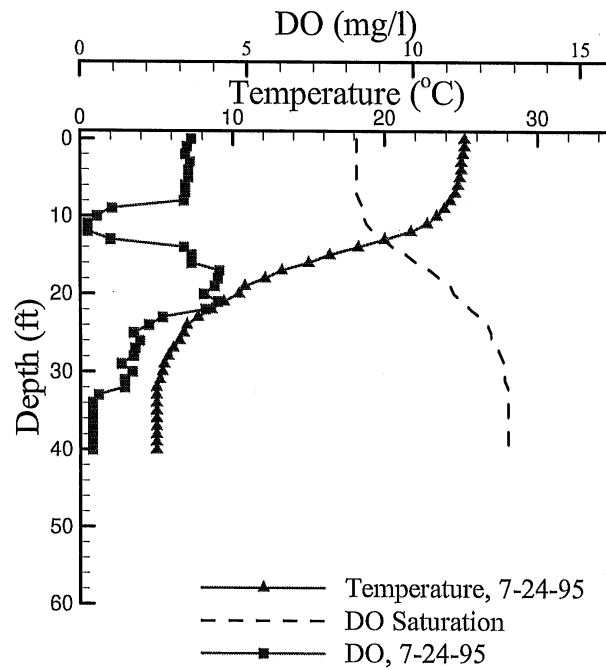


**Figure 2b.** Temperature and DO profiles in Holland Lake in July 24, 1995.

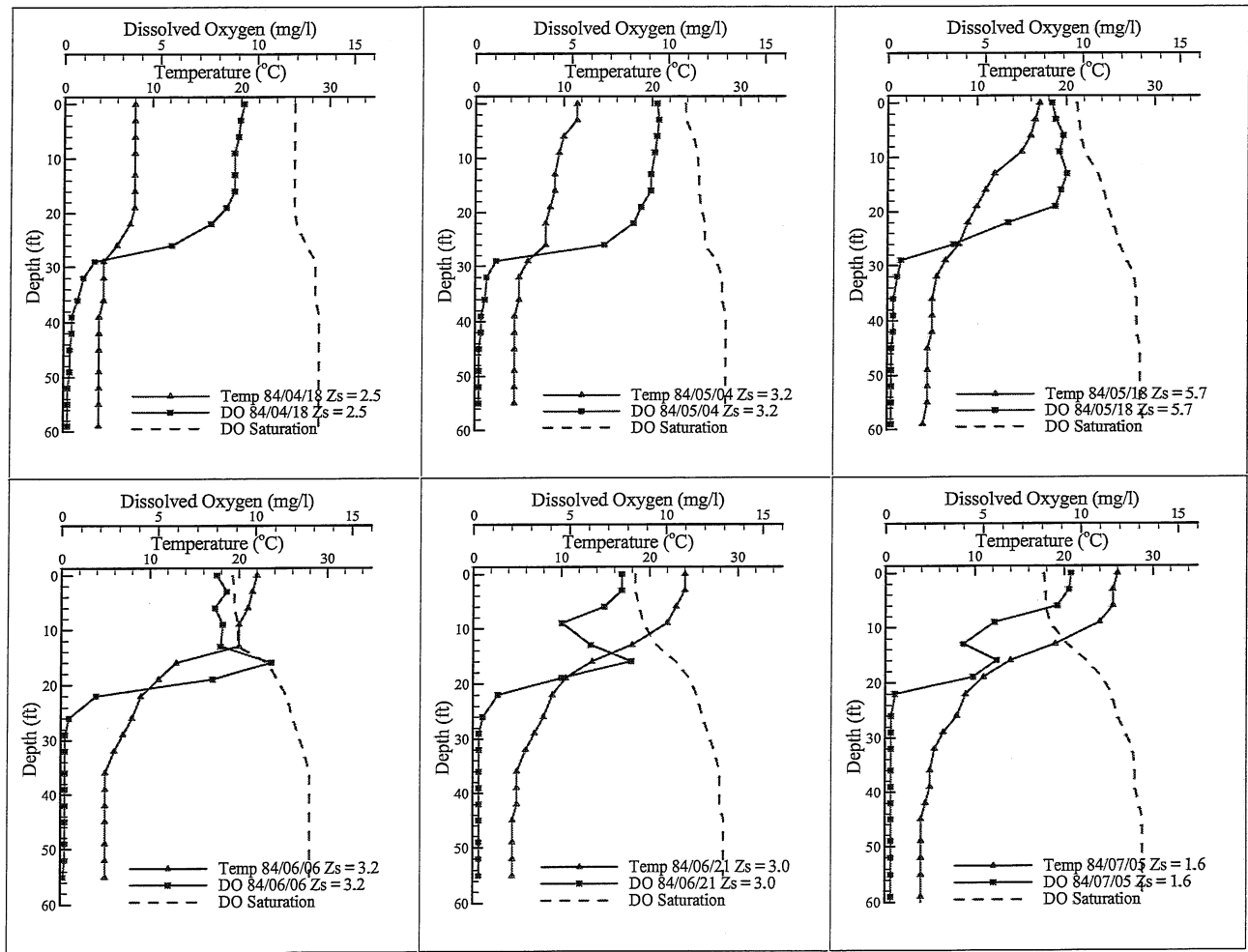
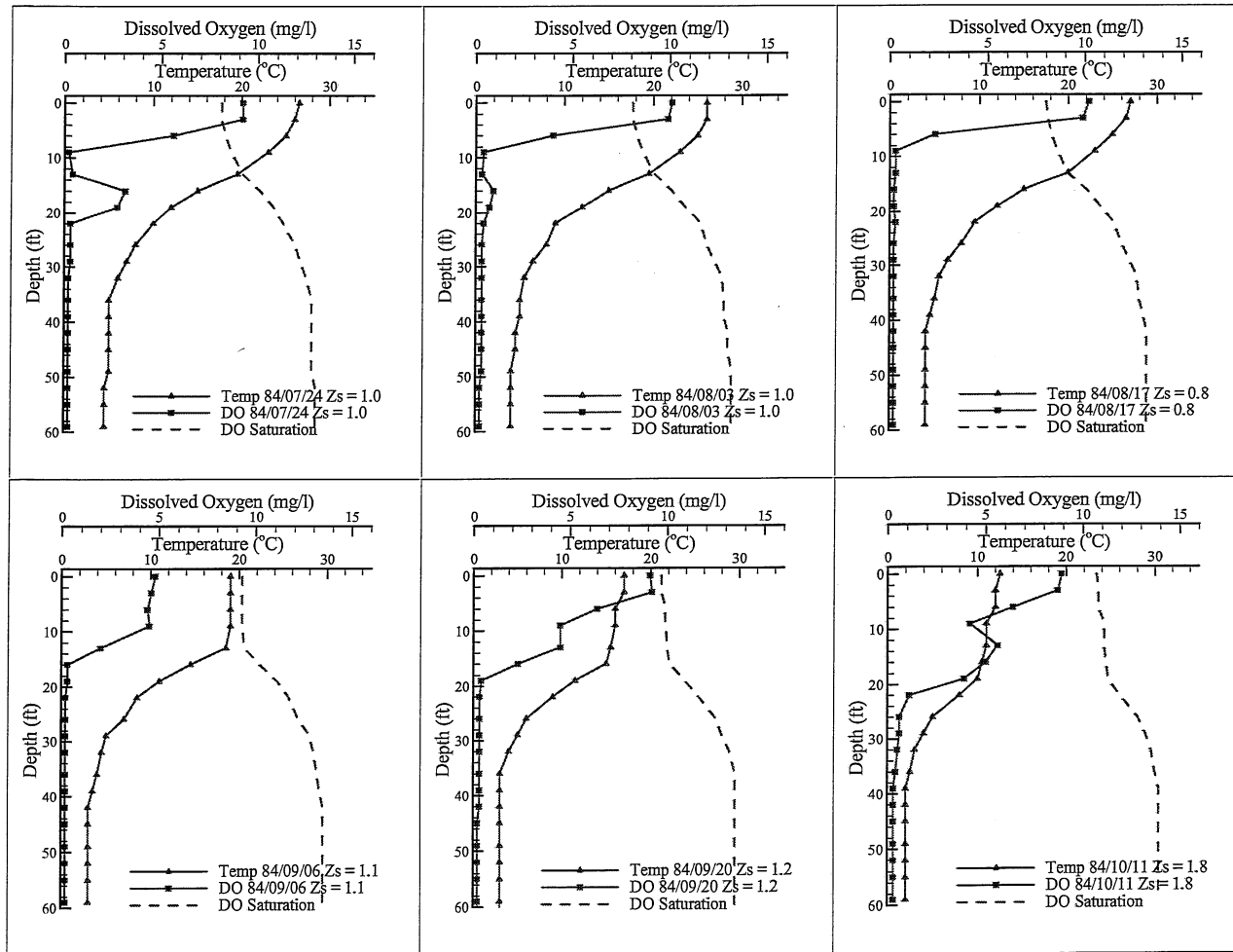


Figure 3a. Temperature, Dissolved Oxygen (DO) and DO Saturation Profiles in Holland Lake in 1984. Data are from the EPA/STORET database.



**Figure 3b.** Temperature, Dissolved Oxygen (DO) and DO Saturation Profiles in Holland Lake in 1984. Data are from the EPA/STORET database.

## IV. Field Work/Data Collection

### IV.1. Water Temperature

Water temperature and DO data were collected at three fixed stations. One thermistor array was placed in the deep subbasin, one in the larger (eastern) shallow subbasin, and one at the boundary between the two subbasins to obtain some evidence of possible interactions between the subbasins, i.e. intrusions (Figure 4). The thermistor chains were supported by  $1.2 \times 1.2$  m floating rafts anchored from three directions. The raft in the deep subbasin was designated as raft 1, the one at the border of the two subbasins as raft 2, and the one in the shallow subbasin as raft 3.

On each raft, a Campbell Scientific CR10 data logger was mounted and connected to an assembly of thermistors (Campbell Scientific model 107B temperature probes) tied to a chain hanging from the raft. The data logger received and recorded water temperatures from thermistors at 1-minute intervals and averaged them over a 10-minute period. The first thermistor was placed at 0.5 ft (0.15 m) below the water surface. The distances between two consecutive thermistors were set at 2 ft (0.60 m).

The thermistors were initially calibrated at room temperatures using a precision (0.1 °F) mercury thermometer. After the rafts were retrieved from the lake, the thermistors were recalibrated. The corrections due to recalibration were applied linearly with time. A quadratic correction with time was only applied to one thermistor. Several thermistors started malfunctioning weeks after they were installed and several others were chewed on by muskrats in the fall. These thermistors were not recalibrated. Instead the missing data were replaced by a linear interpolation from the adjacent thermistors. The calibration corrections and the periods when some thermistors exhibited poor data are shown in Appendix C for the three rafts. The largest adjustments had to be made for probes between 4 and 10 ft (1.2 to 3 m) depth, i.e. in the epilimnion. Probes below 10 ft depths (3 m), i.e. in the thermocline region, held calibration well (the largest adjustment was 0.347 °C).

## **IV.2. Dissolved Oxygen**

Dissolved oxygen concentrations were recorded in situ using a portable YSI Model 58 Dissolved Oxygen Meter. The DO profiles were taken approximately once a week at the locations of the rafts and at the depths where thermistors were recording water temperatures. Since the DO profiles were collected once per visit (often between 10 am and noon), they would not necessarily represent the average daily DO profiles. In order to obtain some information about the diurnal variability of the DO profile and its relationship with late morning measurements, it was decided to make a one-time survey of diurnal DO variations at the three rafts. The diurnal data collection started on August 2, at 10 am and ended on August 3, at 8 am. The time intervals between measurements were 3-4 hours.

## **IV.3. Light**

In addition to temperature and DO profiles, Secchi depth was measured at every trip to the lake, i.e. approximately once a week. For a more accurate estimate of light attenuation, photosynthetic active radiation (PAR) was measured in the water using a spherical PAR collector manufactured by LICOR and connected to a CR10 data logger. PAR profiles were measured three times in the deep subbasin and once in the shallow subbasins at nine locations (Figure 4). When the PAR profiles in the shallow subbasins were measured, macrophytes covered most of the littoral zone of the lake. The nine locations shown in Figure 4 were selected to obtain a representative PAR profile for the shallow subbasins.

## **IV.4. Water Sampling**

To quantify some parameters related to dissolved oxygen depletion, water samples from Holland Lake were collected and analyzed on three occasions.

On August 19, twenty eight (28) samples were collected in 350-ml BOD bottles close to rafts 1 and 3, and from a fourth point in the middle of the western shallow subbasin (Figure 4). The samples were obtained using a peristaltic pump with a funnel mounted at the inlet of the suction pipe to slowly extract water only from the given depth. All bottles, wrapped in aluminum foil and placed in a cooler filled with ice, were taken to the University of Minnesota, Department of Civil Engineering environmental laboratory for the total organic carbon (TOC) analysis. In the laboratory, the samples were analyzed using a Tekmar Dohrmann UV-Persulfate TOC analyzer. The apparatus removes the inorganic carbon by acidification using persulfate and spraying ultra violet rays from a reactor. The resulting carbon dioxide from the reactions is swept through a moisture removal system and a halogen scrubber.

On August 23, twenty eight (28) samples were collected in two liter amber plastic bottles provided by the Ecological Services Section of the MNDNR. The same peristaltic pump was used for collecting the two liter samples. The samples were taken to the

Minnesota Department of Agriculture Laboratory in St. Paul and analyzed for total suspended solids (TSS), total volatile suspended solids (TVSS), phaeophytin concentration and phaeophytin-corrected chlorophyll concentration.

On September 16, thirteen (13) water samples were collected at different depths and incubated in one-gallon plastic bottles for estimating DO uptake/depletion rates at the locations of rafts 1 and 3 in the lake. After taking each sample from a given depth, the DO concentration of that sample was measured using the YSI DO probe. If the DO concentration of the sample was less than 4 mg/l, the bottle was aerated by shaking. Manual aeration would continue until the DO concentration exceeded 4 mg/l. Then, the bottles were wrapped in aluminum foil and tied to a chain hanging from the raft. The bottled samples stayed in the lake at the depths they were collected from. To ascertain whether a 2-day period or a 5-day period would be sufficiently long enough for measuring the respiration rates, two bottles were retrieved on September 18. The DO concentration of the two bottles was measured and it was decided to retrieve the other bottles after a 5-day period. Therefore, on September 21, the remaining 11 bottles were retrieved and their DO concentrations were measured. The difference between the initial and the final DO concentrations over the 5-day period furnished a direct estimate of the oxygen depletion rate.



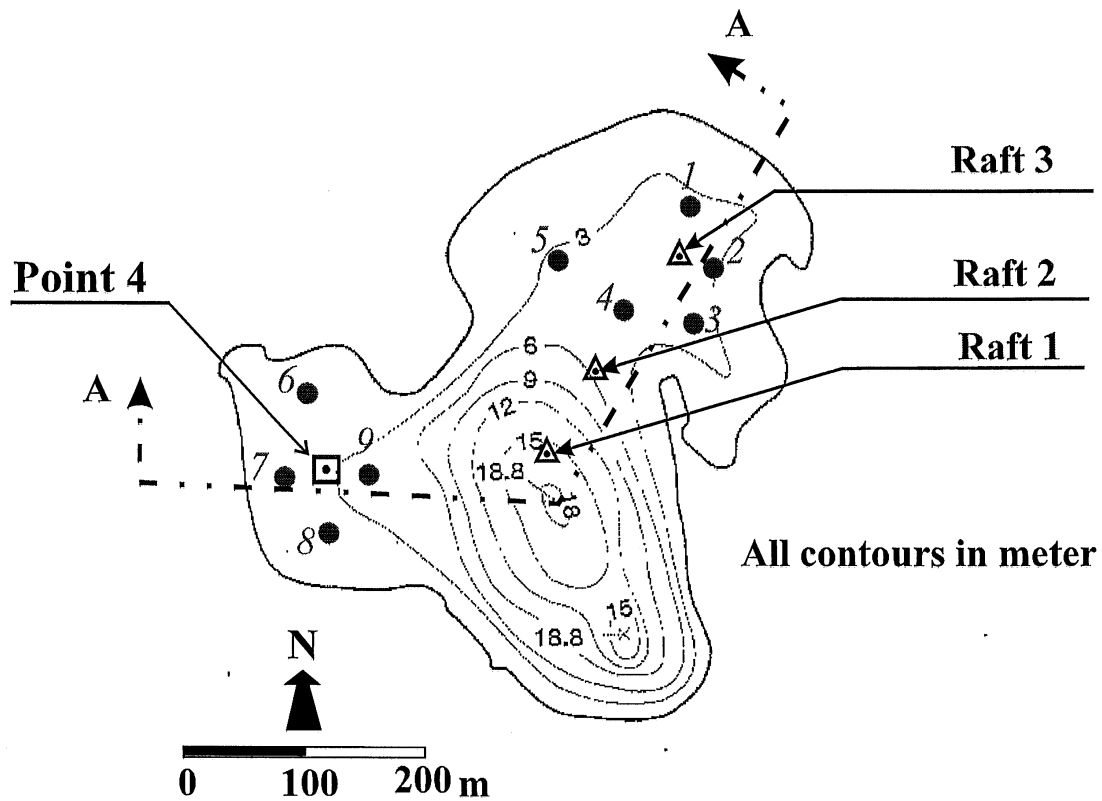


**Figure 4.** Locations of rafts in Holland Lake where DO and temperature profiles were measured, and locations in shallow subbasins where photosynthetically active radiation (PAR) was measured. Triangles with numerals indicate where rafts were located, and circles with italic font numerals indicate where PAR was measured in the shallow subbasins. Point 4 is where the water samples were collected in the western shallow subbasin.

## V. Dissolved Oxygen Profiles

### V.1. Seasonal Trends in DO Concentrations

To determine the seasonal changes in the DO profile, data collected once a month, from October 1998 to May 1999 by the MNDNR and data collected twice a month by the Metropolitan Council from April to July 1999 were combined with those collected by the authors at about weekly intervals from July 1999 to October 1999. The resolution of this database for the summer of 1999 was higher than in any preceding year.

Figures 5a to 5d display twenty one DO profiles, water temperature profiles and associated saturated DO profiles collected between October 1998 and October 1999. Figure 5a shows a complete fall turnover by late November. By January, the DO profile is stratified; the minimum DO concentration (at the bottom of lake) is more than 5 mg/l. By late March, the stratum below the 40 ft (12 m) depth becomes anoxic presumably due to oxygen consumption at the sediment-water interface by decomposition of accumulated organic matter in the sediment. By late May (Figure 5b), the hypolimnetic anoxic stratum has moved up to about 34 ft (10.2 m). At the same time, the DO above the thermocline starts depleting. Consequently, a negative heterograde<sup>§</sup> DO profile is formed in the deep subbasin. By early July, the layer from 10 ft (3 m) depth down to 16 ft (4.8 m) depth, becomes anoxic while the lower stratum of the metalimnion, from 20 ft (6 m) depth to 28 ft (8.4 m) depth, still contains up to 7 mg/l. Apparently, the oxygen depletion rate is lower in these layers than those at the thermocline.

Figure 5b suggests that in midsummer high water temperature at the lake surface and anoxia below the surface would exert stresses on brown trout any time they move upwards to feed near the lake surface. By mid-August (Figure 5c), DO is less than 2 mg/l and the water temperature is above 20 °C above 14 ft depth. It is difficult for brown trout to survive in such an environment. By early September, water temperatures in the surface mixed layer (down to about 16 ft) are still above 20 °C and DO is still near zero below 16 ft (4.8 m) depth. The entire metalimnion is anoxic and a clinograde oxygen profile\*\* is formed in the lake, which is typical for dimictic lakes in the Twin Cities Metro Areas [Osgood, 1989].

Significant nocturnal cooling in fall deepens the surface mixed layer such that by mid-October (Figure 5d) the epilimnion becomes more than 20 ft (6 m) thick and the DO concentration in that layer rises to 10 mg/l due to convective mixing. By mid November, the cycle begins to repeat itself, i.e. there is a fall turnover and DO is more or less uniformly distributed with depth.

---

<sup>§</sup> A heterograde oxygen curve exhibits an irregular slope from the lake surface downwards. High concentrations of animals may produce a negative heterograde distribution if respiration dominates at some mid-depth, or a positive heterograde distribution if photosynthetic organisms are concentrated in the same fashion [Horne and Goldman, 1994].

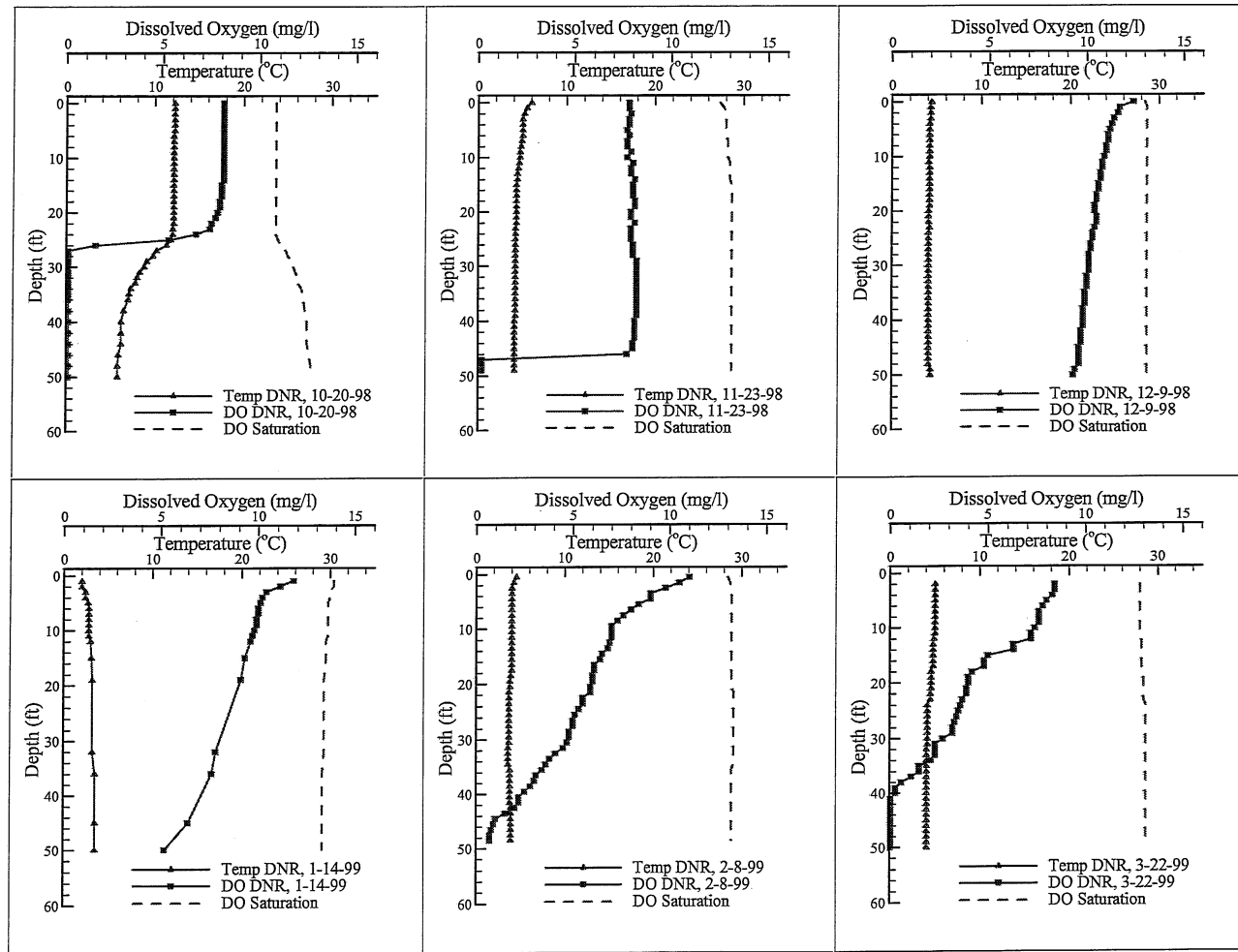
\*\* A clinograde curve is characterized by relatively higher oxygen content near the surface, where photosynthesis releases oxygen [Horne and Goldman, 1994].

To further illustrate the seasonal cycle, DO measurements at different depths have been plotted against time in Figure 6. The DO time series are for the 1998-1999 period. The DO concentrations peak at 10 to 12 mg/l in mid-December. The surface layer exhibits a minimum DO concentration of 4 mg/l in early August. Figure 6 shows fully mixed conditions at about 8 mg/l in the second half of November (fall overturn), but no such event in April or May when spring overturn would be expected. This is due to incomplete mixing in spring, i.e. Holland Lake is more or less a monomictic lake. The deepest layers remain anoxic more than 9 months of the year. These layers exhibit high DO depletion rates ( $0.18 \text{ mg.l}^{-1}.\text{day}^{-1}$ ) during the ice cover period (January and February). The causes of the pronounced oxygen depletion rate is most likely the sedimentary oxygen demand (SOD) due to decaying and deposited macrophyte and phytoplankton material. A very high DO depletion rate is evident in the strata from 10 to 18 ft (3.6 to 5.4 m) depth in early July. The result is a negative heterograde DO profile in early summer as discussed earlier.

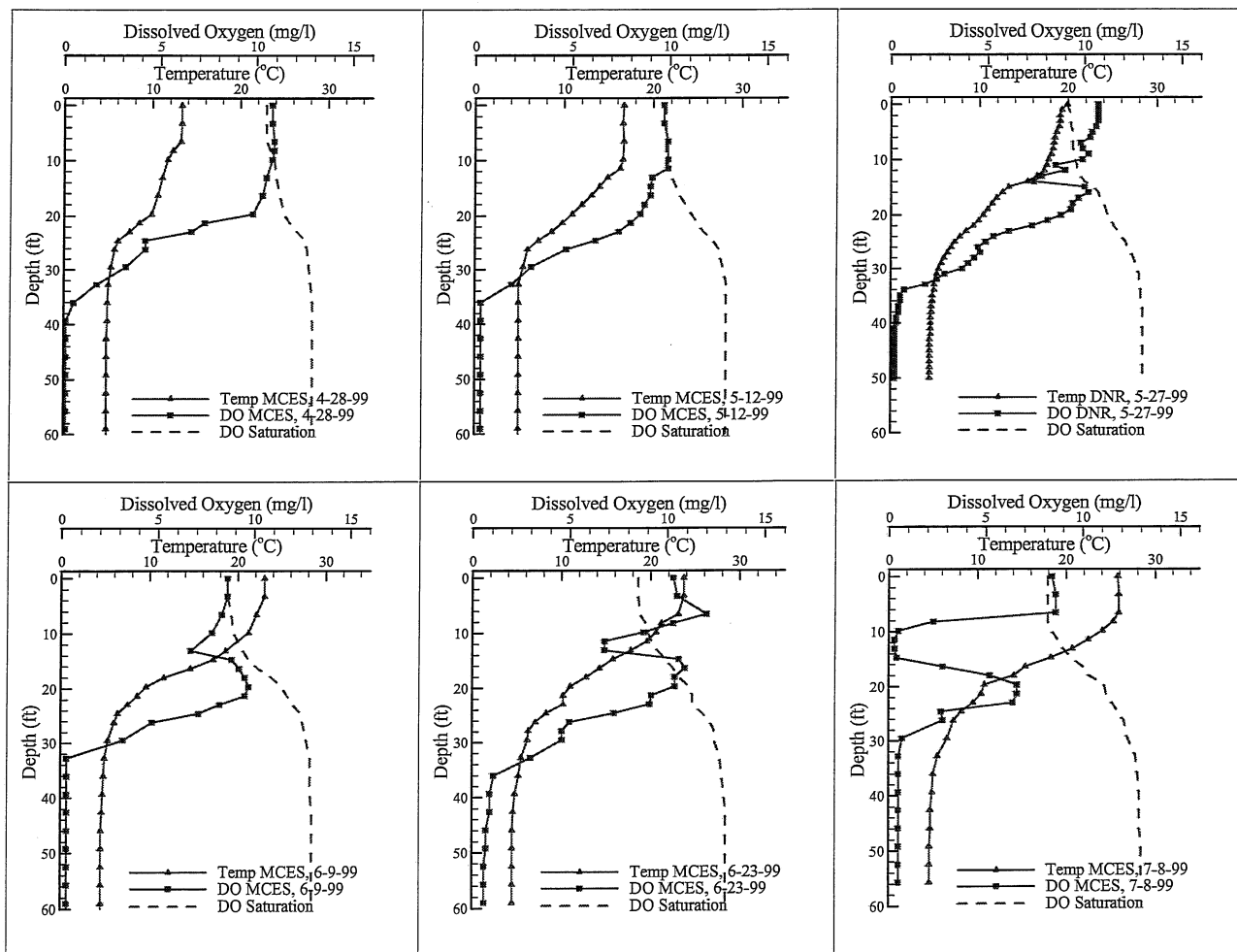
In Figure 7, the water column in the deep subbasin is divided into 5 equally thick strata: The uppermost layer down to a depth of 10 ft characterizes the epilimnion, the second layer from 10 to 20 ft depth encompasses the seasonal thermocline, from 20 to 30 ft depth is the lower stratum of the metalimnion, from 30 to 40 ft depth and from 40 to 50 ft depth is the hypolimnion. Since the DO contents of the last two strata are not significantly different, the average value of the two strata is displayed in Figure 7. Figure 7 shows that the hypolimnion has less than 1 mg DO/l after ice out, which makes the hypolimnion unsuitable for brown trout during the open water season until the fall turnover. From early July until mid-September, the entire metalimnion also becomes anoxic or very low in DO content. Therefore, for a period of more than two months, there is oxygen stress on fish below the epilimnion. The lower stratum of the metalimnion (20 to 30 ft depth) has a smaller DO depletion rate than the stratum above it (10 to 20 ft depth). The DO depletion rates are displayed in Figure 8. The maximum depletion rate of about  $0.47 \text{ mg.l}^{-1}.\text{day}^{-1}$  occurs in the upper stratum of the metalimnion in late June and early July. There are spikes in the rate of change of the DO as large as  $-0.2 \text{ mg.l}^{-1}.\text{day}^{-1}$ , which occur over a very short period in the epilimnion. These rapid changes are probably due to changes in the weather. During overcast days, the rate of photosynthetic oxygen production decreases while the rate of respiration remains more or less the same, if the temperature varies insignificantly.

Figure 9 illustrates the time series of the changes in DO for the entire water column of the deep subbasin. It is evident that the oxygen production rate in spring is lower than the oxygen depletion rate in summer. The DO depletion rate in summer, when the lake is stratified, reaches up to  $4 \text{ g.m}^{-2}.\text{day}^{-1}$ , which is comparable to the DO depletion rate of aged sewage sludge [Thomann and Muller, 1987].

In summary, the hypolimnion of the deep subbasin becomes anoxic soon after the spring turnover. The upper stratum of the metalimnion becomes anoxic by early July while the lower metalimnion still contains some oxygen. By mid-August, there is no oxygen present in both the metalimnion and the hypolimnion of the lake. After fall turnover, the entire water column in the deep subbasin is replenished with DO (more than 8 mg/l).



**Figure 5a.** Measured temperature and dissolved oxygen profiles in Holland Lake in 1999. Data were collected by the MNDNR, the Metropolitan Council and St. Anthony Falls Laboratory.



**Figure 5b.** Measured temperature and dissolved oxygen profiles in Holland Lake in 1999. Data were collected by the MNDNR, the Metropolitan Council and St. Anthony Falls Laboratory.

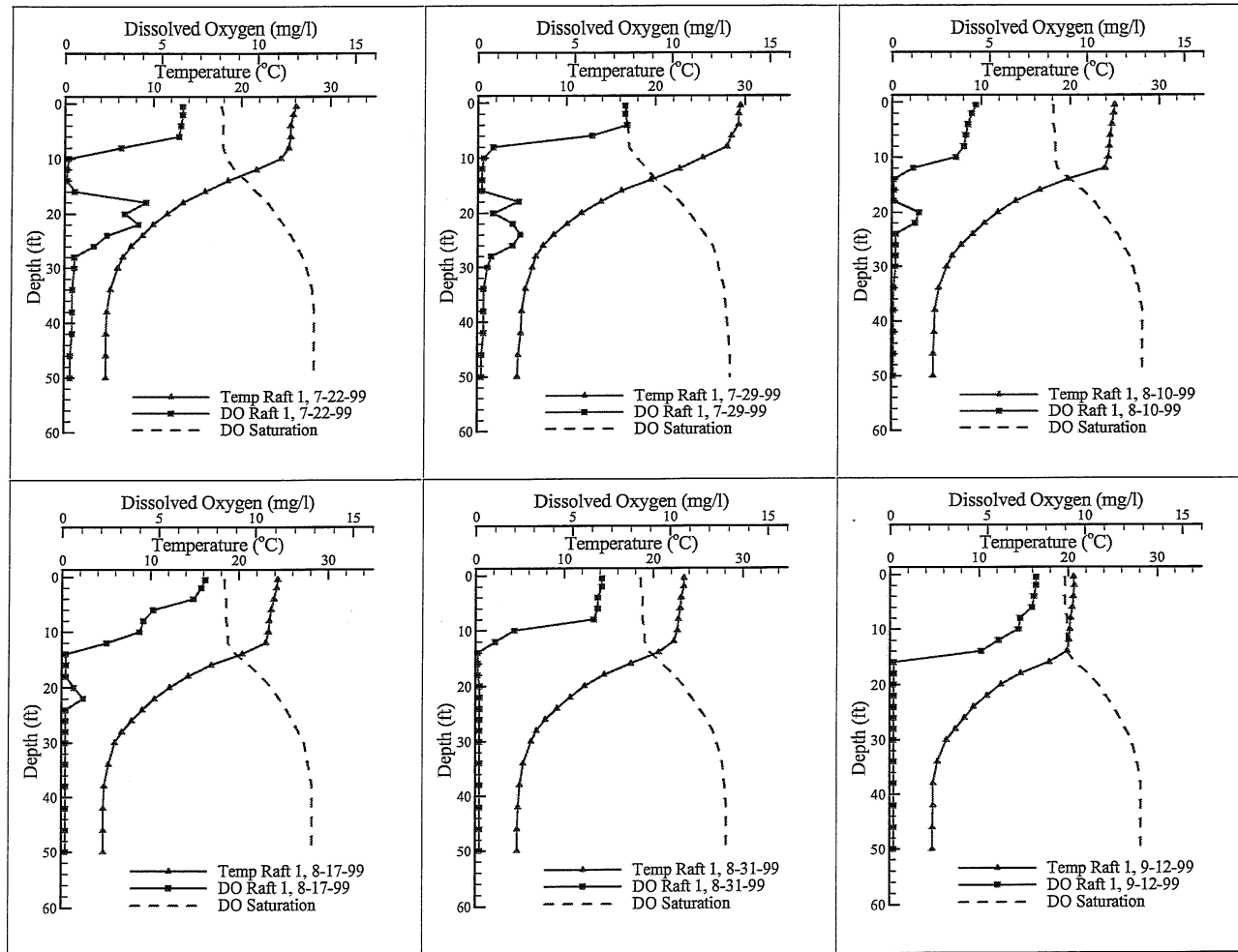


**Figure 5c.** Measured temperature and dissolved oxygen profiles in Holland Lake in 1999. Data were collected by the MNDNR, the Metropolitan Council and St. Anthony Falls Laboratory.

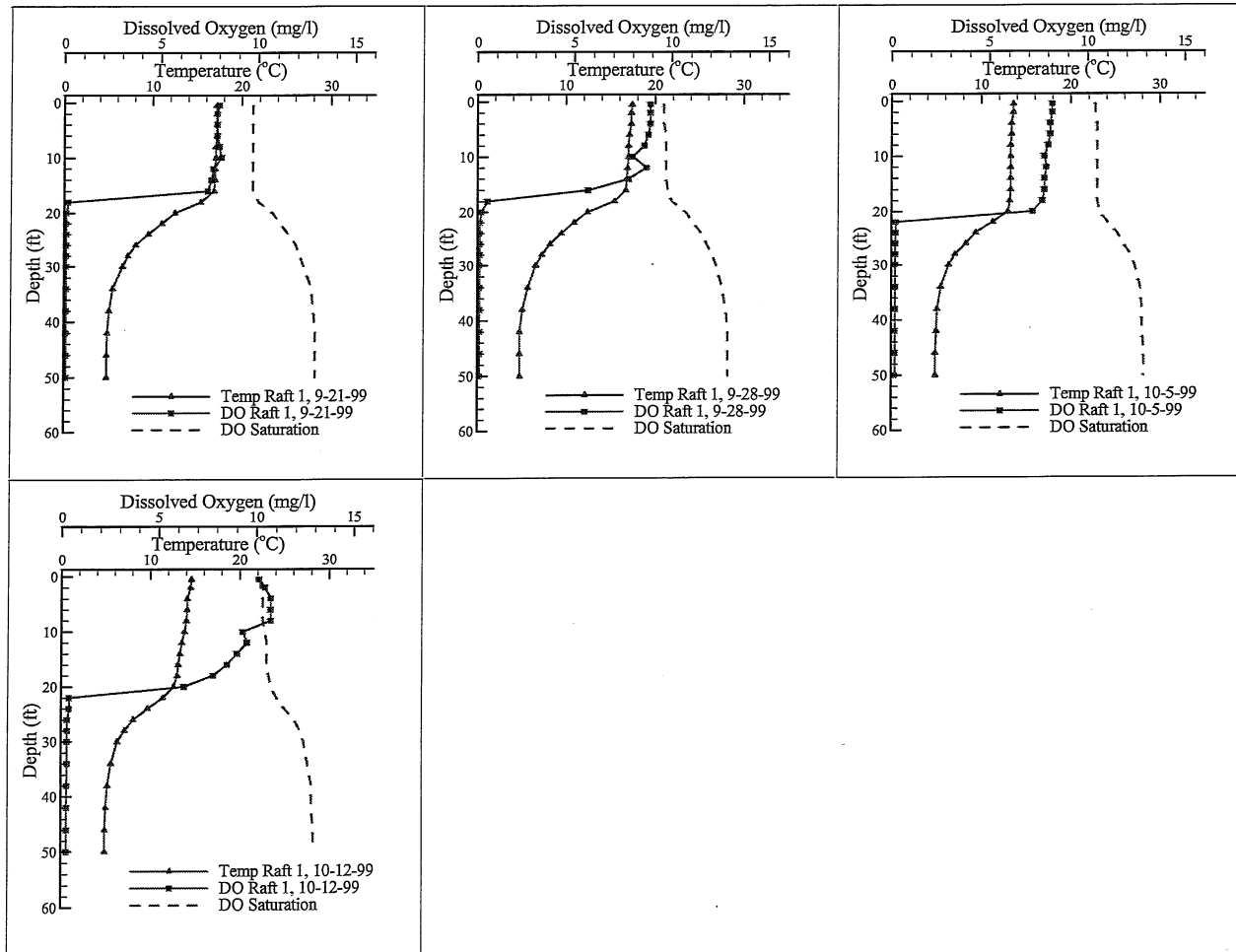


**Figure 5d.** Measured temperature and dissolved oxygen profiles in Holland Lake in 1999. Data were collected by the MNDNR, the Metropolitan Council and St. Anthony Falls Laboratory.

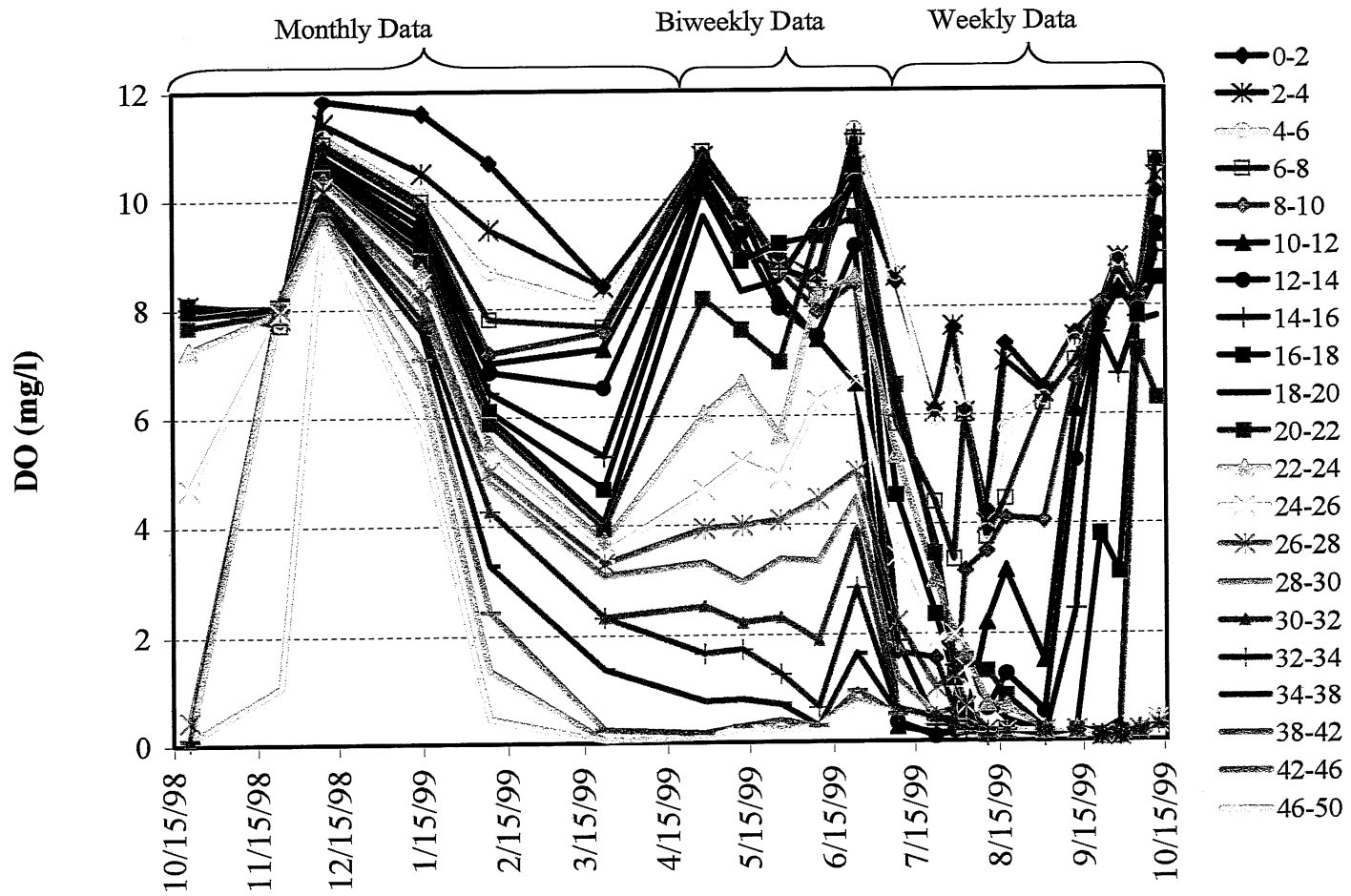


**Figure 6.** Measured dissolved oxygen content of different strata in the deep subbasin of Holland Lake.



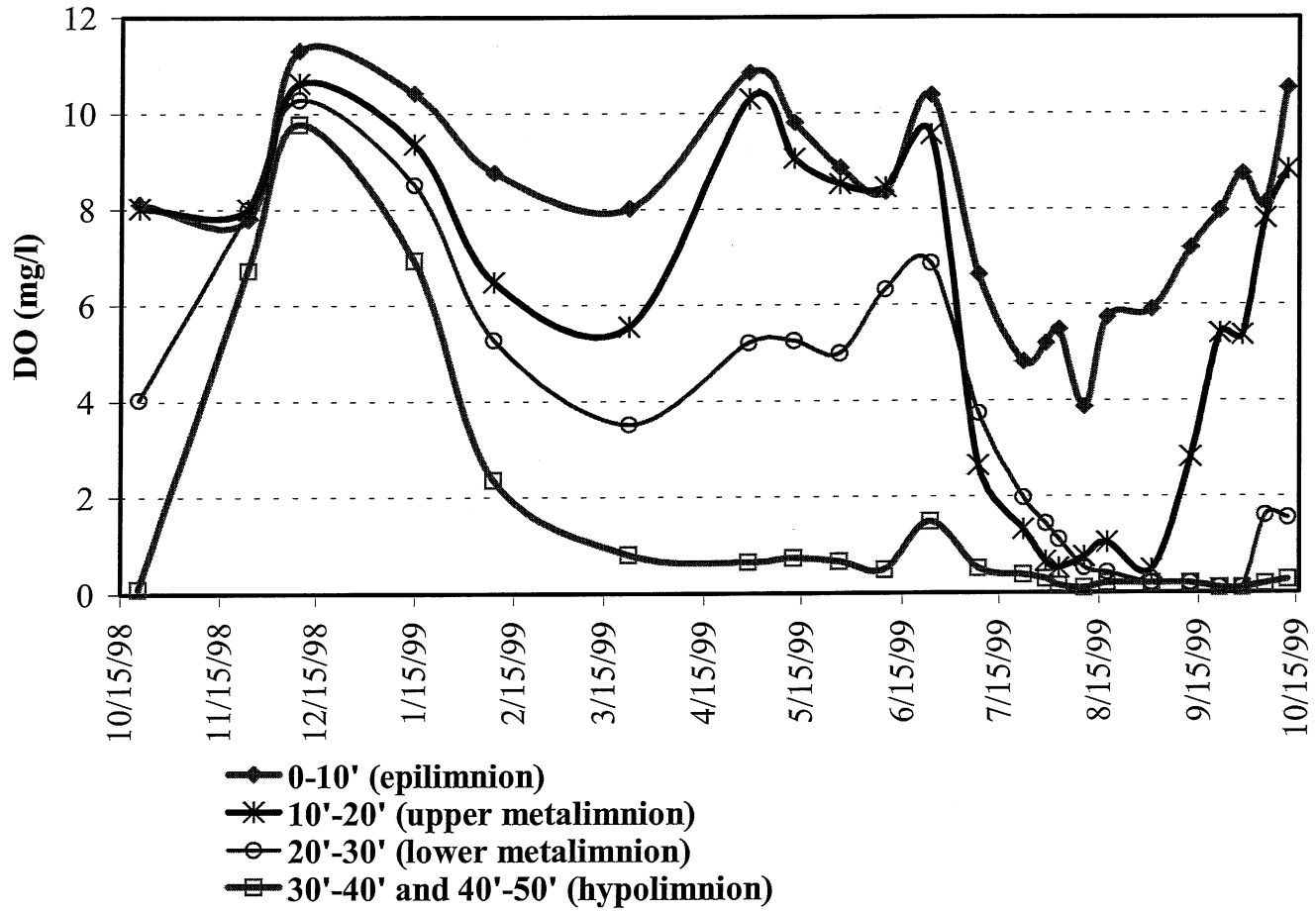


**Figure 7.** Dissolved oxygen content of different strata (thermal regions) in the deep subbasin of Holland Lake.

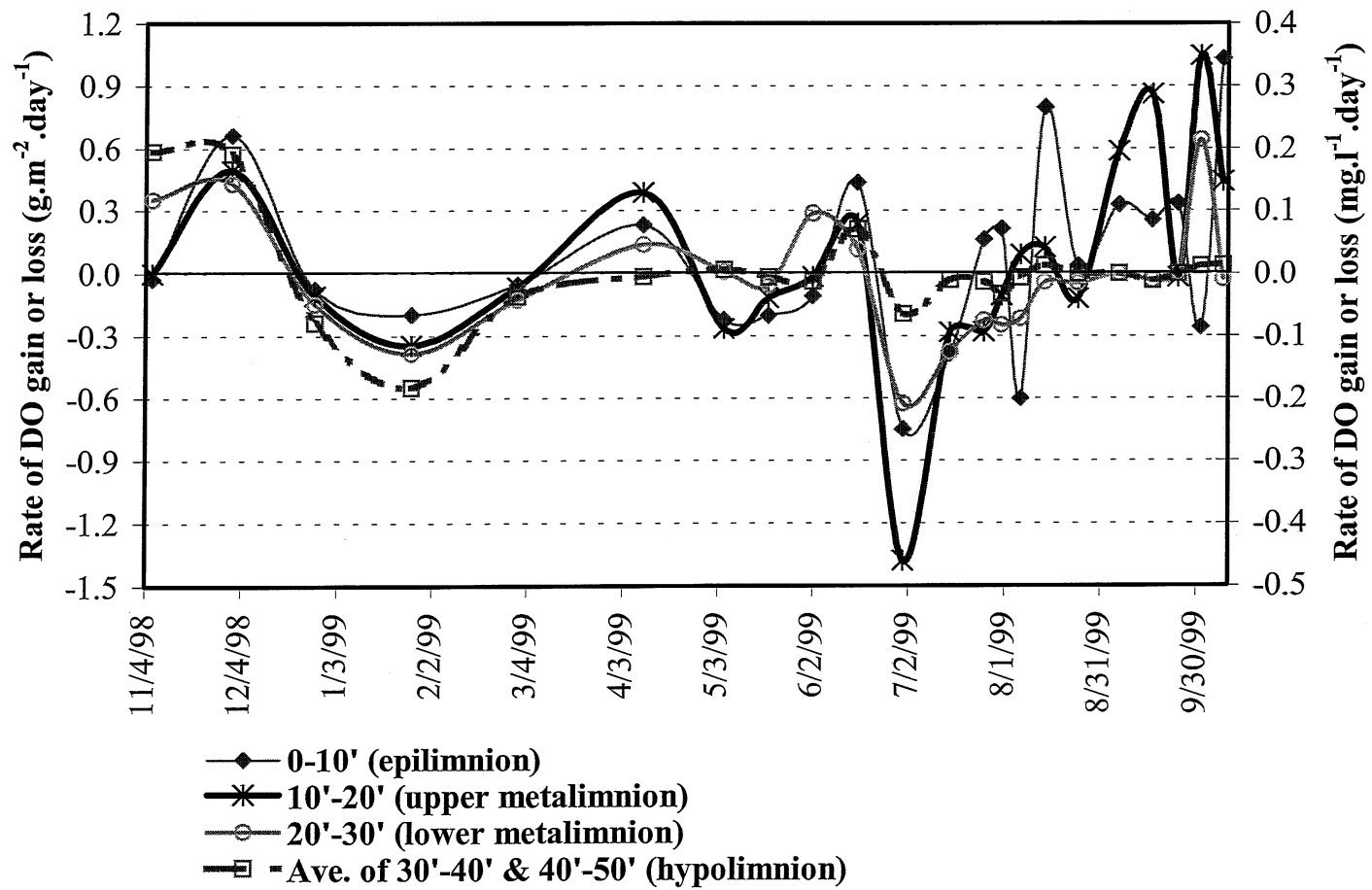


**Figure 8.** Rate of change of dissolved oxygen concentration in different strata (thermal regions) of the deep subsbasin of Holland Lake.

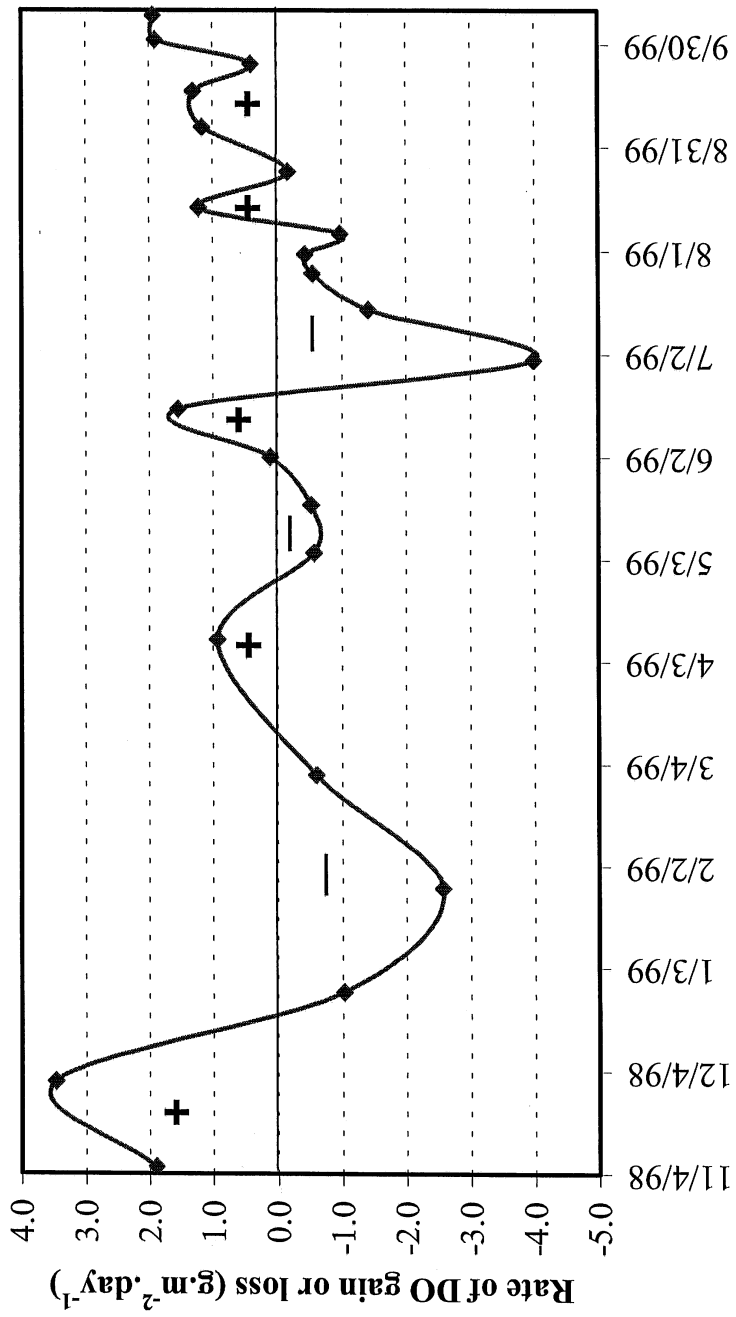


**Figure 9.** Rate of change of dissolved oxygen concentration in the entire water column of the deep subbasin of Holland Lake.

## V.2. Diurnal Changes in DO Concentrations

To ascertain that the seasonal trends discussed above were not significantly influenced by the time of day at which the measurements of DO were made, an intensive diurnal DO survey was conducted. Diurnal changes in DO are known to be quite large in streams, and can in fact be used to determine rates of day time community photosynthesis and night time respiration (Odum's method).

DO profiles at the locations of the rafts were measured seven times during a 24 hour period. The field work started at 10 am on August 2, 1999, a sunny day with no overcast. The morning of August 3 when the last measurements were taken, was partly cloudy, however. In addition to the DO measurements, Secchi depths were measured at the locations of the rafts in the day time.

The seven DO profiles are displayed in Appendix D (Figure D.1). The measurements show that the DO values at raft 1 in the deep subbasin and at raft 2 did not change more than 1 mg/l in a 24 hour period; the changes were mostly near the surface. The spikes in the DO profile of the lower stratum of the metalimnion suggest that intrusions or internal waves were present. Internal waves induce a vertical oscillating motion, which moves water of differing DO from one depth to another. At some depths, the DO probe showed the DO concentration continuously oscillating with an amplitude of about 1 mg DO/l.

The DO profile at raft 3 in the shallow subbasin exhibited a maximum diurnal change of 2.5 mg/l at 5.5 ft (1.7 m) depth probably due to photosynthesis by dense macrophyte populations.

Figure 10 displays the time series of the DO concentrations averaged (simple average, not volume weighted) over layers of 10 ft or more depth at all three rafts. It is evident that the DO content does not change significantly in the deep subbasin; there is only a small change in the epilimnion. Therefore, once a day DO profile measurements in the deep subbasin give errors only in tenths of mg/l. The shallow subbasin is more dynamic and some diurnal changes are evident. An evening DO measurement would give the largest error from the daily mean. Measurements around noon would supply values near the daily averages. The DO content in the upper 10 ft of the water column was similar at the three rafts. The largest difference of 1 mg/l was in the afternoon and between raft 3 and the other two rafts (Figure D.2).

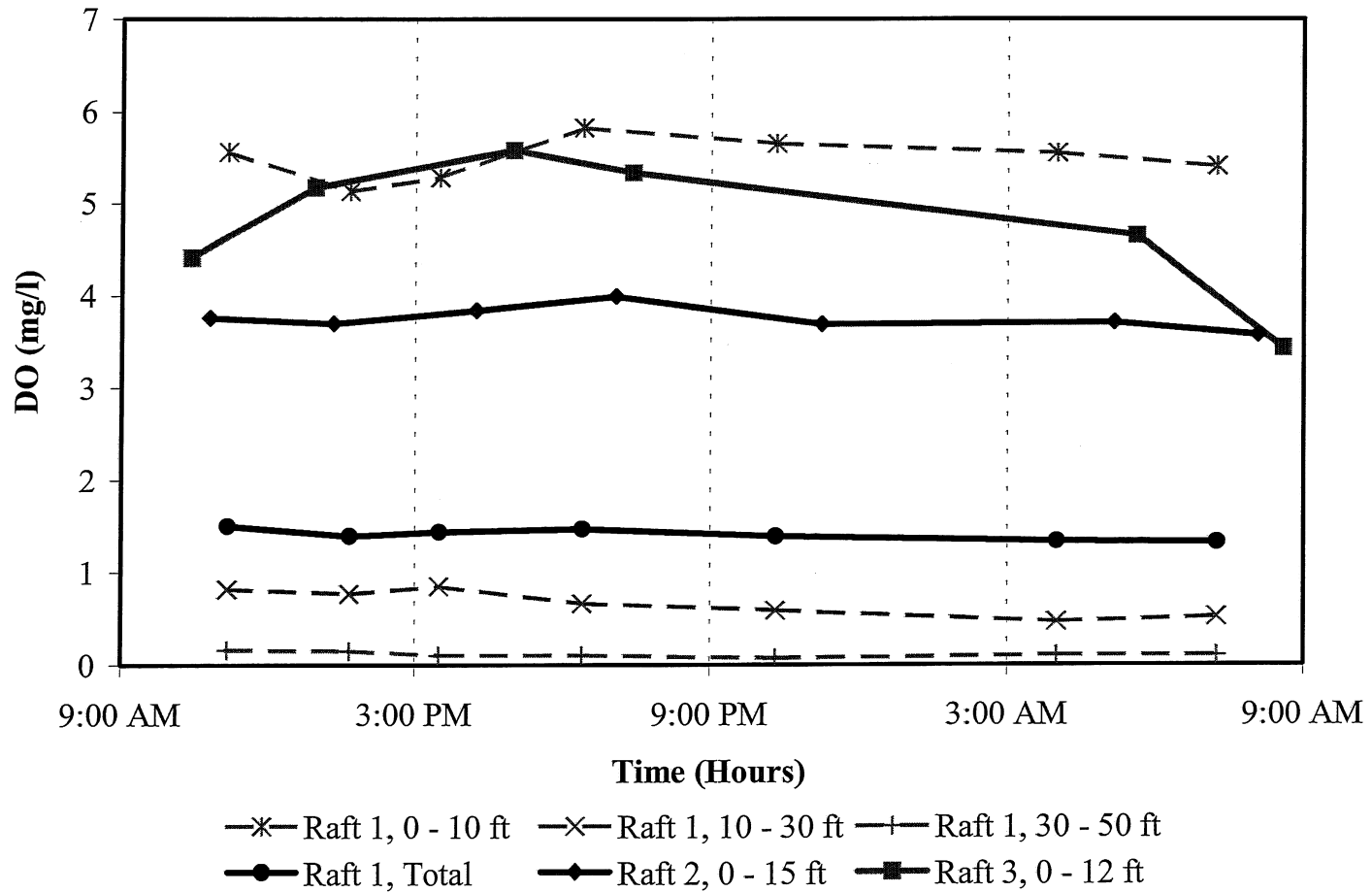


**Figure 10.** Diurnal dissolved oxygen variation in Holland Lake, August 2 and 3, 1999. Simple average concentrations for several layers and locations are plotted versus time of day.

## VI. Processes Affecting Dissolved Oxygen

The dissolved oxygen concentration in any layer of the lake is a function of oxygen production, depletion and transport processes in that layer, which can be listed as follows:

1. Gas exchange across the air/water interface. This surface aeration or deoxygenation affects only the topmost water layer directly.
2. Oxygen production by photosynthesis, which is a function of available light and the concentration of macrophytes and algal populations.
3. Oxygen uptake through plant respiration, which is a function of the concentration of macrophytes and algal populations.
4. Oxygen uptake by biochemical decomposition of dead particulate or dissolved organic matter in the water column, i.e. biological oxygen demand (BOD), which is a function of the detritus concentration and dissolved organic carbon (DOC).
5. Oxygen uptake by the sediment, i.e. sediment oxygen demand (SOD), which is a function of the type of sediment and the bathymetry of the lake.
6. Mixing in vertical directions, which depends upon wind and buoyancy. Mixing is controlled by weather conditions (seasons) and diurnal heating and cooling. The wind effects also depend upon lake morphometry and topography and land use around the lake.
7. Horizontal dispersion of detritus, algae and DO between the subbasins.
8. External advection. Holland Lake has a small drainage basin and currently no storm sewage is being discharged into the lake. The most significant advective flow appears to be the groundwater flow through the lake.

In the following sections, these processes will be discussed and quantified using the field data obtained in Holland Lake.

### VI.1. Photosynthesis

Secchi depth (SD) is an indicator of light attenuation in a lake. It is usually measured in the open water of a lake where only color and particulate suspended matter affect the measurement. It is unusual to measure Secchi depth in or near a macrophyte canopy. If macrophytes are present the traditional Secchi depth/chlorophyll-*a*/total phosphorous relationships do not hold. Because Secchi depth is easily measured, a substantial amount of Secchi depths data exist for Holland Lake. The data collected by the Metropolitan Council and the MNDNR contain Secchi depth transparencies in the deep subbasin of Holland Lake. Secchi depth normally corresponds to a depth where approximately 10% of surface light is still present [Wetzel, 1983]. In eutrophic lakes, it corresponds approximately to one third of the depth of the photic zone (1% of surface light). Figure 11 shows that the Secchi depth in Holland Lake peaks in spring and drops to its minimum in summer. However, the seasonal pattern varies somewhat from one

year to another. From 1983 to 1985, the summer Secchi depth was at its lowest, which could have been due to storm runoff discharge into the lake. From 1983 to 1984, there was an approximate 21% increase in the phosphorus concentration at the lake surface which caused a 65% increase in algal abundance [Osgood, 1985]. This substantial response decreased the water clarity from 1983 to 1984. In 1985, the Secchi depth was less than 2 ft (0.6 m), which corresponds to the transparency of eutrophic lakes. In 1988, after the City of Eagan had stopped discharging storm runoff into the lake, the Secchi depth increased to 5 ft (1.5 m) in summer. The most transparent conditions in the deep subbasin on record occurred in summer of 1993 when Secchi depth did not drop below 9 ft (2.7 m). In the summer of 1999, Secchi depth fluctuated between the values of 1988 and 1993. Based on the Secchi disk transparency measurements Holland Lake has been considered a mesotrophic lake, since 1988.

The Secchi disk transparency data collected in 1999 (Figure 12) were measured at the locations of the three rafts. The Secchi depth at raft 3 was frequently affected by the vicinity of macrophytes and does not necessarily represent the entire shallow subbasin, because macrophytes were not uniformly distributed over the entire subbasin. Similar trends in both the deep subbasin and the shallow subbasin are evident in Figure 12. Smaller Secchi depths in the shallow subbasin (at raft 3) from late July to early September correspond to the growth of a dense vegetation in that subbasin (Figure 13) and larger Secchi depths in late September and October correspond to the decay of the dense vegetation. Figure 13 displays the approximate distribution of the dense vegetation in the eastern shallow subbasin on four days of site observations.

An empirical relationship between the Secchi depth and the attenuation coefficient [Poole and Atkins, 1929; Idso and Gilbert, 1974] adapted to Minnesota Lakes [Hondzo and Stefan, 1993] is

$$\eta = \frac{1.84}{z_s} \quad (1)$$

It has been used to plot the values of  $\eta$  in Figure 12. In equation 1,  $\eta$  is the attenuation coefficient ( $\text{ft}^{-1}$ ) and  $z_s$  is the Secchi depth (ft). The deep subbasin attenuation coefficient varies from 0.2 to 0.4  $\text{ft}^{-1}$  throughout the summer and early fall. In the shallow subbasin, during the same period, the attenuation coefficient varies within a significantly larger range (0.2 to 0.7  $\text{ft}^{-1}$ ). The stronger light attenuation coefficient (0.7  $\text{ft}^{-1}$ ) is due to the presence of macrophytes.

The attenuation coefficients obtained from the measured PAR (photosynthetically active radiation) profiles in the deep subbasin are in agreement with those estimated from the Secchi depths (Figure 14). The PAR profiles in the deep subbasin show that the photic depth is about 18 ft (5.4 m). Consequently, it is unlikely to have any significant photosynthetic oxygen production below 18 ft (5.4 m) in the deep subbasin.

The light attenuation in the deep subbasin is due to the presence of phytoplankton populations. Figure 15 illustrates the chl-*a* profiles in Holland Lake. The chl-*a* concentration varies between 5 to 8 mg/l in the epilimnion. There are several spikes in the metalimnetic chl-*a*. The presence of these spikes cannot be well explained. The largest spike is at the 16 ft depth and could be due to plant material imported from the

shallow subbasins. Spikes in the chl-*a* profile at greater depths (24 ft and 30 ft) are possibly associated with bacteria. Some types of microbial organisms show up in the chl-*a* test, but do not photosynthesize and are only oxygen sinks in the water column. The persistently higher DO values in the lower stratum of the metalimnion at 20 to 30 ft depth (Figure 5b and Figure C1 in Appendix C) can therefore not be due to photosynthesis because the photic depth is less than 20 ft.

To quantify the effects of macrophytes in the shallow subbasins on light attenuation, nine locations for PAR measurements were chosen (Figure 4). Based on the abundance of vegetation (macrophytes) they were categorized as: no visible vegetation, decaying vegetation and dense vegetation (Figure 16). Not surprisingly, the PAR profiles in areas with decaying vegetation or dense vegetation did not follow the typical exponential relationship [Wetzel, 1983]. In areas with dense vegetation, there was almost no light below 4 ft (1.2 m). The photic depth in the areas with decaying vegetation was about 7 ft (2.1 m). The attenuation coefficient varied with depth by an order of magnitude (from 0.18 ft<sup>-1</sup> to 1.8 ft<sup>-1</sup>) in the shallow subbasins (Figure 17). Average attenuation coefficients were defined by the Beer-Lambert law

$$\eta = \frac{\ln I_0 - \ln I_z}{z} \quad (2)$$

where  $I_0$  and  $I_z$  are PAR values right below the surface and at depth  $z$ , respectively. Equation 2 gives average values of the attenuation coefficient  $\eta$  over depth  $z$ . The values in Figure 17a were calculated using the data in Figure 16 and equation (2) for each location, and then averaging the estimated attenuation coefficients at each depth for a vegetation category. Figure 17b gives the local attenuation coefficients at each depth.

The site observations and the PAR measurements show that as some types of macrophytes grow towards the water surface, other macrophytes or phytoplankton residing in deeper areas do not receive enough light for continued photosynthesis. They become senescent and eventually must die and decay. An increase in the attenuation coefficient at a lower depth in the area with dense vegetation (Figure 17b) suggests that different types of macrophytes might be in those areas and one type is photo inhibiting the other types. The shorter plants are most likely senescent or dead over the time and hence a large source of oxygen demand (BOD).

The important conclusion of this part of the study is that light attenuation in the shallow subbasin is substantially stronger than in the deep subbasin. In summer photosynthesis in the shallow subbasins is therefore confined to a much more shallow photic zone (typically less than 10 ft deep) than in the deep subbasin. Below this depth plant material will senesce and become an oxygen sink.



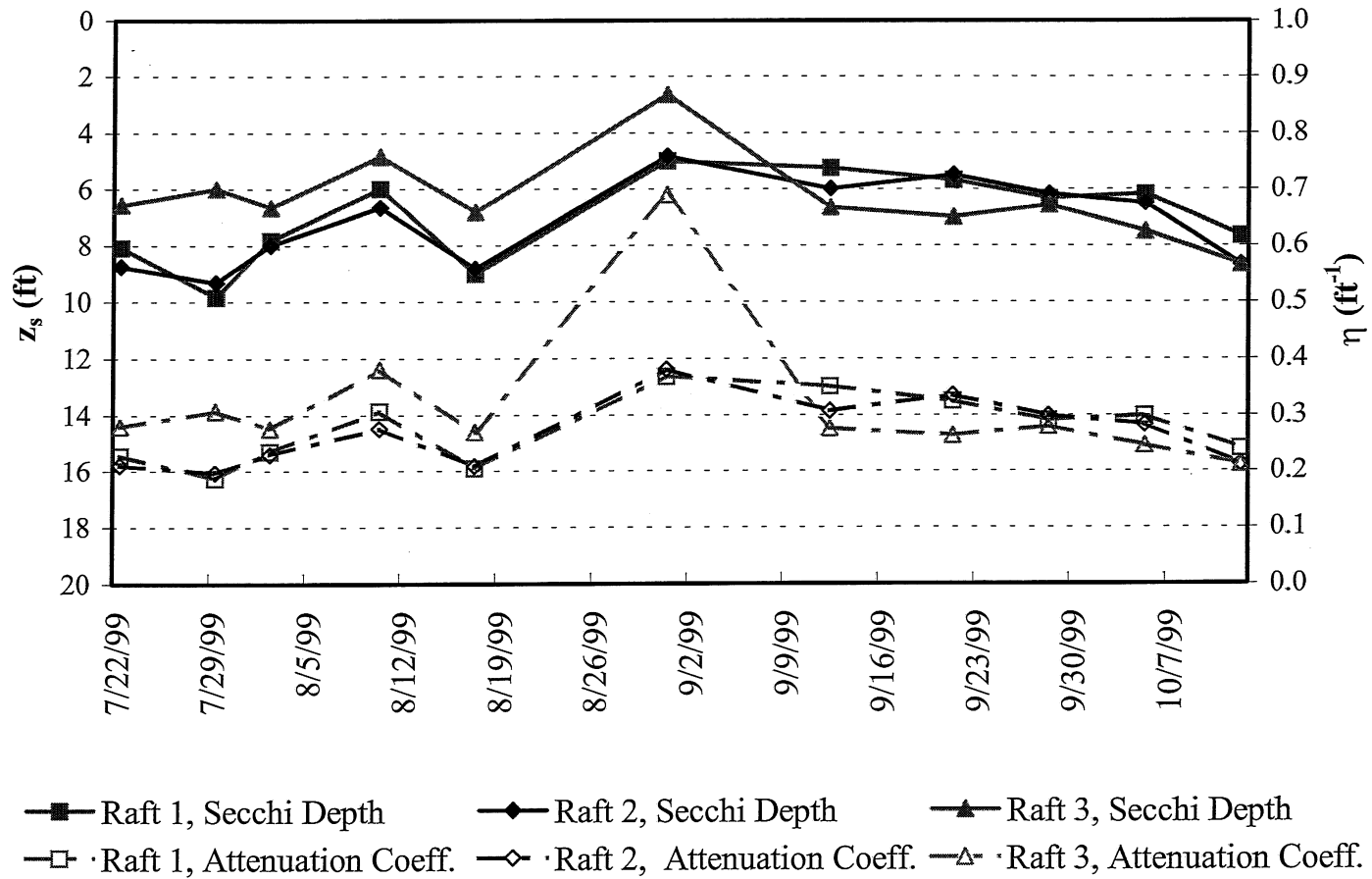


**Figure 12.** Measured Secchi depth transparency  $z_s$  and estimated coefficient of attenuation  $\eta$  in subbasins of Holland Lake.

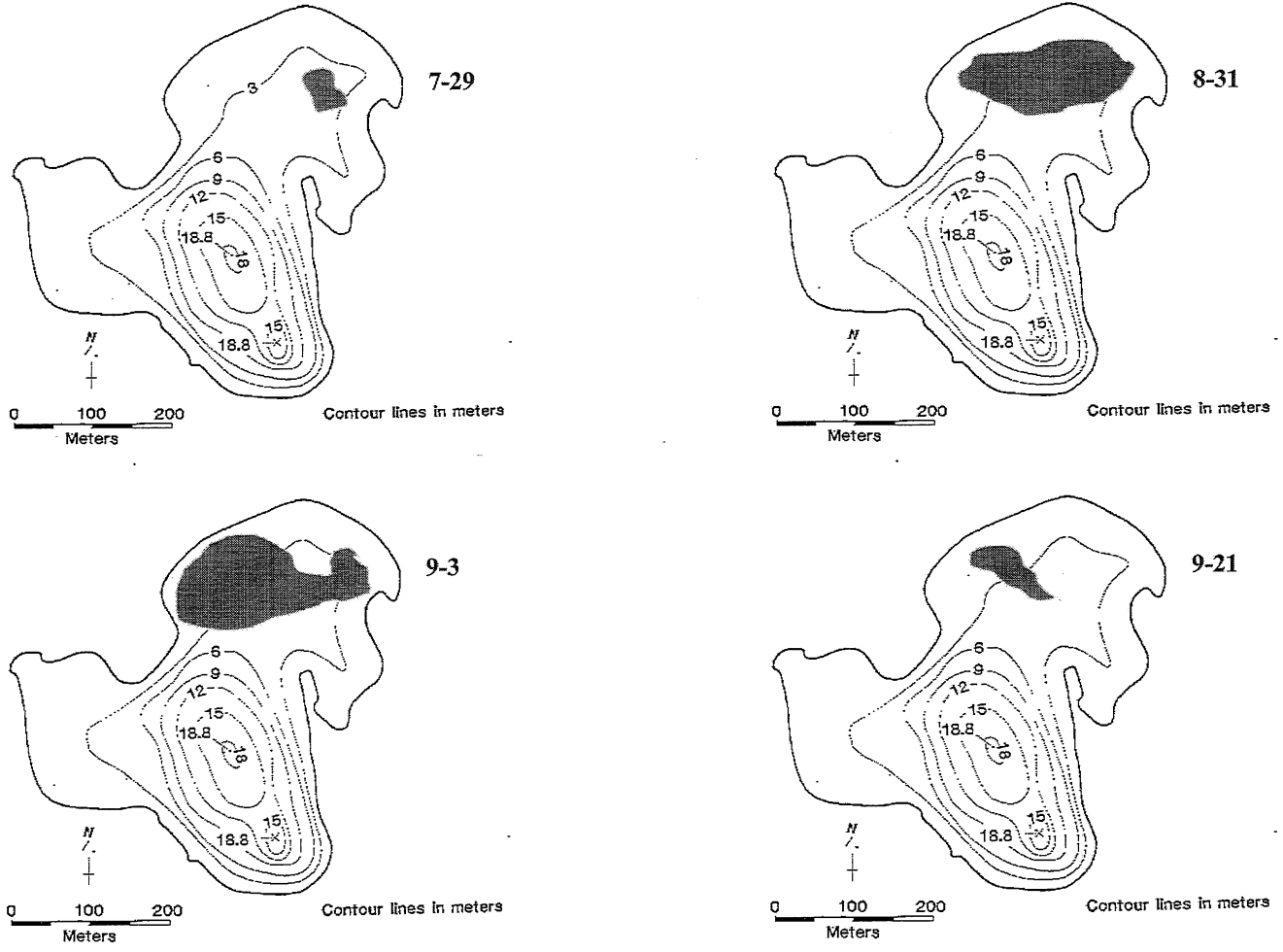
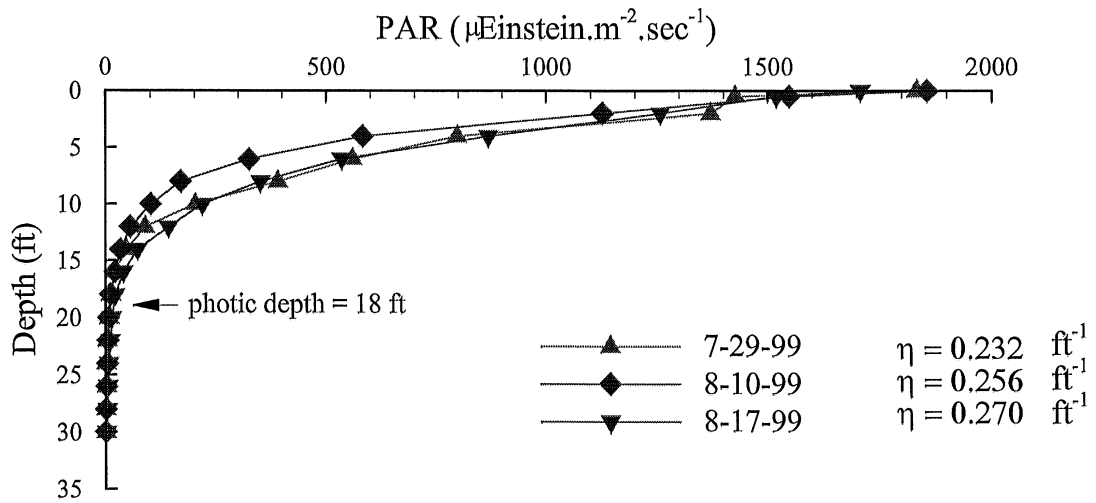
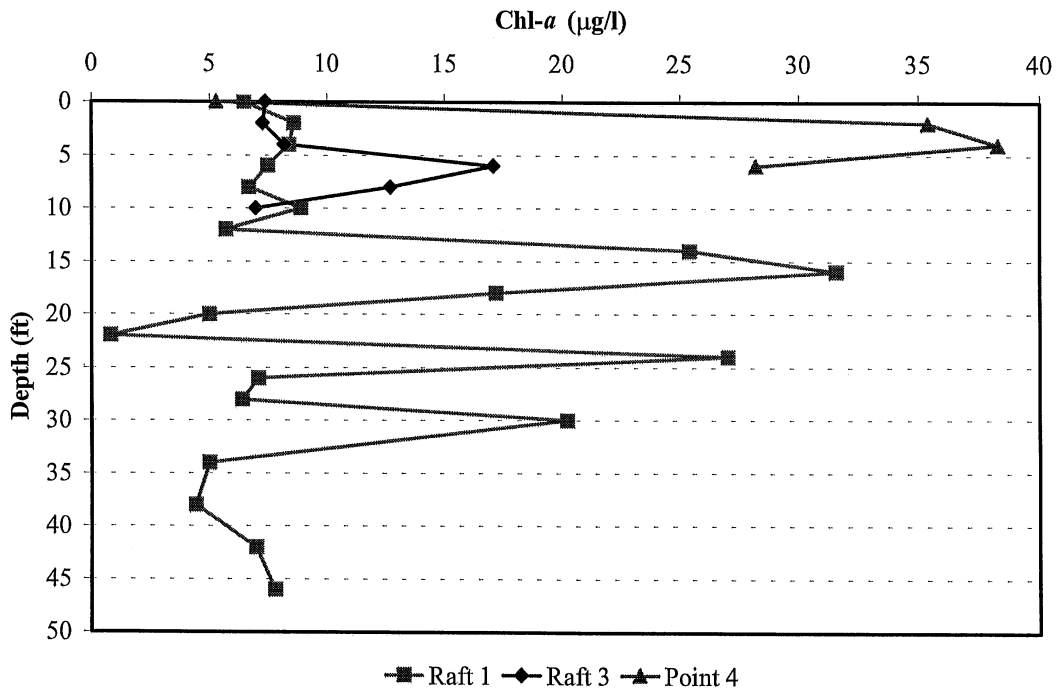


Figure 13. Areas (shaded) of dense macrophyte vegetation in the eastern shallow subbasin of Holland Lake in summer 1999.



**Figure 14.** Measured photosynthetically active radiation (PAR) in the deep subbasin of Holland Lake. The attenuation coefficients are estimated by fitting an exponential function to the three measurements.



**Figure 15.** Chlorophyll *a* (chl-*a*) concentration profiles measured on 8/23/1999 at three locations in Holland Lake. Point 4 was within the smaller (western) shallow subbasin (Figure 4).

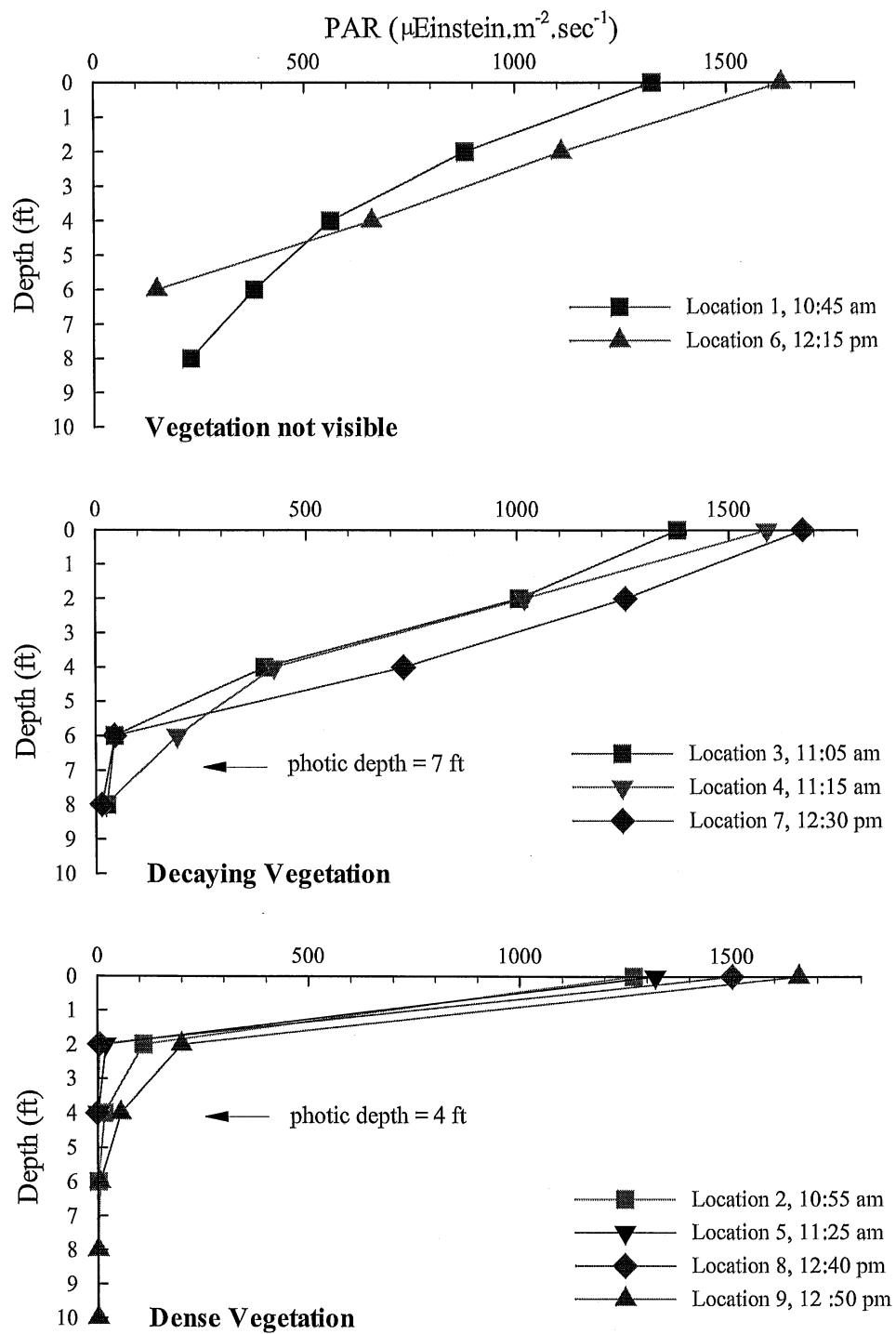


**Figure 16.** Measured photosynthetically active radiation (PAR) in the shallow subbasins of Holland Lake. The locations of the measurements are shown in Figure 4.

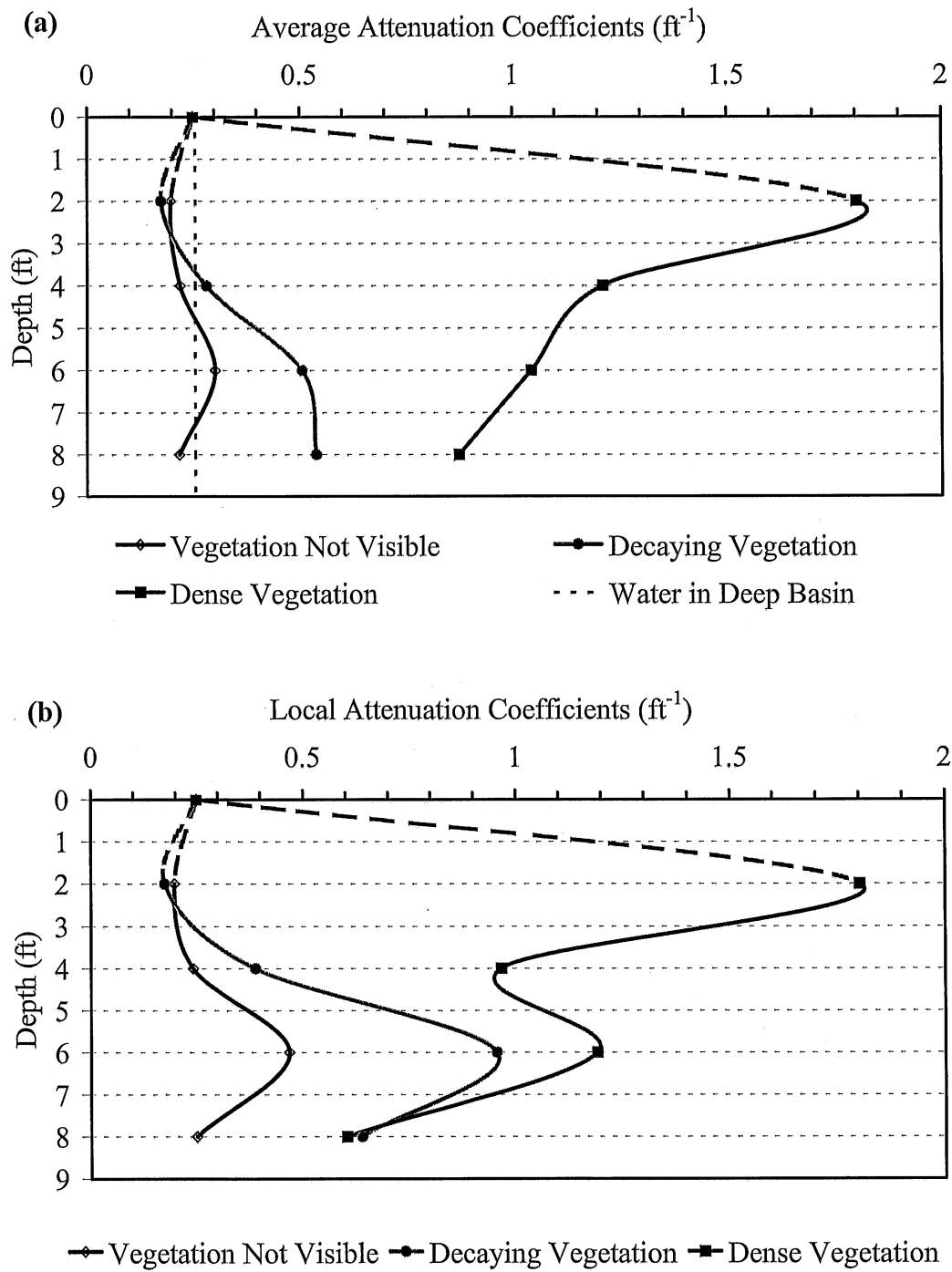


**Figure 17.** Attenuation coefficients  $\eta$  estimated at different depths in the shallow subbasins of Holland Lake. The dashed lines are hypothetical extrapolations.

## VI.2. Respiration

To identify and quantify the potential sinks of oxygen at any given depth, water samples along a lake water column were collected as explained in section IV.4. The parameters related to respiration and measured in the water samples were: total suspended solids (TSS), total volatile suspended solids (TVSS), total organic carbon (TOC), chlorophyll *a* (chl-*a*), and phaeophytin (PHY). Respiration rates were also measured directly by incubation of water samples at different depths as described in section IV.4.

### VI.2.1. Total Suspended Solids (TSS)

Figure 18 displays the vertical distribution of TSS in the deep subbasin and the two shallow subbasins. In the deep subbasin, the TSS concentrations vary from 1 to 3 mg/l at most depths. However, substantially larger values were measured in samples from 12 to 18 ft depth and below 38 ft depth. The spike in the upper stratum of the metalimnion (from a depth of 10 to 20 ft) is at a depth that has the largest temperature gradients. The 10 to 20 ft layer is also where the maximum chl-*a* concentrations (Figure 15) and the highest oxygen depletion rates had been observed (Figure 8). The high TSS in the deepest part of the lake may be due to the resuspension of bed materials.

### VI.2.2. Total Volatile Suspended Solids (TVSS)

The water sample analyses show that about 76% of the TSS were volatile (Figure 19). The non-volatile residue of 24% is typical of organic material. This indicates that most if not all TSS is organic material, i.e. phytoplankton and detritus. This is plausible since runoff from the watershed is small, and any inorganic and therefore heavier material would settle out near the periphery of the lake and not reach the deep subbasin.

### VI.2.3. Total Organic Carbon (TOC)

Total organic carbon (TOC) profiles were also measured in Holland Lake (Figure 20). The range of TOC in natural waters is 1 to 30 mg/l [Wetzel, 1983]; higher values are encountered in polluted environments. Based on Figure 20, the deep subbasin of Holland Lake has a relatively uniform TOC concentration of about 7 mg/l along the water column. The profile, however, shows a weak spike at 16 ft depth of about 9 mg/l. The TOC is larger in the upper strata (10 to 20 ft) of the metalimnion than in any other thermal region of the lake. Comparing the TVSS profile with the TOC profile shows that the higher concentration of TOC at 16 ft depth is also found in the TVSS.

TOC comprises both dissolved (DOC) and particulate organic carbon (POC). Since only a fraction of the TVSS is POC, and since TVSS is much less than TOC, a very large portion of the organic carbon in Holland lake has to be in the dissolved form. Meybeck [1982] studied 500 Wisconsin lakes and found a ratio of 11 to 1 between dissolved organic matter and particulate organic matter, respectively. Since a large fraction of the organic matter is carbon, 11:1 might also be the approximate ratio between DOC and POC in Holland Lake.

Dissolved organic carbon (DOC) mainly originates from macrophytes, algae and the decomposition of dead organic material. Typically detrital DOC exceeds by many times the live DOC in the form of bacteria. Consequently, it can be expected that a significant fraction of the measured TOC is detrital DOC. In brief, since DOC is larger than POC, DOC is likely the main oxygen sink in the deep subbasin water column. However, in the upper stratum of the metalimnion (10 to 20 ft depths), where the high DO uptake is of concern additional POC is present (Figure 19).

The water samples for the TOC analysis were collected four days earlier than those for the TSS and the TVSS analyses. The correlation coefficient (Table 1) between TOC and TSS (or TOC and TVSS) in the hypolimnion and the lower strata of metalimnion (depths larger than 20 ft) is 0.88 or better, which indicates a strong relationship among those water quality parameters. The high correlation coefficients suggest that the upward or downward movement of particulate matter is very slow and insignificant within a four-day period. However, small and negative correlations at the 10 to 20 ft depths (Table 1) may be attributed to the four-day difference between collecting the water samples for the TOC analyses and the TSS/TVSS analyses. Water movements induced by changes in weather conditions could make the particulate materials move one or two feet upward or downward within the thermocline.

By stoichiometry, potential carbonaceous biological oxygen demand (CBOD) was estimated using the TOC profiles in the lake (Figure 21). The average CBOD is 18.7 mg/l, with a maximum of 24 mg/l at the 16 ft depth. Since the ratio of potential CBOD to the 5-day CBOD is about 1.2 [Chapra, 1997], the potential oxygen depletion rate (CBOD) is about  $3 \text{ mg.l}^{-1}.\text{day}^{-1}$  for the water column with a maximum of  $4 \text{ mg.l}^{-1}.\text{day}^{-1}$  at the 16 ft depth. This is an upper limit for the oxygen depletion rate in Holland Lake.

#### VI.2.4. Phaeophytin

The laboratory analyses gave also phaeophytin profiles in the lake (Figure 22). Phaeophytin represents degraded chlorophyll. The phaeophytin profile has characteristics similar to those obtained for the TSS and the TVSS (Table 1), and particularly a spike within the upper stratum of the metalimnion (from 10 to 20 ft depth). More than  $10 \text{ }\mu\text{g/l}$  of phaeophytin within depths of 10 to 20 ft indicates the presence of substantial degraded plant material which is a significant oxygen sink within those depths.

If there is an influx of organic, oxidizable materials from the shallow subbasins into the deep subbasin, it must occur at depths of 10 to 20 ft because of the temperature stratification. Such fluxes are the most likely cause of spikes of 16 ft depth evident in the TSS, TVSS, TOC, chl-*a* and phaeophytin profiles. Some spikes at greater depths do not match, however. The chl-*a* profile (Figure 15) shows two other spikes, but only one of them (24 ft) can be identified in the other profiles. The spike in phaeophytin at the 30 ft depth cannot be explained by interactions among the subbasins. The phaeophytin profile also does not exactly follow the chl-*a* profile.

### VI.2.5. Potential Respiration Rates

The oxygen uptake rates calculated from DO profiles in section V.1 represented net bulk respiration rates. Those rates were, however, limited by the frequency of the DO profile measurements. It was desirable to measure potential respiration rates directly and in situ. Total potential respiration rates were measured directly in Holland Lake by incubation of water samples at 11 depths in the deep subbasin, and three depths in the eastern shallow subbasin. Total respiration rates measured in this way include phytoplankton (plant) oxygen uptake, microbial decomposition of detritus and biochemical oxidation of DOC. The samples were left at the depths where they were obtained for a 5 day period (9/16-9/21). This procedure kept the samples' water temperatures at the water temperatures in the lake. All bottles were wrapped with aluminum foil to prevent any photosynthetic oxygen production. The direct measurements of respiration were done a month after the water samples collected for the TOC or the TSS analyses. The results show (Figure 23) that despite a one month difference between the two experiments, the largest respiration rate, or oxygen sink is the upper stratum of the metalimnion, which was also where the maxima for TOC and TSS had been observed.

The average respiration rate in the deep subbasin was  $0.25 \text{ mg.l}^{-1}.\text{day}^{-1}$  with a maximum of  $0.52 \text{ mg.l}^{-1}.\text{day}^{-1}$  at a depth of 17 ft. Samples with more visible particulate matter content exhibited a higher rate of respiration. The respiration rate at 20 to 25 ft depths is significantly lower ( $0.1 \text{ mg.l}^{-1}.\text{day}^{-1}$ ). However, another peak in the respiration rate profile ( $0.3 \text{ mg.l}^{-1}.\text{day}^{-1}$ ) is evident at the 27 ft depth, where a secondary spike was also observed in the TSS, TVSS, TOC, chl-*a* and phaeophytin profiles.

The profile (Figure 23) also shows a data point greater than zero, at the 30 ft depth. Since there was not enough light for photosynthesis at that depth, this is believed to be in error.

To investigate whether live plant (phytoplankton) respiration made a significant contribution to total respiration, the chl-*a* profile in Figure 15 was correlated with the total respiration profile shown in Figure 23. Respiration due to chl-*a* was estimated as follows

$$R = a_{op} \mu_R 1.08^{(T-20)} P \quad (3)$$

where  $R$  is the respiration rate in  $\text{mg.l}^{-1}.\text{day}^{-1}$ ,  $a_{op}$  is the  $\text{mg DO}/\mu\text{g chl-}a$  produced, which varies from 0.133 to 0.267,  $\mu_R$  is a coefficient with a range of 0.05-0.25  $\text{day}^{-1}$  [Thomann and Mueller, 1987],  $T$  is the water temperature in  $^{\circ}\text{C}$ , and  $P$  is the concentration of phaeophytin-corrected chl-*a* in  $\mu\text{g.l}^{-1}$ . In Figure 24, the estimated respiration rates due to chl-*a* using minimum and maximum  $a_{op}$  and  $\mu_R$ , have been plotted next to the total respiration rates measured in Holland Lake. The water temperatures used in equation 2 were obtained from the water temperature data measured on September 21, however, the  $P$  values were obtained from the chl-*a* profile measured on August 23. Interestingly, the profiles' shapes are very similar although spikes at greater depths do not match. It is apparent that the estimated maximum chl-*a* respiration rates are unrealistic, but the estimated minimum chl-*a* respiration rates suggest that at least 30% of total respiration in Holland Lake is due to live organisms.



#### *VI.2.6. Summary of Oxygen Uptake Rates*

The overall results show that oxidization of particulate and dissolved organic matter plays an important role as an oxygen sink in the deep subbasin. All profiles, TSS, TVSS, TOC, chl-*a*, phaeophytin and total respiration rate exhibit a maximum in the upper part of the metalimnion (10 to 20 ft depth). The average CBOD gives a DO depletion rate of  $3 \text{ mg.l}^{-1} \text{ day}^{-1}$ , with a maximum of  $4 \text{ mg.l}^{-1} \text{ day}^{-1}$  in the upper stratum of the metalimnion if decay were to occur over 5 days. The total potential respiration rate was measured to be  $0.52 \text{ mg.l}^{-1} \text{ day}^{-1}$  ( $0.68 \text{ mg.l}^{-1} \text{ day}^{-1}$  with a 2-day measurement) within the same stratum, and the net rate of oxygen depletion is as high as  $0.47 \text{ mg.l}^{-1} \text{ day}^{-1}$  in mid summer. The CBOD value is an upper limit based on the amount of material in the water column. The DO depletion rate computed from the DO profiles gives net oxygen uptake but it's limited to the time interval between the DO profile measurements, therefore it may give an underestimated value for the oxygen uptake. The total potential respiration rate gives the oxygen uptake, when there is no oxygen production. However, the respiration rates measured in the incubated bottle was for a stagnant water, therefore, excluding the boundary layer effect on the oxygen uptake by detritus and algae. Consequently, for any aeration purposes all three numbers must be taken into account.

Due to the strong temperature gradient in the metalimnion, organic particulate matter floats in the thermocline and does not settle down until fall turnover. The question is why does the organic matter sit at a depth of 14 to 20 ft, and why is there a second influx of organic matter at a larger depth (25 to 27 ft).

**Table 1.** Correlation coefficients between the total suspended solids (TSS), total volatile suspended solids (TVSS), chlorophyll-a (chl-*a*), phaeophytin (PYT) and total organic carbon (TOC) in different strata.

<b>0-10'</b>	<b>chl-<i>a</i> (ppb)</b>	<b>PYT (ppb)</b>	<b>TSS (ppm)</b>	<b>TVSS (ppm)</b>
<b>PYT (ppb)</b>	0.26			
<b>TSS (ppm)</b>	-0.33	0.22		
<b>TVSS (ppm)</b>	-0.06	0.52	0.00	
<b>TOC</b>	0.29	-0.29	-0.34	-0.78
<b>10'-20'</b>	<b>chl-<i>a</i> (ppb)</b>	<b>PYT (ppb)</b>	<b>TSS (ppm)</b>	<b>TVSS (ppm)</b>
<b>PYT (ppb)</b>	0.78			
<b>TSS (ppm)</b>	0.74	0.76		
<b>TVSS (ppm)</b>	0.80	0.72	0.98	
<b>TOC</b>	0.31	-0.28	-0.29	-0.16
<b>20'-30'</b>	<b>chl-<i>a</i> (ppb)</b>	<b>PYT (ppb)</b>	<b>TSS (ppm)</b>	<b>TVSS (ppm)</b>
<b>PYT (ppb)</b>	-0.83			
<b>TSS (ppm)</b>	0.92	-0.78		
<b>TVSS (ppm)</b>	0.95	-0.78	0.97	
<b>TOC</b>	0.91	-0.55	0.88	0.92
<b>30'-46'</b>	<b>chl-<i>a</i> (ppb)</b>	<b>PYT (ppb)</b>	<b>TSS (ppm)</b>	<b>TVSS (ppm)</b>
<b>PYT (ppb)</b>	0.89			
<b>TSS (ppm)</b>	0.93	0.94		
<b>TVSS (ppm)</b>	0.93	0.93	1.00	
<b>TOC</b>	0.82	0.82	0.96	0.96

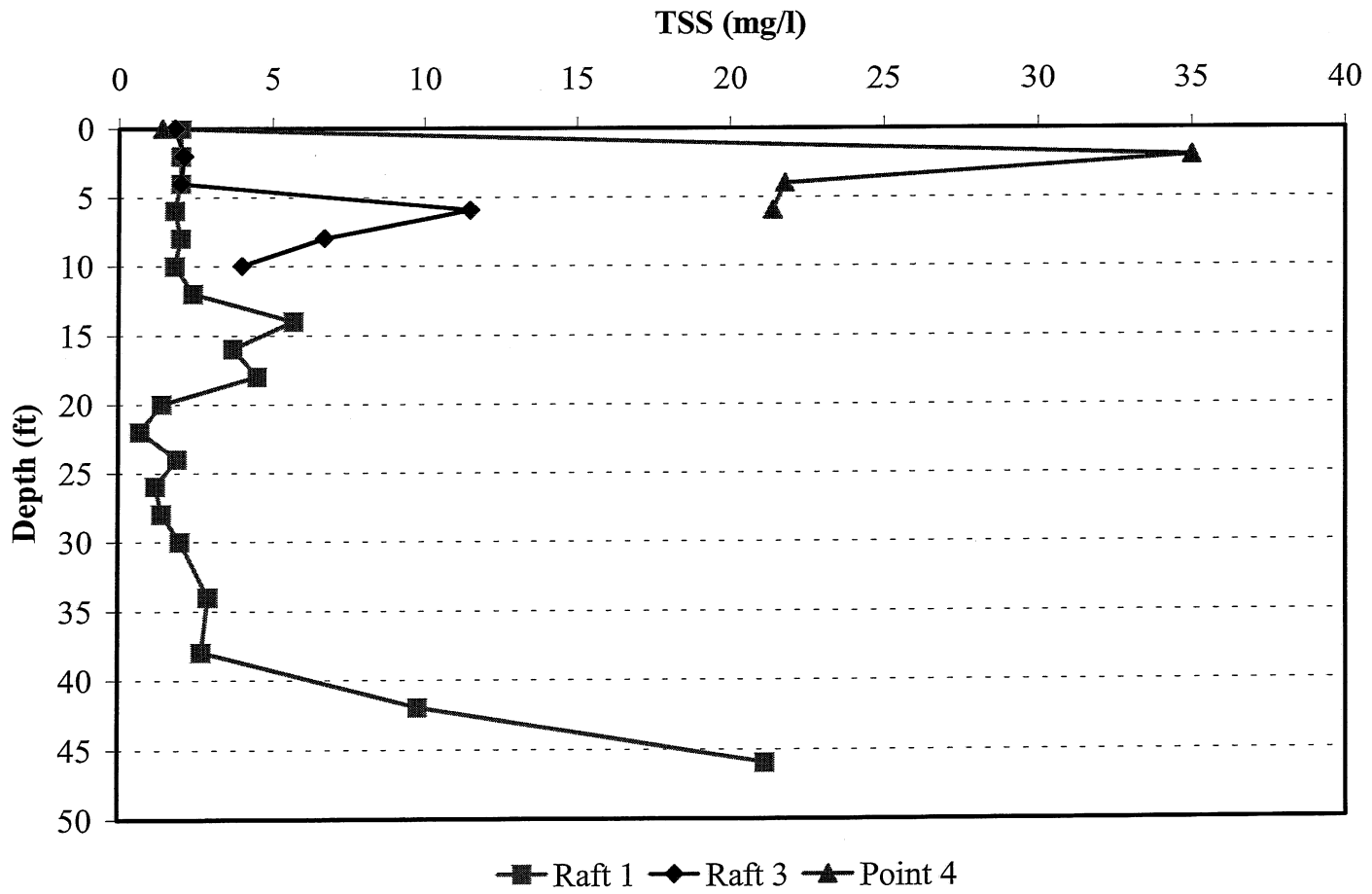
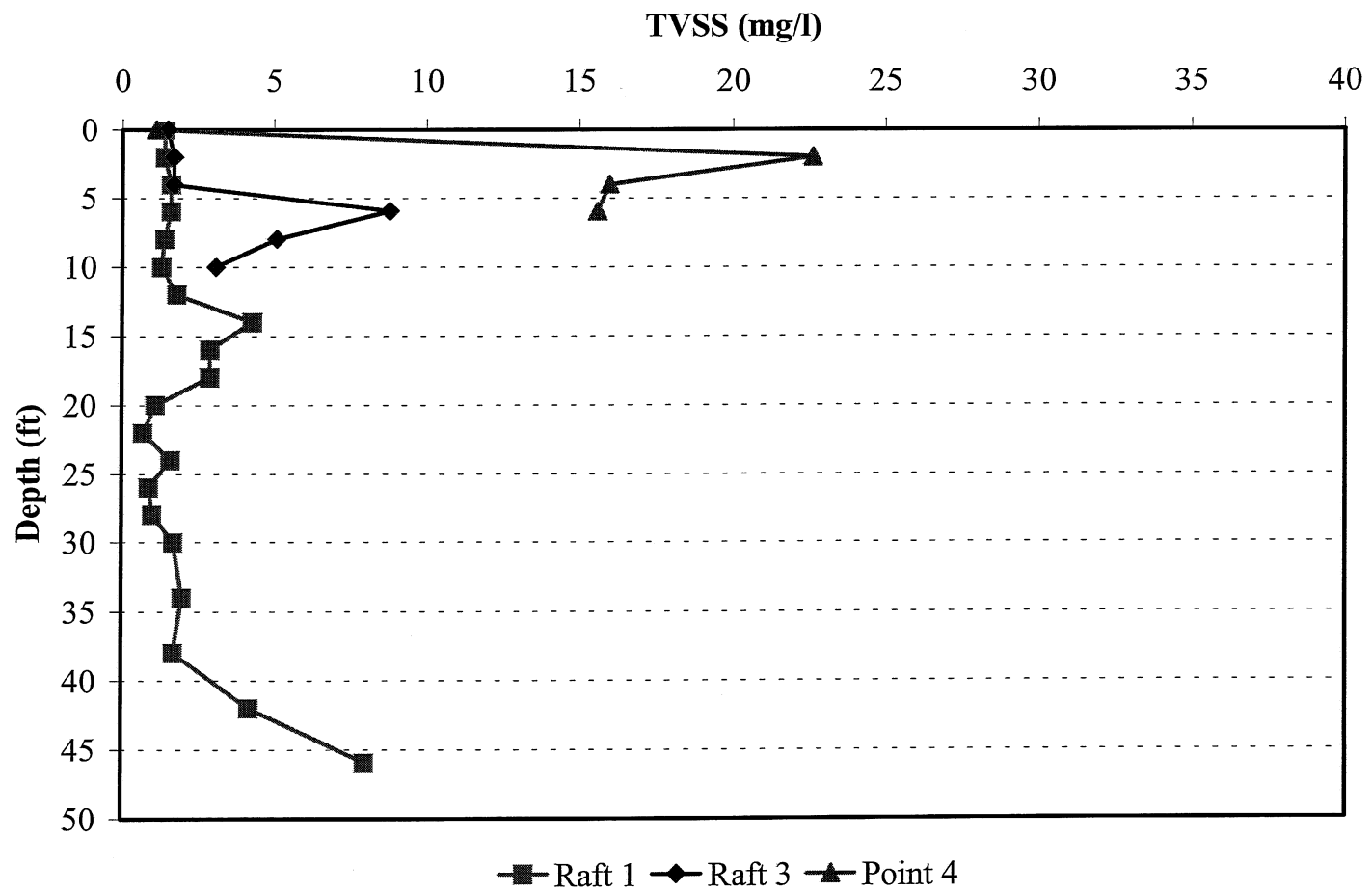
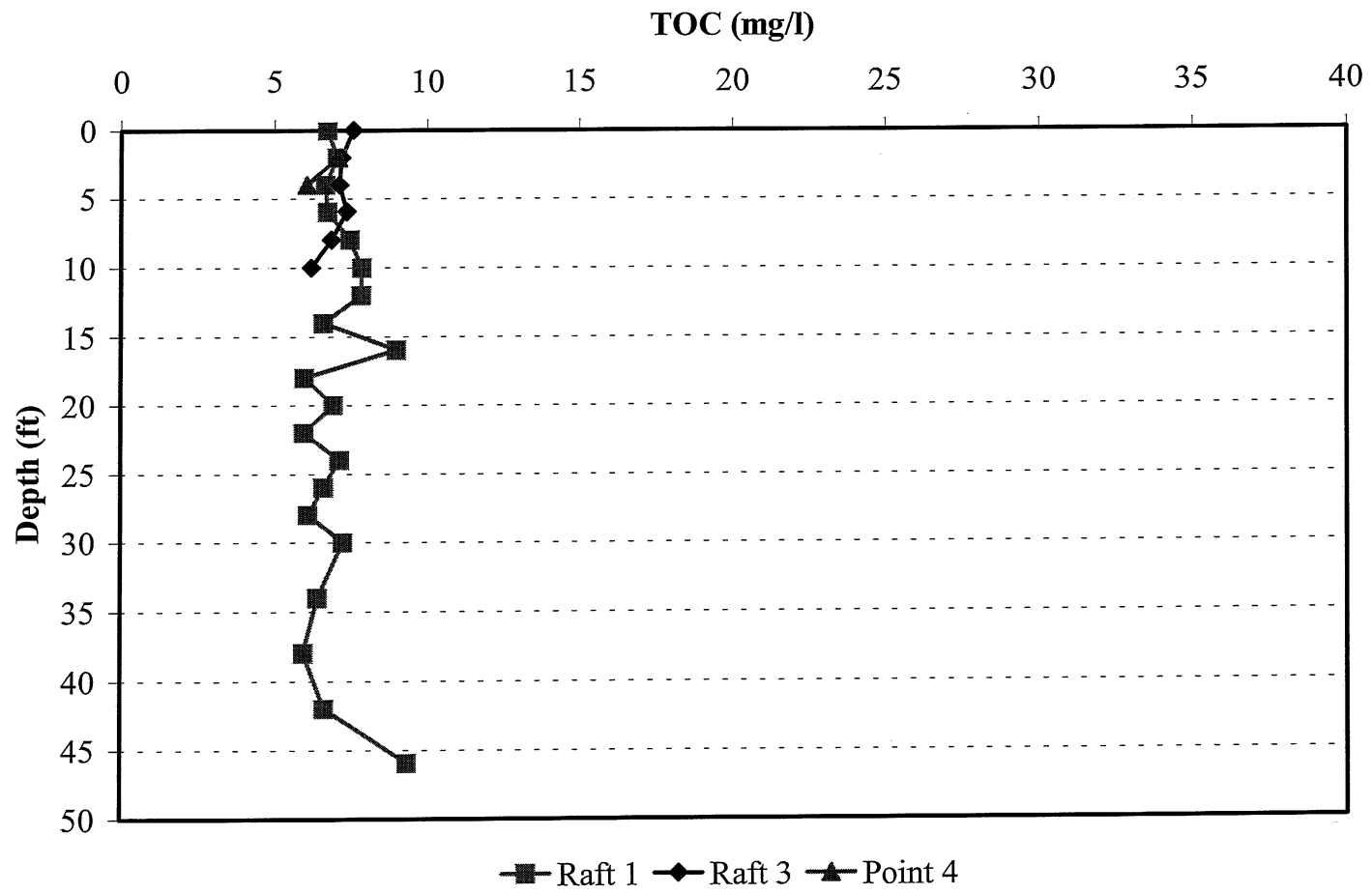


Figure 18. Total suspended solids (TSS) profiles measured at three locations in Holland Lake, 8/23/99.



**Figure 19.** Total volatile suspended solids (TVSS) profiles measured at three locations in Holland Lake, 8/23/99.



**Figure 20.** Total organic carbon (TOC) profiles measured at three locations in Holland Lake, 8/19/99.

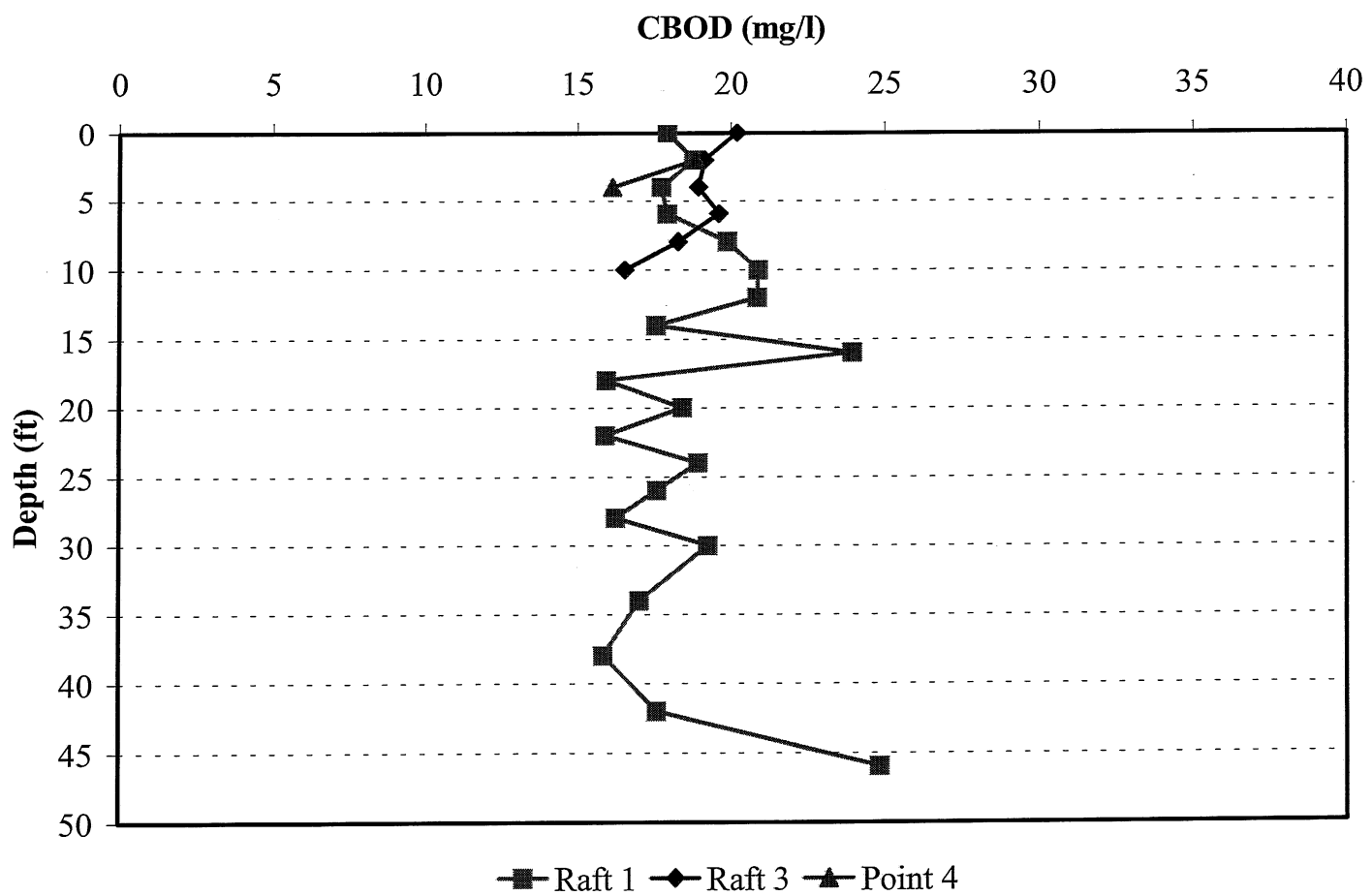


**Figure 21.** Carbonaceous biochemical oxygen demand (CBOD) profiles estimated from TOC at three locations in Holland Lake.

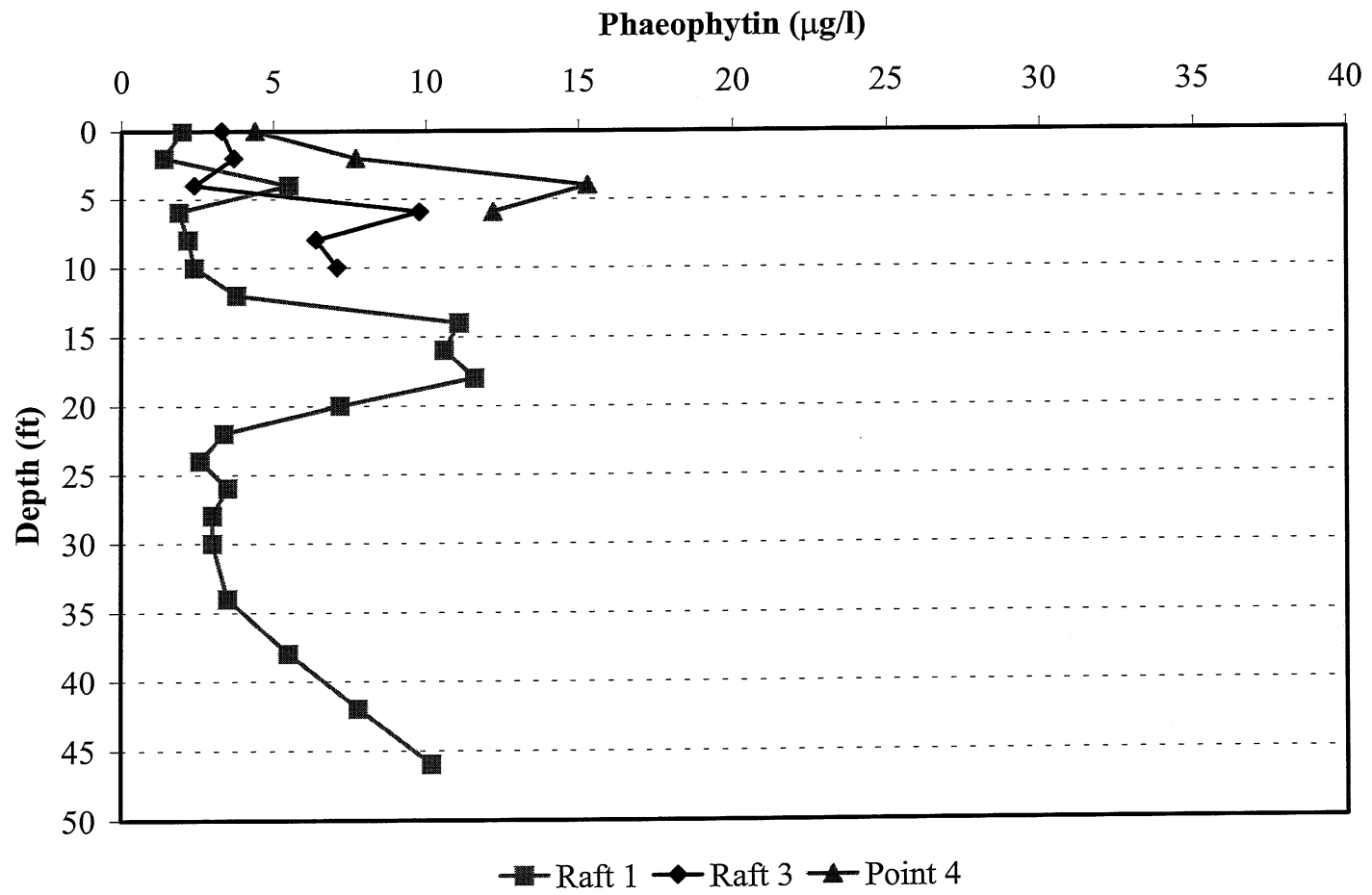
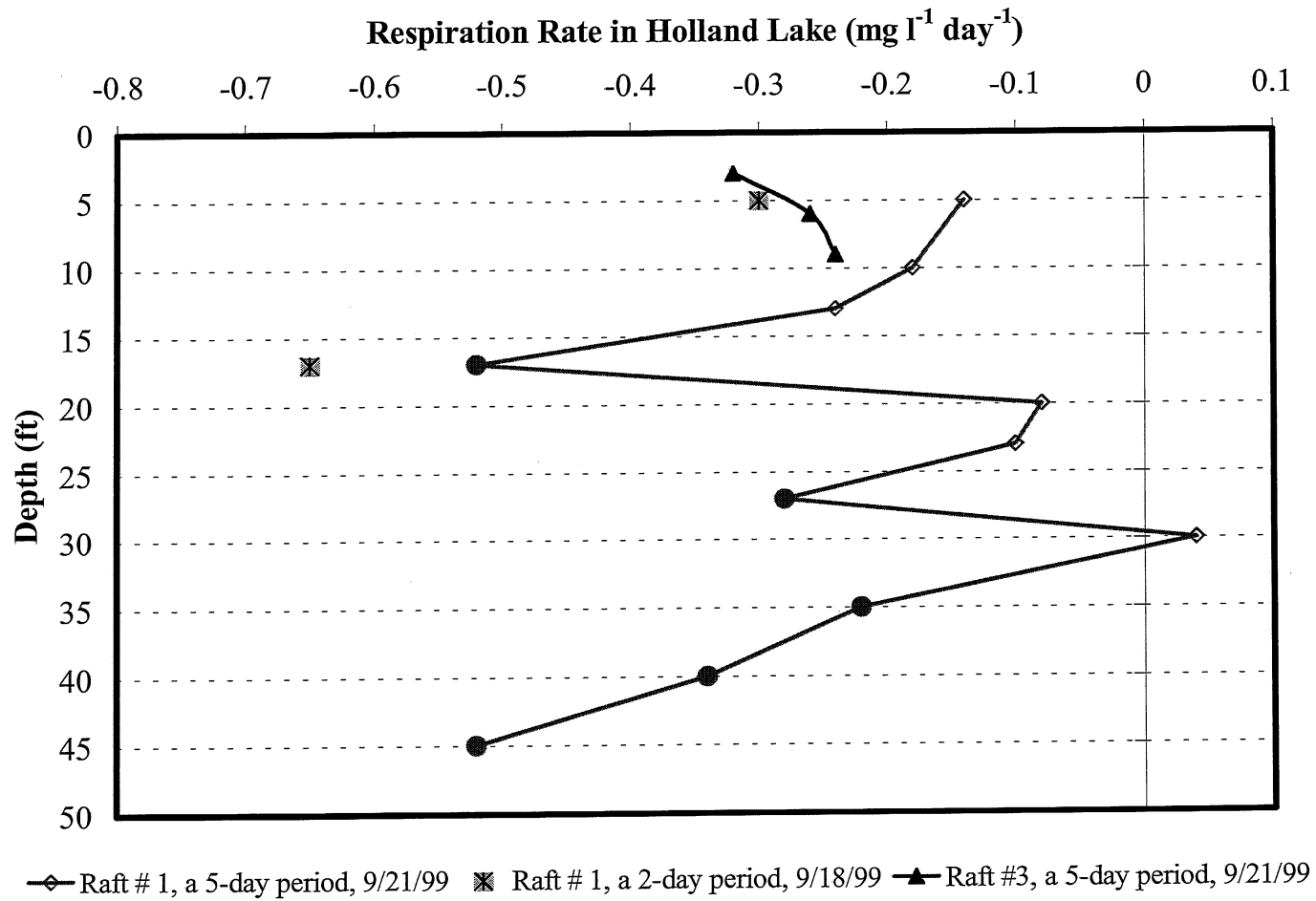
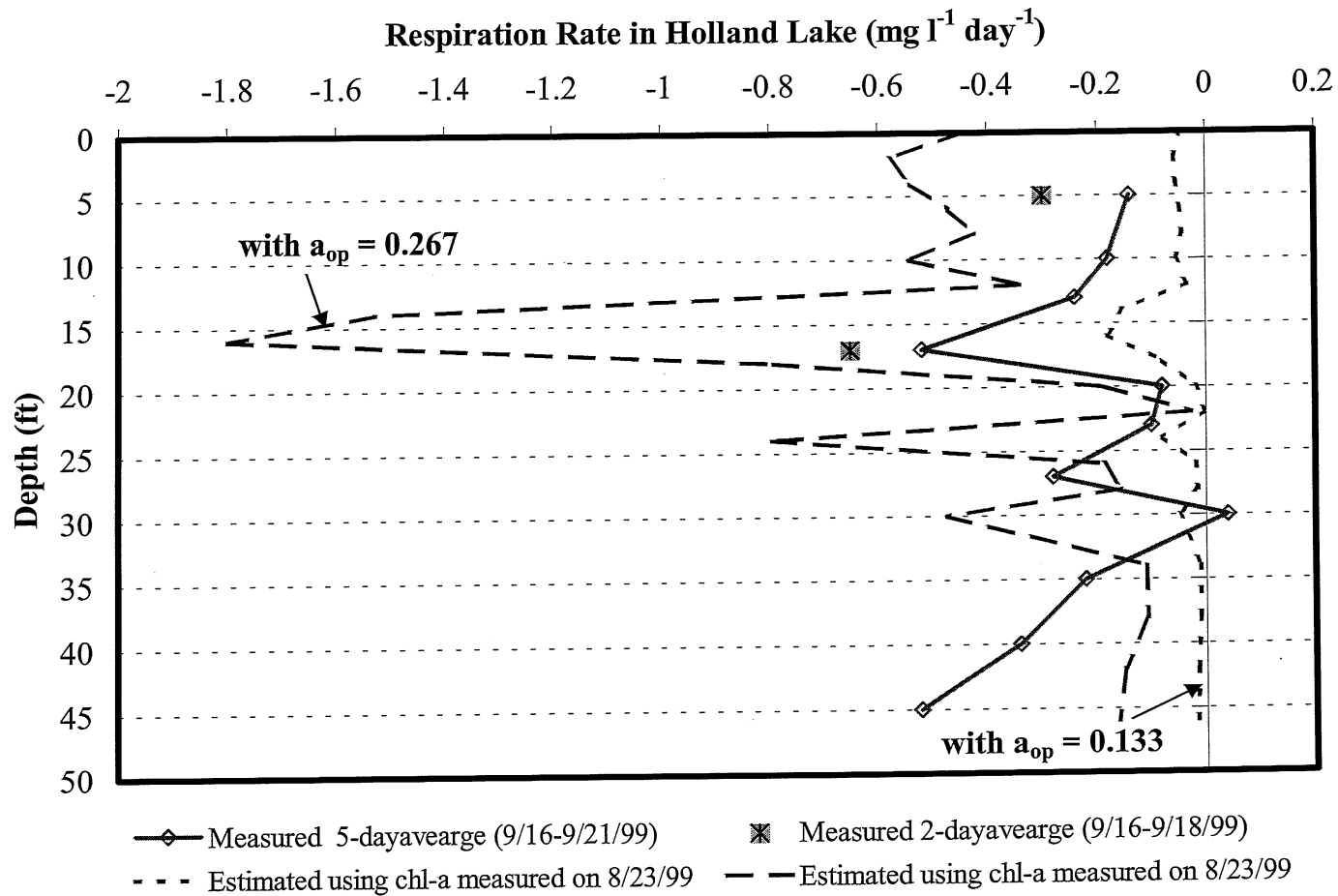


Figure 22. Phaeophytin concentration profiles measured at three locations in Holland Lake, 8/23/99.



**Figure 23.** Respiration rates measured in Holland Lake. The large filled circles identify samples with a significant content of particulate matter.





**Figure 24.** Measured and estimated respiration rates in Holland Lake. Solid line gives values measured on 9/21/99 by dark bottle incubation. Dashed lines are estimated respiration rates using the chl-*a* profile and the water temperature profiles measured on 8/23/99 and 9/19/99, respectively.

### VI.3. Sedimentary Oxygen Demand (SOD)

Lake sediments consist in general of organic matter in various stages of decomposition, particulate mineral matter, and an inorganic component of biogenic origin [Wetzel, 1983]. The oxygen uptake by sediments depends upon the amount of organic matter in the sediment and the nature of the benthic community. In deep water, nearly all metabolism is microbial. Microbial populations in the surficial sediment are important oxygen sinks that can be several orders of magnitude greater than in an equivalent weight of the overlying water. Hypolimnetic anoxia therefore occurs often in stratified lakes with high sediment oxygen demand (SOD).

Sedimentary oxygen demand (SOD) was not measured directly in Holland Lake. Oxygen depletion rates calculated from measured DO profiles in 2 to 10 ft layers include SOD since each layer is in contact with lake sediment. The total respiration rate measured near the bottom of the deep subbasin and presented in Figure 23 gives an idea of the magnitude of SOD. Referring to Figure 23, the total respiration rate at a depth of 45 ft was  $0.52 \text{ mg.l}^{-1}.\text{day}^{-1}$  (the water samples from the deepest part of the lake contained a significant amount of particulate matter). If this oxygen depletion rate were entirely attributed to SOD in the bottom-most 2 ft layer of the deep subbasin, the SOD, converted to 20 °C using

$$\text{SOD}_T = \text{SOD}_{20} \theta^{(T-20)} \quad (4)$$

would be  $0.9 \text{ g.m}^{-2}.\text{day}^{-1}$  (with an average value of 1.065 for  $\theta$ ).

SOD at the bottom of the shallow subbasins may vary more significantly throughout the year than the SOD in the deep subbasin. From the measured bulk respiration rate, an oxygen depletion rate (at 20 °C) in the bottom most 2 ft layer of the shallow subbasin was also estimated for the period from 9/16/1999 to 9/21/1999. Its value was  $0.2 \text{ g.m}^{-2}.\text{day}^{-1}$ , however, the total potential respiration rate measured in the bottom most 2 ft layer of the shallow subbasin does not necessarily represent the SOD in the shallow subbasin since macrophytes cover the sediment bed in the shallow subbasins. An estimate of mid-summer SOD in Holland Lake is probably 0.2 to  $1 \text{ g.m}^{-2}.\text{day}^{-1}$ .

#### VI.4. Hydrodynamic Transport

Mixing, i.e. vertical exchange of water by advection (flow), including internal waves, turbulence and wind-driven currents, was not measured directly. However, the stratification dynamics were documented by temperature profile time series at the three rafts (Figures 25 to 27). The data start on July 9 and end on October 12. Holland Lake is a monolithic lake with a strong stratification in summer. In summer 1999, there were several days with a 25 °C temperature difference from the bottom to the surface of the deep subbasin. The thermocline defined as point of maximum temperature gradient with vertical distance, was at 12 to 16 ft for most of the summer (Figure 25). The surface mixed layer in the deep subbasin, in July, was about 8 ft deep at night and became 2 to 4 ft deep in daytime. The surface mixed layer deepened down to 12 ft until mid-August and stayed at 12 ft until early September. By early October, the surface mixed layer became 20 ft deep with a temperature of about 15 °C. Until early September, the upper 12 ft of the lake was warmer than the maximum temperature tolerance (20 to 22 °C) of brown trout.

Although the shallow subbasins are less than 15 ft (4.5 m) deep, they are also stratified (Figure 27). Temperature stratification of the shallow subbasins may be affected by several factors: groundwater inflow with temperatures of about 10 to 15 °C, intrusion of cold water from the deep subbasin by internal wave motion, and the presence of dense macrophyte beds that attenuate incident solar radiation in the upper few feet of water and suppress vertical turbulent mixing. Some of these factors are evident in some traces in Figures 25 to 27. For instance, the water temperature for the months of July and August is about 1 °C colder at a depth of 12 ft in the shallow subbasin (Figure 27) than the temperature at a depth of 14 ft in the deep subbasin. This condition implies that there is no favorable condition for water from the deep subbasin to intrude into the shallow subbasin. The low bottom temperatures in the shallow subbasins imply that there is not enough energy available to warm up the colder water at the subbasin bed level. As discussed in section VI.1, macrophytes prevent light from penetrating the shallow subbasins. Therefore, there is not enough radiative heat input to increase the water temperature at the bed level. Mixing due to the kinetic energy produced by wind is not strong in Holland Lake due to two factors: the small size of the lake which does not allow a large fetch and the tall trees around it, which shelter the lake from strong winds. Continuous stratification evident in the deep subbasin (e.g. the temperature profiles in Figures 5b and 5c) is evidence of the limited wind effect on the surface mixed layer. In the shallow subbasins, a third factor is in effect: the presence of dense macrophytes, which dampen the kinetic energy, produced by wind. Consequently, the shallow subbasins exhibit a strong seasonal stratification. Another explanation is that there must be a source of cold water at the bottom of the shallow subbasin, which keeps the water temperatures low at 16 to 18 °C. This source is most likely groundwater.

Despite weak wind mixing in the lake, the signature of the wind effect is evident in the metalimnion and hypolimnion in the form of temperature oscillations (internal waves). The amplitudes of the internal waves cause substantial temperature changes during storm events. The largest amplitude of the temperature oscillations (internal waves) in the record (Figure 25) are due to a storm on July 26. The second largest

temperature oscillation occurred four days later on July 31. A heat wave (Figure 31), associated with a high dew point temperature (90% relative humidity) did not allow any significant evaporative cooling from the lake and the surface temperature increased to 34 °C, which may be a record.

The temperature time series below the surface mixed layer are significantly different in the shallow subbasin and in the deep subbasin. The difference is in the form and shape of the water temperature oscillations due to internal waves. The same large excursions in temperatures due to storms, as evident in the deep subbasin (Figures 25), are visible in the shallow subbasin temperature time series (Figure 27). However, during calm (no storm) periods, oscillations in the temperature time series have significantly smaller amplitudes in the shallow subbasins. This phenomenon is due to the presence of macrophytes in the shallow subbasins, which dampen the internal waves.

When water temperatures in the shallow subbasin are compared with those in the deep subbasin, it becomes evident that there must be a significant interaction between the basins. In July and August, the bottom temperature in the shallow subbasin is about 2 to 3 °C colder than at the same depths in the deep subbasin (Figures 28 and 30). This temperature difference must cause a density current from the shallow subbasins into the deep subbasin. The slope of the bed in the shallow subbasins is toward the deep subbasin, which helps this plunge flow. The current carries water from the shallow subbasins' sediment bed into a depth of 12 to 15 ft in the deep subbasin. The spikes evident in the TSS, TVSS, TOC, chl-*a* and phaeophytin at depths of 10 to 20 ft and more specifically at depths of 14 to 18 ft, are attributed to this process. The intrusion in July and August most likely moves detritus from the bottom of the shallow basins into the upper stratum of the metalimnion, where it depletes the oxygen content of the water. By late August, the temperature differences at depths of 10 to 12 ft in the subbasins reverse due to hypolimnetic warming. In late August and September, the surface mixed layer in the shallow subbasin is warmer than in the deep subbasin (Figures 25 and 27). Therefore, water from the surface mixed layer of the deep subbasin intrudes into the surface mixed layer of the shallow subbasin pushing out more water from the bottom of the shallow subbasin into the deep subbasin.

In summary, the bathymetry of the lake and the presence of macrophytes in the shallow subbasins help the shallow subbasins to stratify in early summer with relatively cold temperatures at their bed levels. These relatively cold water temperatures cause a density current into the deep subbasin, which probably transports a substantial amount of suspended solids and detritus into the upper stratum of the metalimnion in the deep subbasin. This material ultimately appears as a major oxygen sink with a high rate of DO depletion in that stratum.

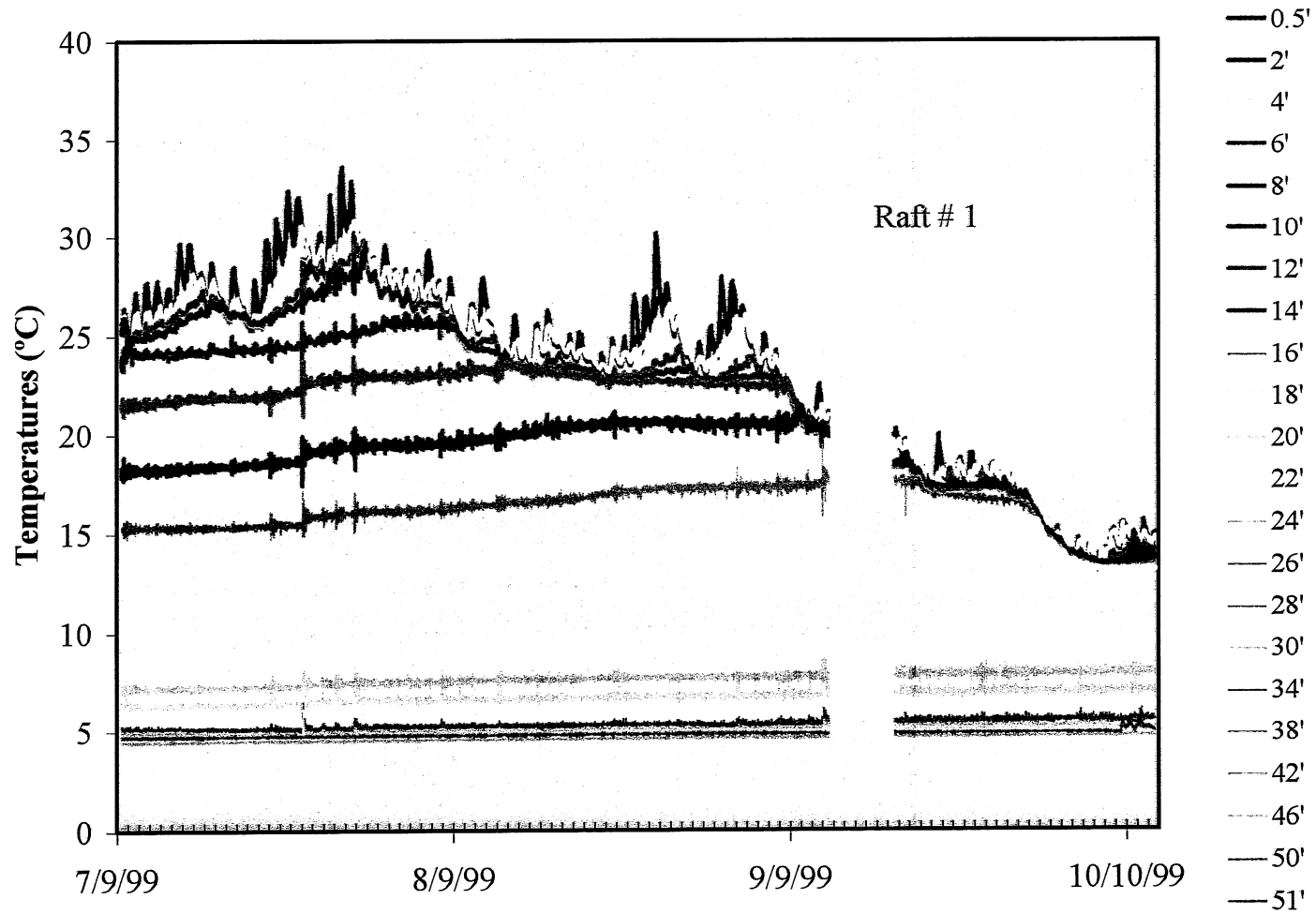


**Figure 25.** Temperature profile time series in the deep subbasin (raft # 1) of Holland Lake, summer 1999.

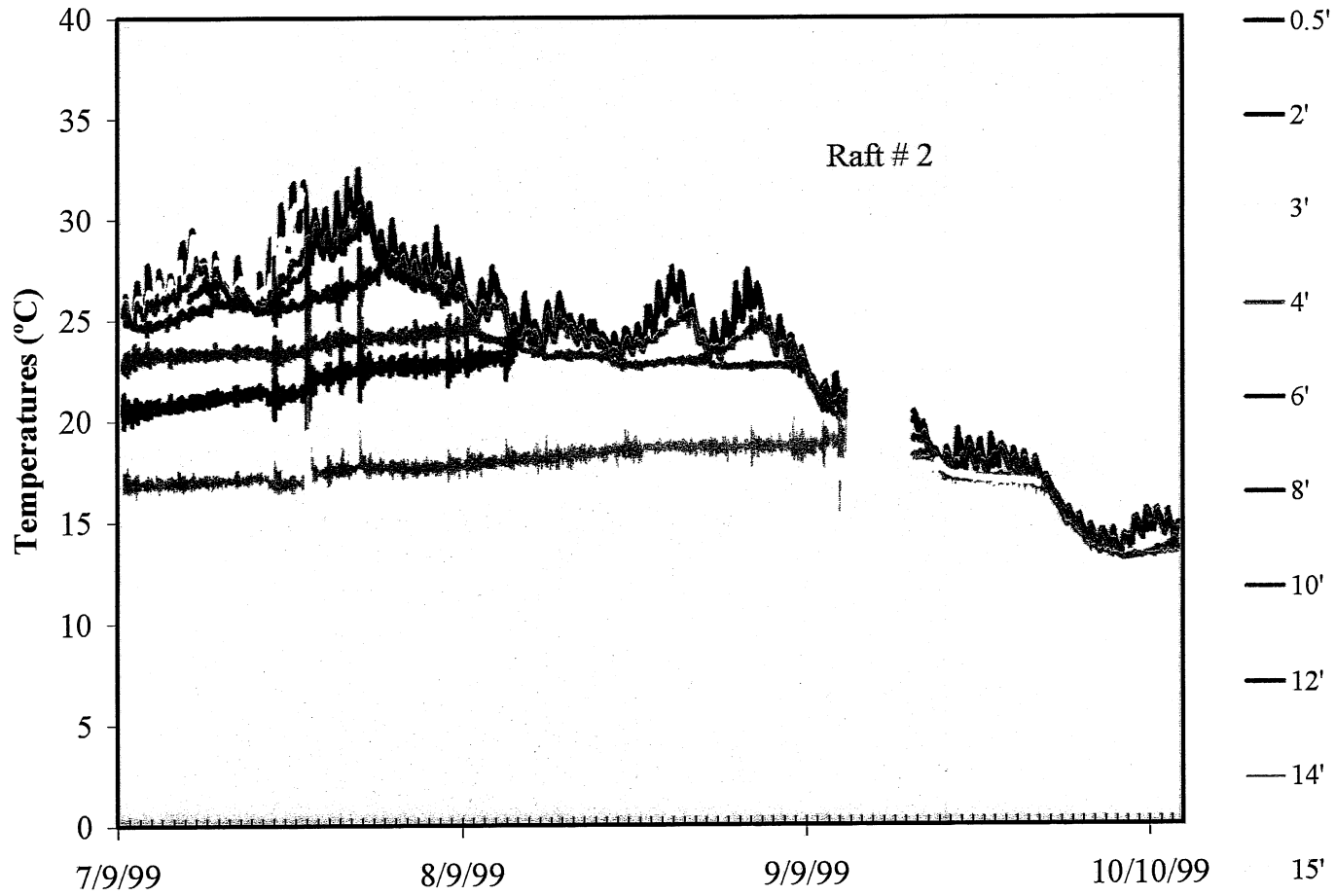


**Figure 26.** Temperature profile time series at the border of the deep subbasin and the eastern shallow subbasin of Holland Lake, summer 1999.

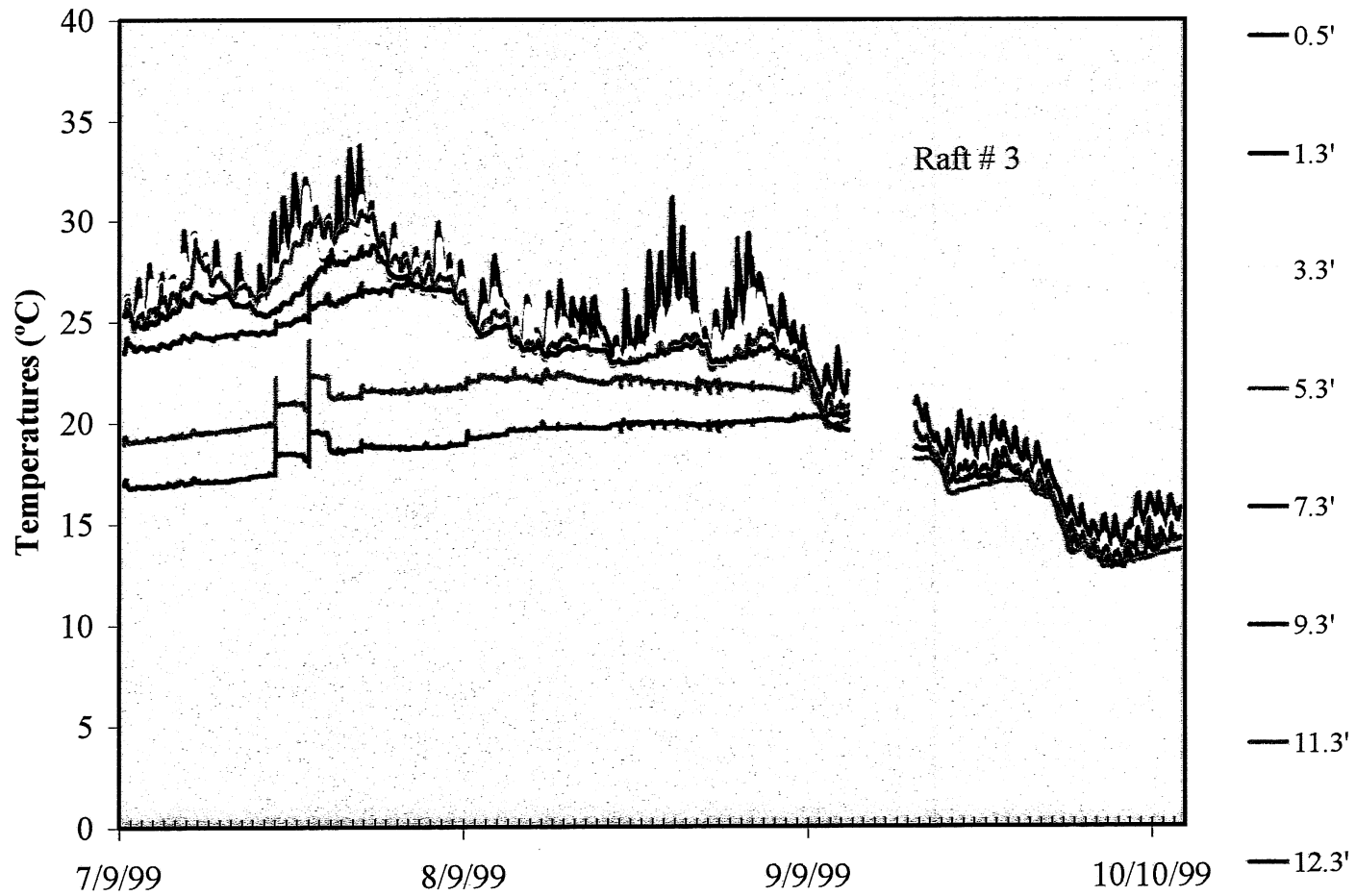


**Figure 27.** Temperature profile time series in the shallow subbasin of Holland lake, summer 1999.

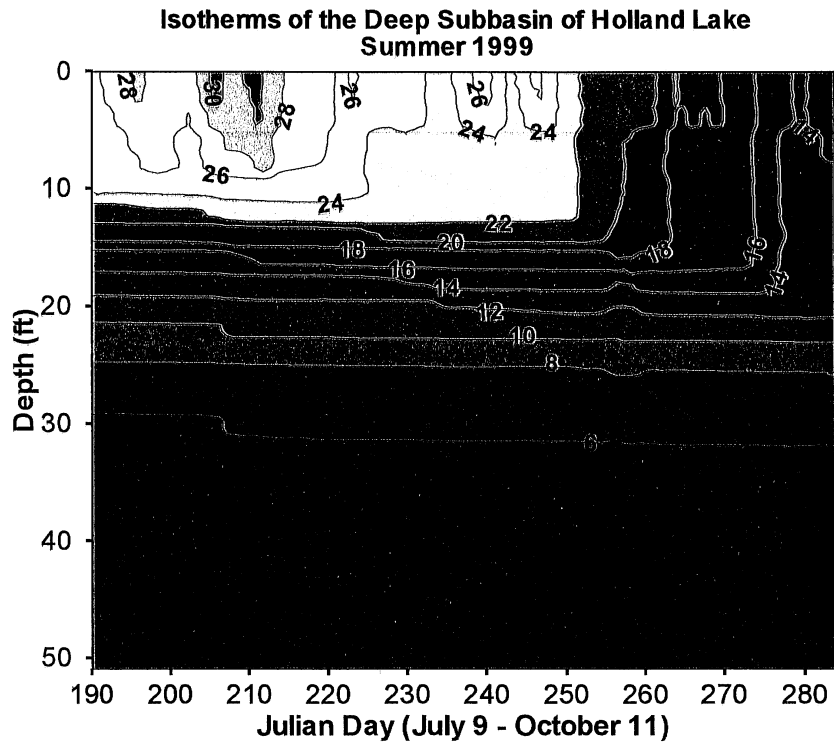


**Figure 28.** Isotherms of the deep subbasin of Holland Lake.



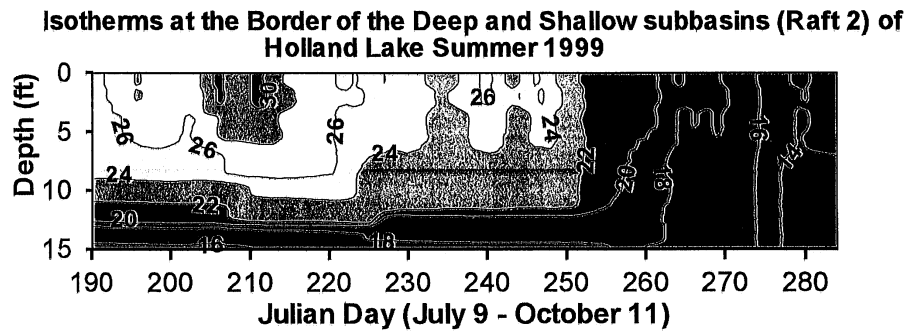


**Figure 29.** Isotherms at the boundary of subbasins of Holland Lake.

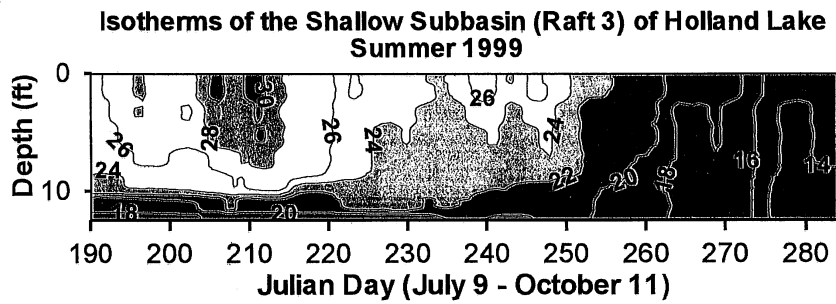


**Figure 30.** Isotherms of the shallow subbasin of Holland Lake.

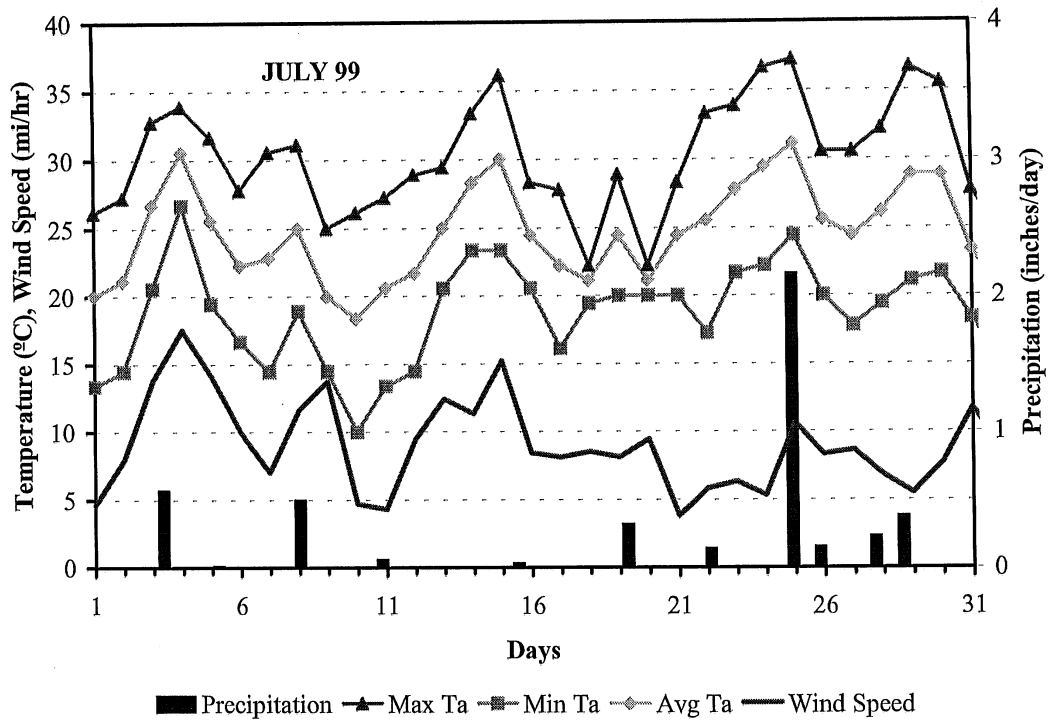


**Figure 31.** Daily weather parameters at the Twin Cities airport in July 1999.

## VI.5. Advection

### VI.5.1. Advection by Groundwater

Since the low water temperatures measured at the bottom of the shallow subbasins relative to the deep subbasin are hard to explain by shading alone, we have made an assessment of the potential groundwater flow into and out of Holland Lake. This investigation was beyond the scope of the work, but has provided important information that explains some of the inlake observations.

Holland Lake is located in glacial deposits of sand and gravel of the Rosemount outwash. It intercepts a Quaternary aquifer. Figure 32 gives elevation of the groundwater table and general groundwater flow directions in the proximity of Holland Lake [*Minnesota Geological Survey, 1990*]. The water table was determined from the static water levels reported in driller's records and observation wells. The aquifer is confined and has an average hydraulic conductivity of 1000 gallons.ft<sup>2</sup>.day<sup>-1</sup> (40.7 m. day<sup>-1</sup>). The thickness of the saturated layer is about 80 ft (24 m) around the lake. The potentiometric surface of the aquifer along the arrows of Figure 32 is shown in Figure 33. The potentiometric head of the aquifer drops by 50 ft (15 m) from the southwest side of the lake to its northeast side.

An attempt was made to identify areas with groundwater inflow along the periphery of the shallow subbasins of the lake by measuring temperatures in the surficial sediments and in the overlying water. About 45 temperatures were measured around the lake periphery on two occasions. Measurements 2 inches into sediments were from 1.5 to 3.5 °C colder than lake water, which was between 22 to 27 °C. This may be due to groundwater intrusion, but is not proof.

Another observation suggesting groundwater inflow into Holland Lake is the presence of several lakes to the west and south of Holland Lake with significantly higher lake stages (Figure 34). In particular, O'Brian Lake has an elevation of 908 ft (277 m) amsl compared to Holland Lake's 867 ft (265 m), and it is only 500 m away. It appears that groundwater flow from the vicinity of these lakes may converge towards Holland Lake as a focal point. Based on these characteristics a substantial amount of groundwater flow into and out of the lake can be expected.

In the Twin Cities, the mean annual precipitation and lake evaporation are about 28 inches (710 mm) and 30 inches (760 mm), respectively. Precipitation over the lake more or less compensates for evaporation. Provided no change in the lake stage occurs on an annual basis, the groundwater must be compensated by surface water and groundwater outflow. To roughly estimate the average groundwater flow through Holland Lake, the following equation for confined aquifers can be utilized

$$q = \frac{K (\phi_1 - \phi_2)}{L} \quad (5)$$

where  $q$  is flow per unit area,  $K$  is hydraulic conductivity, and  $L$  is the distance between two points with known piezometric heads  $\phi_1$  and  $\phi_2$ . Estimating the inflow from the piezometric head gradient of  $125/12000 = 0.01$  and a  $K$  value of  $133.5 \text{ ft.day}^{-1}$  (Figure 33), and assuming that the groundwater from the 80 ft (24 m) thick aquifer flows all

through Holland Lake gives a groundwater inflow of  $120 \text{ ft}^3 \cdot \text{ft}^{-1} \cdot \text{day}^{-1}$  ( $11 \text{ m}^3 \cdot \text{m}^{-1} \cdot \text{day}^{-1}$ ). Figure 35 illustrates the approximate capture zone of Holland Lake based on the hydrogeological map of the region [USGS, 1990]. The flow gradient varies within the lake capture zone; it is smaller in the west and south, and reaches a maximum in the southwest. Assigning an average gradient of 0.01 for the entire capture zone, and assuming a width of 2900 ft (870 m) for the capture zone, total groundwater inflow becomes  $348,000 \text{ ft}^3 \cdot \text{day}^{-1}$  ( $9570 \text{ m}^3 \cdot \text{day}^{-1}$ ).

Groundwater inflow into Holland Lake is quite significant with respect to the lake volume, which is  $25,380,000 \text{ ft}^3$  ( $720,000 \text{ m}^3$ ). With the above values, groundwater has a hydraulic residence time on the order of 73 days in Holland Lake. Since groundwater usually contains little or no DO, the effect of groundwater flow through a lake would be to remove DO from the lake.

A whole lake mass balance equation gives

$$C_2 = \frac{C_1 \left( \frac{V}{\Delta t} \right) + C_i Q}{Q + \frac{V}{\Delta t}} \quad (6)$$

where  $C_1$  and  $C_2$  are initial and final DO concentrations of the Lake,  $C_i$  is inflow concentration,  $V$  is the volume of the lake,  $Q$  is the groundwater inflow (which herein is assumed to be equal to the groundwater outflow), and  $\Delta t$  is the time interval. For an inflow concentration  $C_i=0$ , the relative concentration change in the lake becomes

$$\frac{\Delta C}{C_1} = - \frac{Q \Delta t}{V} \quad (7)$$

For a one day time step, this value is about 1.4%. But a 1.4% decrease in the DO concentration, or 73 days of residence time is only true when groundwater mixes with the entire water of the lake, as may be the case during the fall turnover. In summer, when the lake is temperature stratified, groundwater enters only into some of the layers. The groundwater temperature is slightly above the mean annual air temperature of the region, which is about  $10 \text{ }^\circ\text{C}$  in the Twin Cities area. Consequently, in summer, when the deep subbasin is stratified, groundwater enters only layers, which have a temperature greater than  $10 \text{ }^\circ\text{C}$ . According to Figure 28, groundwater must enter above a depth of 22 to 24 ft (6.6 to 7.2 m) in the deep subbasin. In the shallow subbasins, it enters the bottom of the basins and mixes with the bed layers. Low temperatures at a depth of 12 ft ( $16$  to  $18 \text{ }^\circ\text{C}$ ) in the shallow subbasin are likely associated with groundwater inflow in addition to shading (Figure 30). In summer, the groundwater residence times must be estimated using the thickness of the layers, with which the groundwater is mixing. Table 2 gives estimates of the groundwater residence times using the capture zone in Figure 35. For each subbasin, an appropriate width of the capture zone is assigned based on the figure.

**Table 2.** Estimates of the groundwater residence times in subbasins of Holland Lake in summer.

Subbasin	Inflow Width (ft)	Inflow (ft <sup>3</sup> . day <sup>-1</sup> )	Inflow depths	Volume (ft <sup>3</sup> )	Residence time (day)
Western shallow subbasin	1250	150,000	Bottom 3 ft	37,000	0.3
Eastern shallow subbasin	450	54,000	Bottom 3 ft	158,000	2.9
Deep subbasin	1250	150,000	18-24 ft depth	1,223,000	8.2

The estimates of the groundwater residence times in Table 2 are only crude estimates, however, they indicate that the groundwater inflow may have a significant impact on thermal stratification of the shallow subbasins as well as DO dynamics. It also implies that, it is most likely that the western shallow subbasin has a colder bottom temperature than the eastern shallow subbasin. However, there are no measurements from the western shallow subbasin to verify this potential difference.

One can summarize the estimates presented in Table 2 as follows: Groundwater enters the bottom of the western shallow subbasin with a residence time of less than a day and decreases the bed water temperatures. The bottom water in the shallow subbasins is cooler and therefore denser than the surface water and enters the deep subbasin as density current. The density current intrudes into a region with the same temperature (14 to 15 ft depth in July). High concentrations of TSS and TVSS were measured at those depths in the deep subbasin. They may be attributed to plant material carried by the density current from the shallow subbasins into the deep subbasin. Since the groundwater usually carries little or no DO it may gradually displace oxygen richer water and replace it by water with a high oxygen demand from the shallow subbasins. If the groundwater comes from the upper lakes it will have some DO in it.

Overall it is believed that groundwater flow into Holland lake contributes to the observed DO dynamics especially the DO depletion in the upper metalimnion by July as shown in section V.1. The second spike in the TSS and the TVSS profiles at a depth of 24 ft may be associated with direct groundwater inflow into the deep subbasin. Resuspension of sediments at those depths in the deep subbasin would increase the TSS.

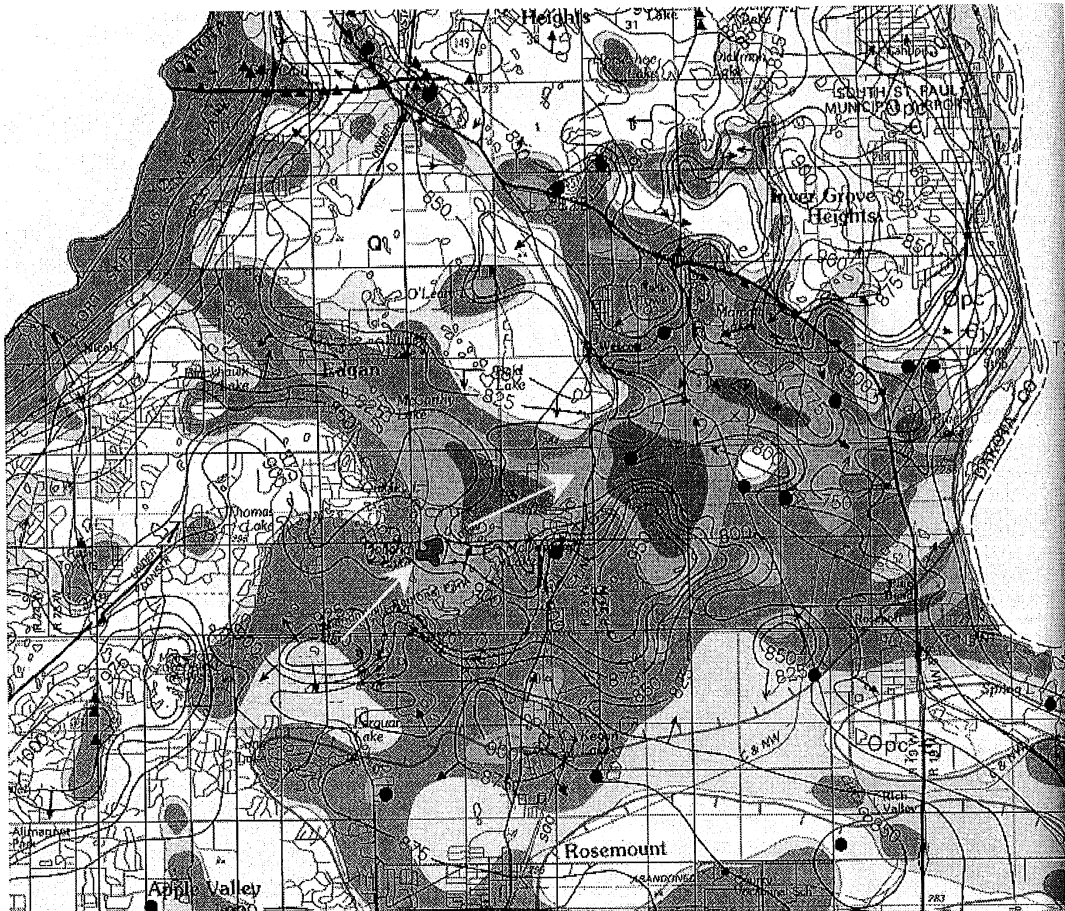


**Figure 32.** Hydrogeological map of the region around Holland Lake [after *Minnesota Geological Survey*, 1990]. The lake is between the white arrows.

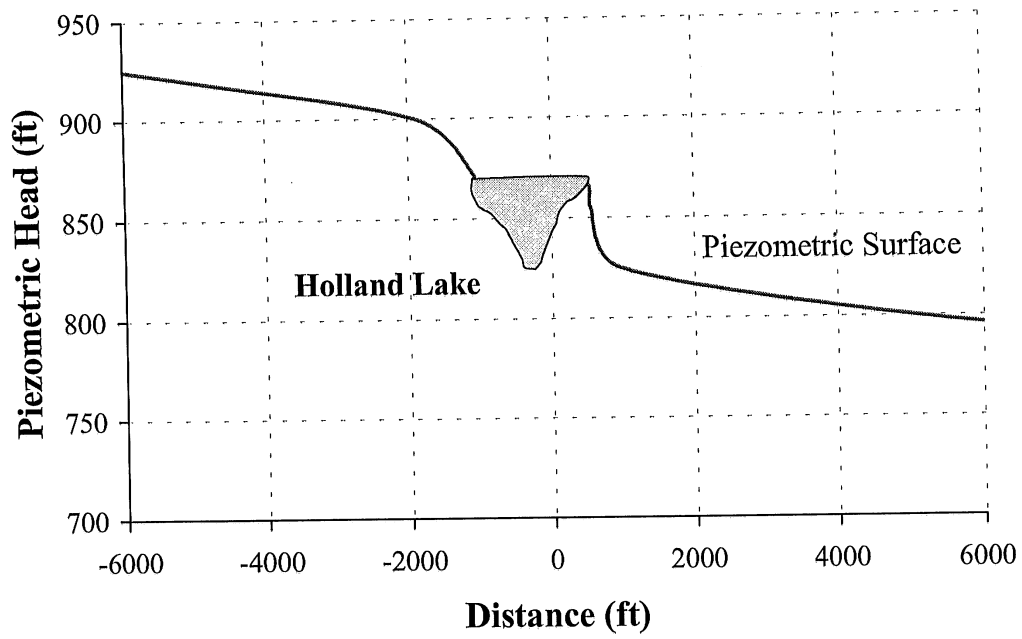


**Figure 33.** Piezometric groundwater surface of the Rosemount outwash in a cross section through Holland Lake (elevation data are from the *Minnesota Geological Survey*, 1990).





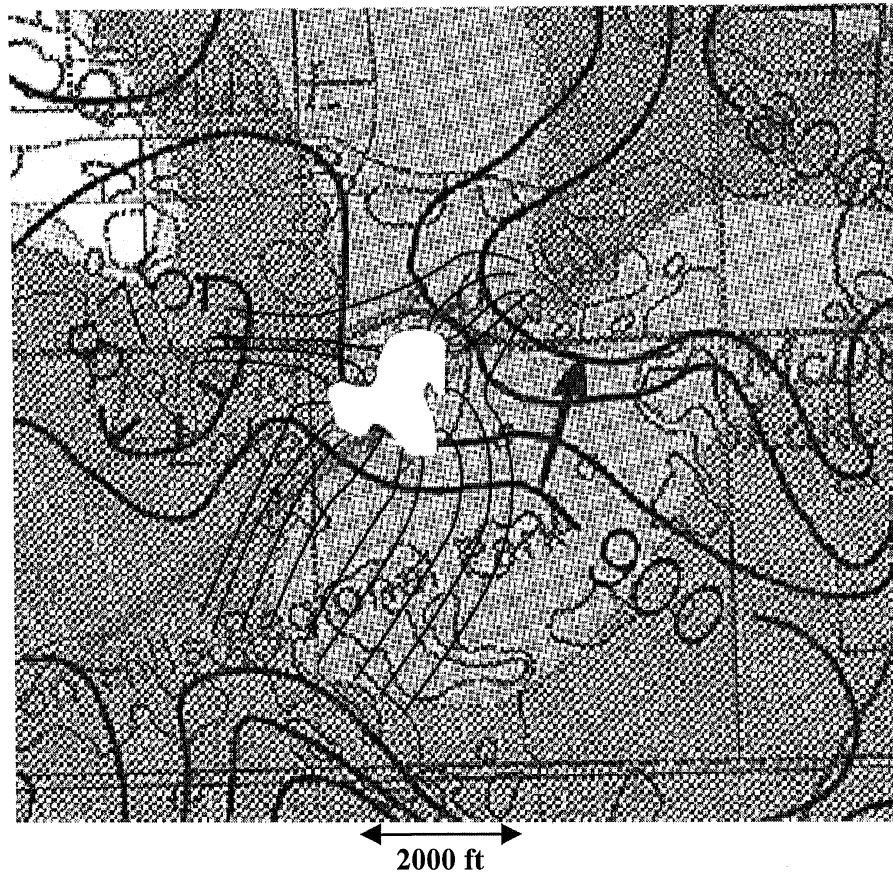


**Figure 35.** The Holland Lake capture zone of the aquifer. Approximate groundwater streamlines and equal piezometric head lines around Holland Lake showing the capture zone of groundwater.

### *VI.5.2. Advection by Internal Waves*

The water temperature stratification in Holland Lake, as in any other real lake, is not static. As wind and wind shear on the lake surface change with time, internal Seiches (standing waves) are generated. The occurrence of such internal waves is evident in the water temperature records from depths below 10 ft (in the metalimnion) and at all three rafts (Figures 25-27). Maximum temperature changes over a day have been extracted from the data and are plotted as time series in Figures 36 to 38, and as monthly averages in Figures 39 to 41. These changes are either due to diurnal heating and cooling or due to internal waves or both. The amplitudes of maximum temperature changes due to internal waves are frequently less than 1 °C in the deep subbasin (raft 1) and less than 0.5 °C for the shallow subbasin (raft 3). However, these amplitudes are often more than 1 °C at the boundary between the deep and the shallow subbasins (raft 2) due to the impingement and reflection of internal Seiche motion on the bed/boundary between the deep and the shallow subbasins.

Internal standing waves moving into and out of the shallow subbasin could transport organic material (BOD, TOC, etc.) from the bottom of the shallow subbasins into the deep subbasin. However, internal waves are not large enough in small lakes and are only effective in transport of material during storm events. The largest diurnal temperature changes in Figures 36 to 38 are due to storms on July 26, 1999. Figure 42 displays temperature time series with 10-minute intervals in the deep subbasin of Holland Lake for July 25-28, 1999. It is evident that temperature changes in 10 minute intervals are less than 0.5 °C until the early hours of July 26. The wind speed time series in Figure 42 (measured over Lake McCarrons) shows an abrupt increase in wind speed due to a storm event, i.e. a front moving into the region. At the same time, the amplitude of temperature changes increases by 2 to 3 °C in the metalimnion and parts of the hypolimnion. The internal waves had dissipated by the end of the day. The period of these standing waves in Holland Lake is about an hour.

The daily temperature changes plotted in Figures 36 to 38 can be translated into approximate vertical amplitudes if the mean water temperature profile with depth is known. This was done for July 26, 1999 which had the largest recorded maximum changes in diurnal temperature in the summer of 1999 (Figure 43). The figure gives the median daily temperature profile at each raft. The horizontal bars show temperature ranges which were recorded by the thermistors on that day. The vertical bars give the potential maximum displacements (amplitudes of internal waves) that match the temperature range indicated by the horizontal bars. The maximum height of vertical displacement during the storm of July 26 could not exceed 2 ft in the thermocline. They are usually much less than 2 ft. This result shows that internal waves are not significantly strong to produce much exchange between the shallow and deep subbasins, mainly due to the size, shape and wind sheltering of Holland Lake. Consequently, the mean transport of particulate material is not by internal waves in Holland Lake.

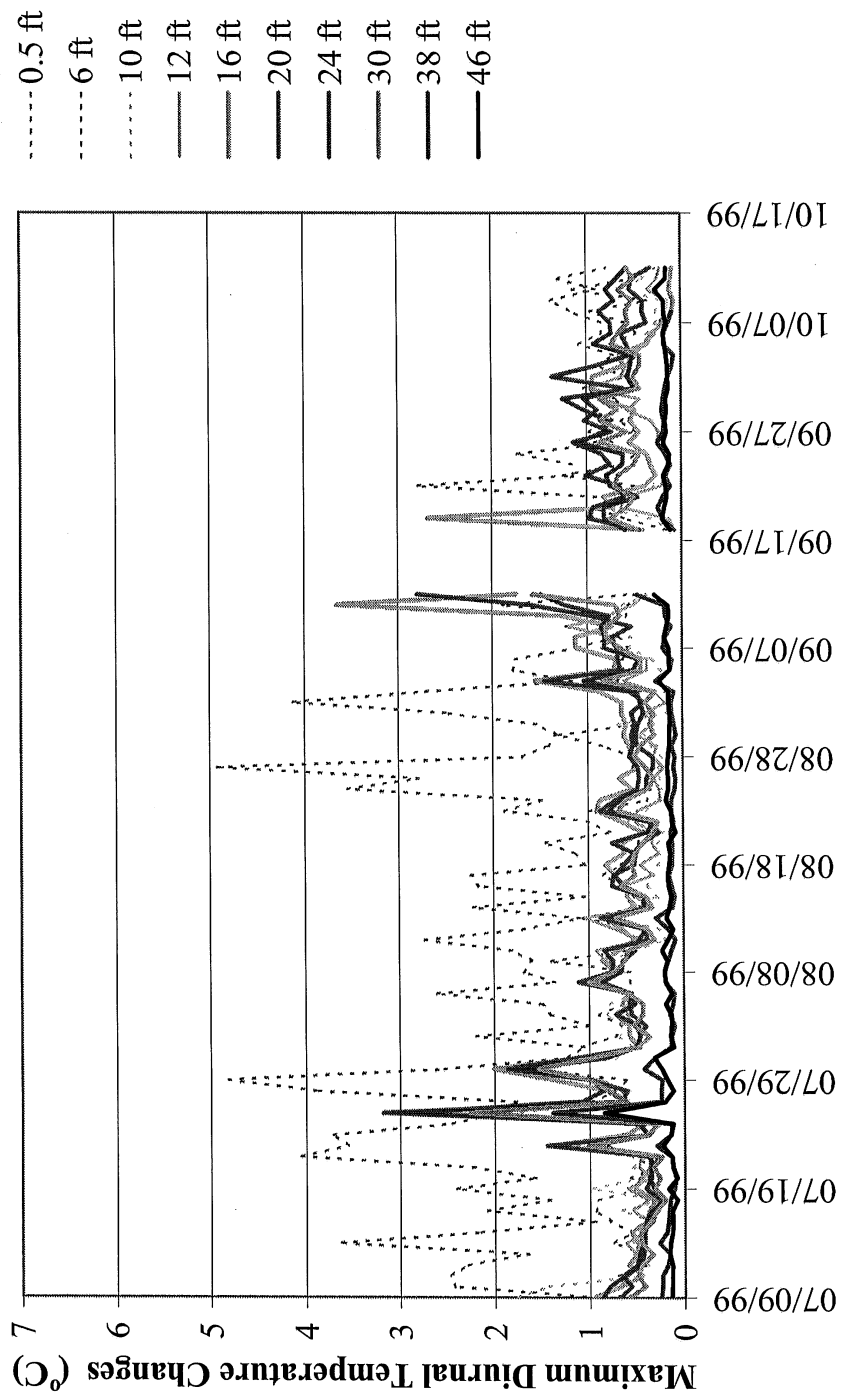
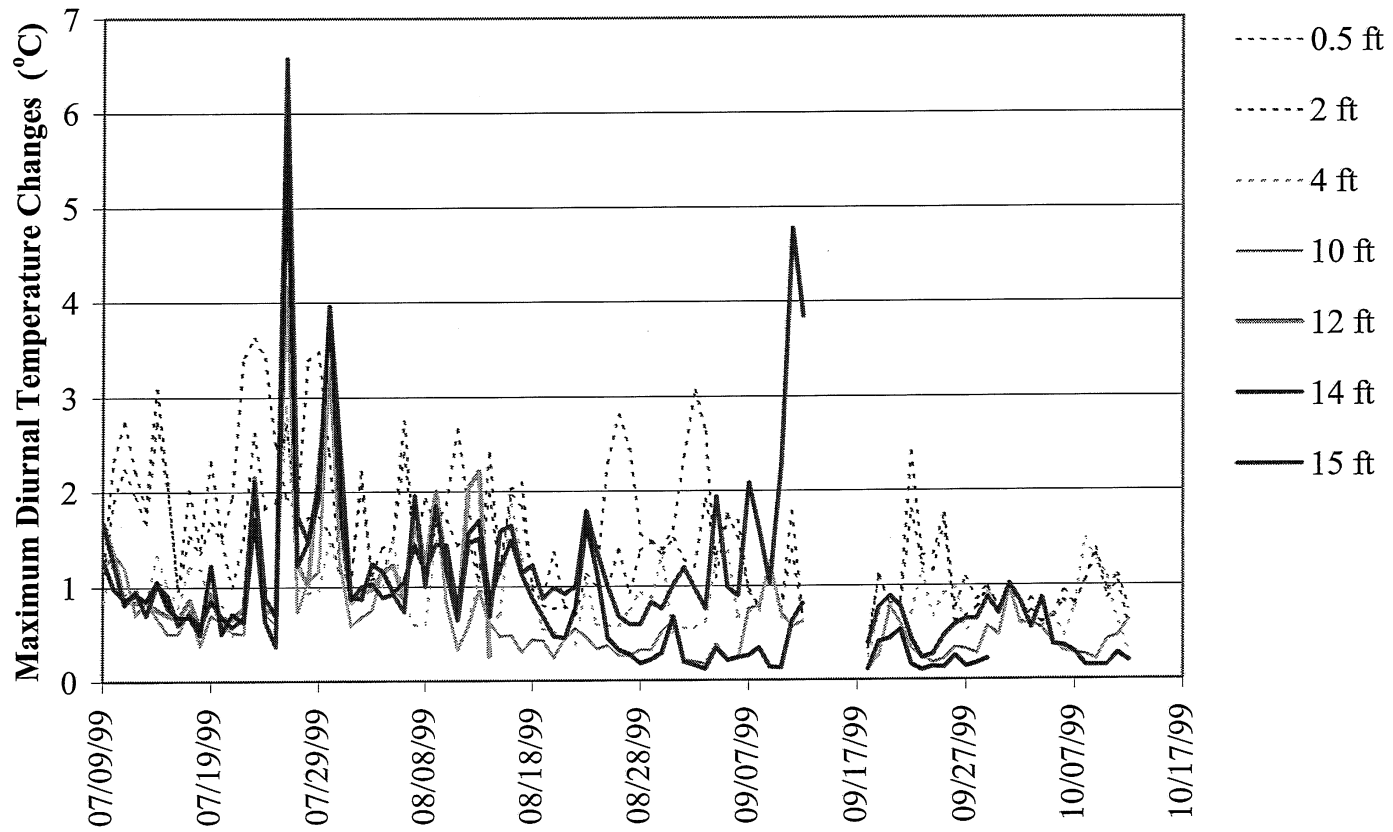


Figure 36. Maximum daily amplitude of temperature changes in the deep subbasin of Holland Lake (Raft 1).



**Figure 37.** Maximum daily amplitude of temperature changes between the deep subbasin and the eastern shallow subbasin of Holland Lake (Raft 2).

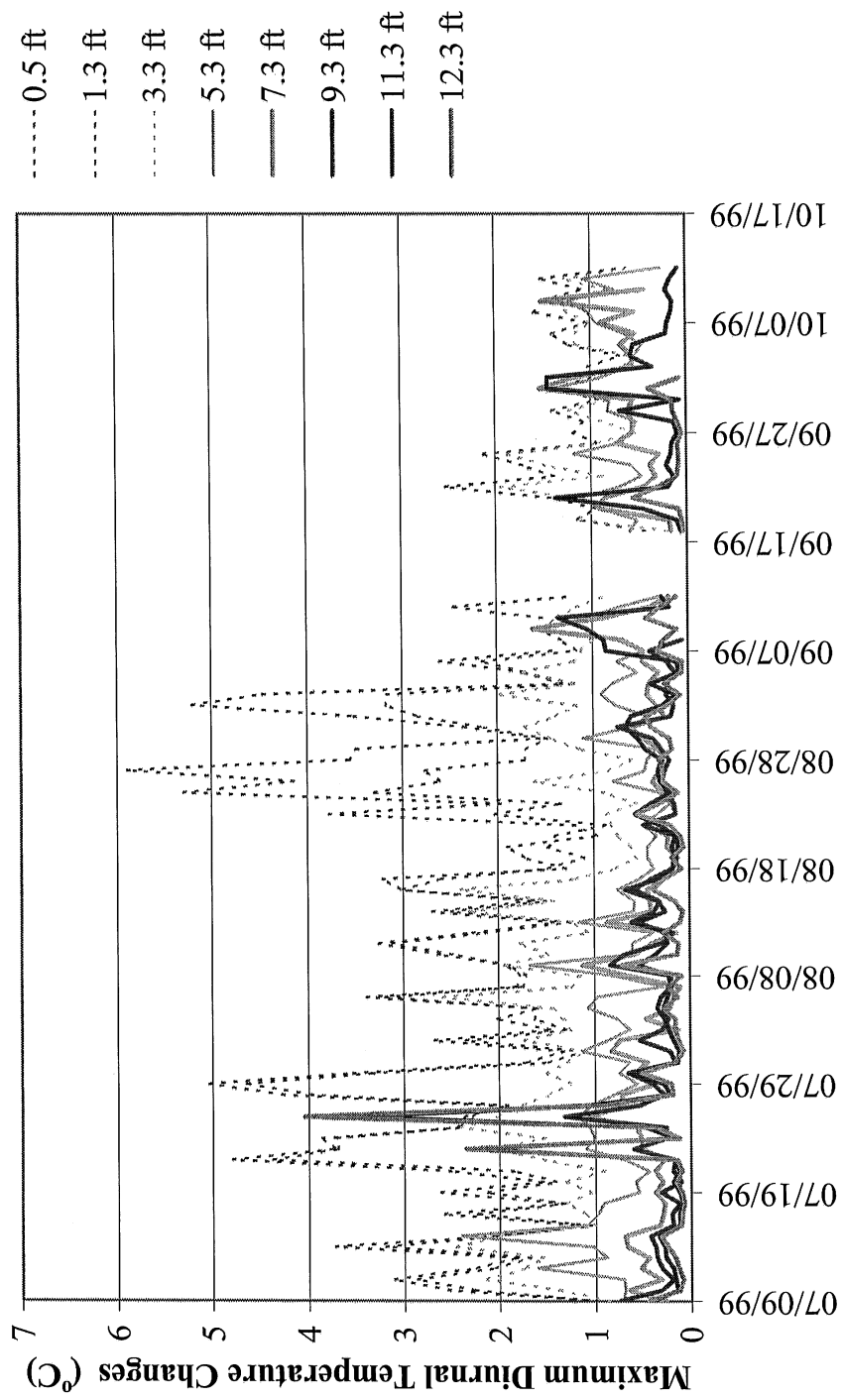


Figure 38. Maximum daily amplitude of temperature changes in the shallow subbasin of Holland Lake (Raft 3).

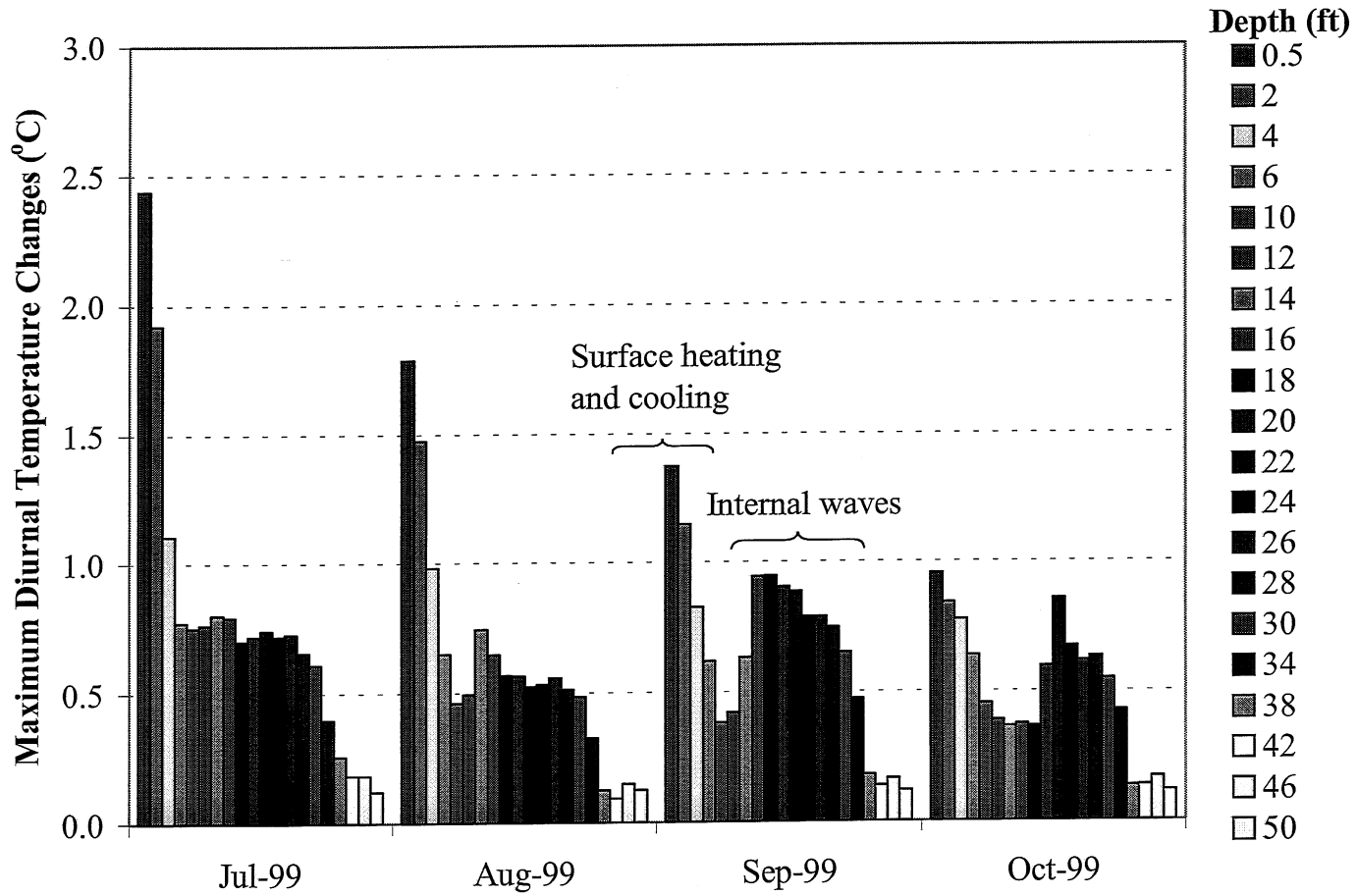
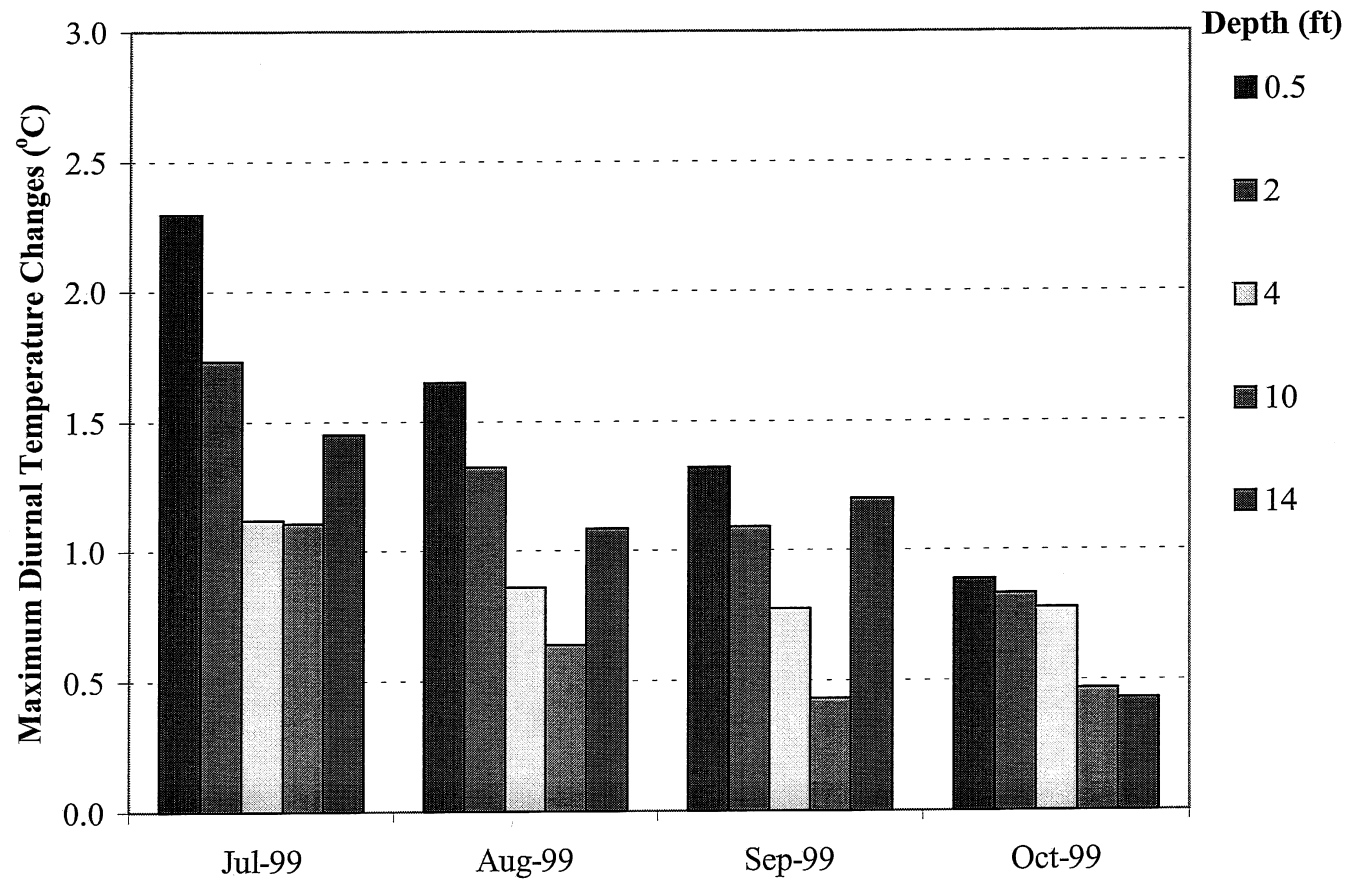
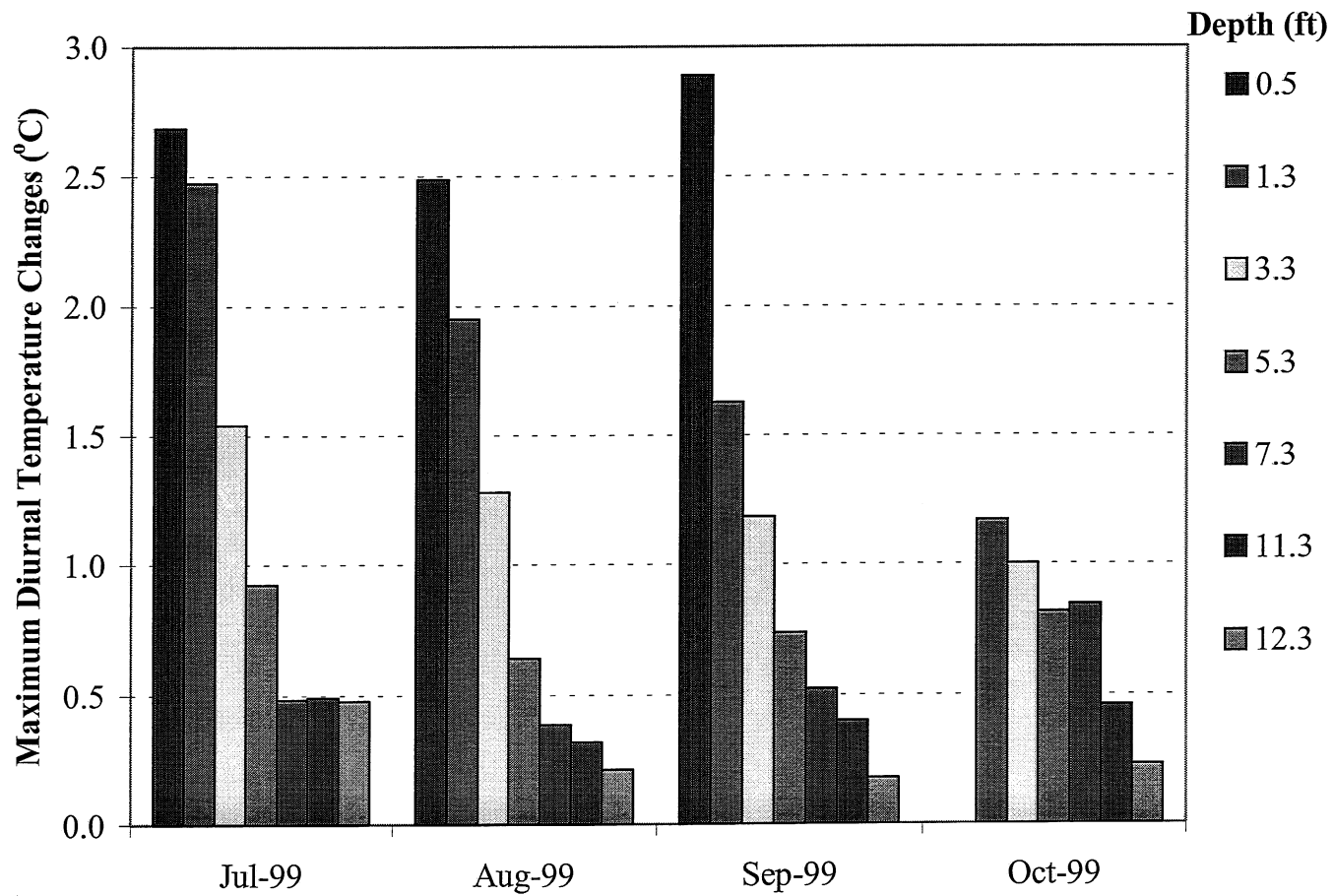


Figure 39. Monthly averages of maximum diurnal temperature changes in the deep subbasin of Holland Lake (Raft 1).



**Figure 40.** Monthly averages of maximum diurnal temperature changes at the border of the deep subbasin and the eastern shallow subbasin of Holland Lake (Raft 2).



**Figure 41.** Monthly averages of maximum diurnal temperature changes in the shallow subbasin of Holland Lake (Raft 3).



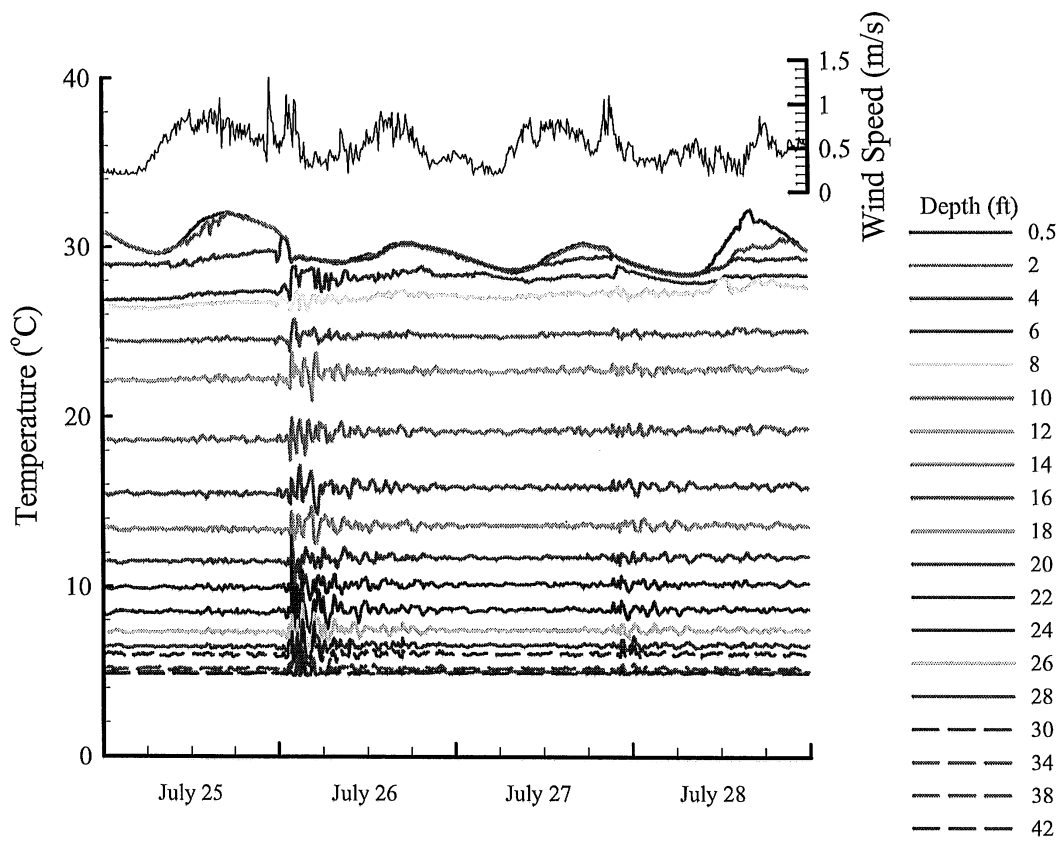


**Figure 42.** Ten minute averaged water temperature and instantaneous wind speed time series for July 25-28, 1999, in Holland Lake. Wind speed data were measured over Lake MaCarrons, MN, by the Metropolitan Council.

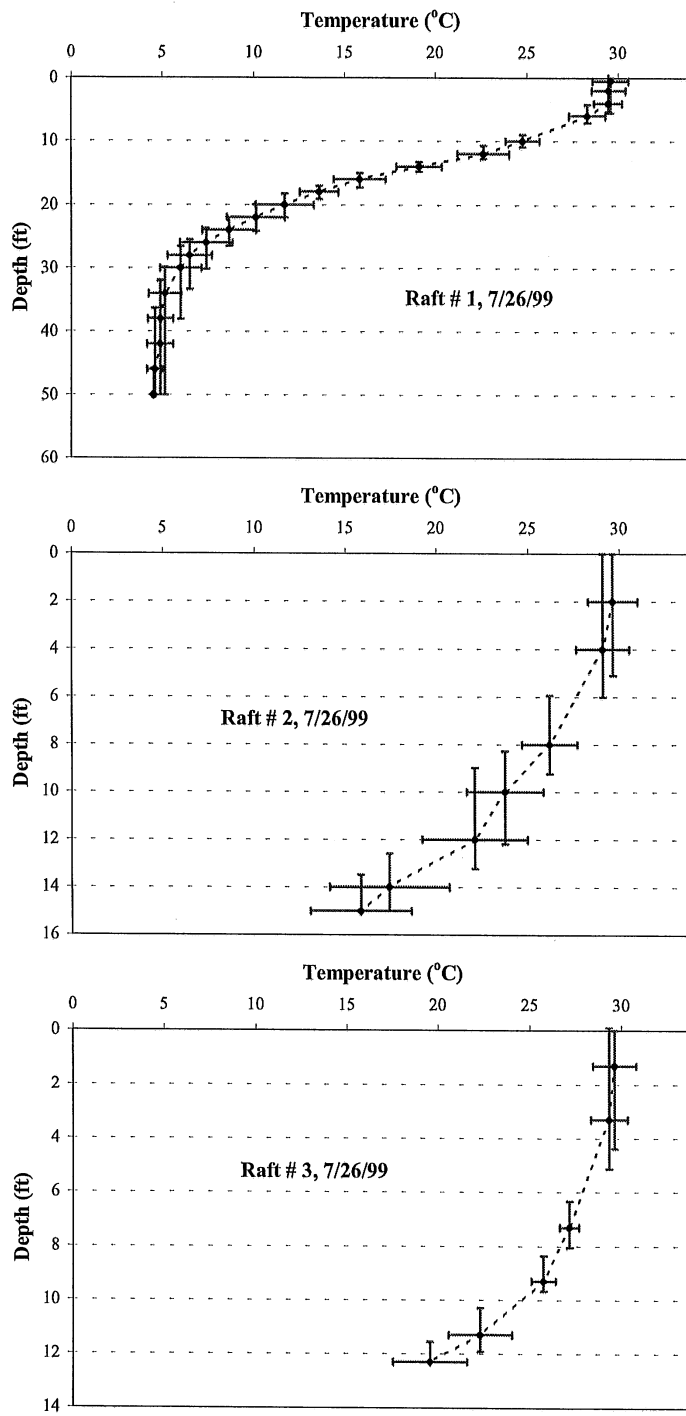


**Figure 43.** Maximum diurnal changes in temperature and the corresponding potential vertical water movements in Holland Lake during the storm event of July 26, 1999.

## VII. Summary and Conclusions

Holland Lake in Dakota County has been considered for stocking with brown trout. Holland Lake is suitable for this purpose because it is exceptionally deep in comparison to other lakes in the Metro Area and has relatively good water quality due to a limited drainage area. However, for a period of two to three months the strata below the surface mixed layer become anoxic. Consequently, midsummer high water temperature at the lake surface and anoxia below the surface would exert exceptional stresses on brown trout endangering their survival.

A field study was conducted in the summer of 1999, to quantify some of the factors affecting the dissolved oxygen (DO) dynamics in Holland Lake. Temperature profiles were measured continuously at 10 minute intervals at three locations, from July 9 to October 12. DO profiles were measured approximately once a week. Other parameters measured in Holland Lake were: Secchi depth, PAR, TSS, TVSS, chl-*a*, TOC and total respiration rates.

The historical data and the data collected in summer 1999 in Holland Lake show that the water below the surface mixed layer in the deep subbasin (from about 10 to 20 ft depth) approaches anoxia at a depletion rate of about  $0.47 \text{ mg.l}^{-1}.\text{day}^{-1}$ , when the stratum below it (20 to 30 ft depth) still contains more than  $3 \text{ mg DO.l}^{-1}$ . The entire metalimnion (10 to 30 ft depth) becomes anoxic by early September. The total respiration rate in the deep subbasin at a depth of 10 to 20 ft was measured to have a maximum of  $0.52 \text{ mg.l}^{-1} \text{ day}^{-1}$  ( $0.68 \text{ mg.l}^{-1} \text{ day}^{-1}$  with a 2-day measurement). It was estimated that at least one third of the total respiration rate is due to live plants. The TSS, TVSS and TOC profiles show that a significant amount of organic matter in the upper layer of the metalimnion is responsible for the high oxygen depletion rate within the thermocline.

The temperature profiles in the shallow, well stratified subbasins in addition to the hydrogeological map of the region suggest that substantial amounts of groundwater enter the bottom of the shallow subbasins. This decreases the bed water temperatures. The bottom water in the shallow subbasins (10 to 12 ft depth) is therefore cooler and denser than the surface water and intrudes into the deep subbasin as a density current. The density current plunges into a stratum with the same temperature at 14 to 15 ft depth in July. The density current transports detritus and plant material from the shallow subbasins into the deep subbasin. In summary, the presence of a substantial amount of plant material (macrophyte) in more than 50% of the lake, the particular morphometry of the lake, and a significant groundwater inflow cause high oxygen depletion rates and a negative heterograde DO profile in the upper metalimnion in early summer in Holland Lake. By late summer the water below a depth of 12 ft has become anoxic. To create brown trout fish habitat, artificial aeration and/or partial mixing will be required.

## VIII. Recommendations

To create a reliable habitat for brown trout in Holland Lake, depletion of dissolved oxygen in portions of the lake metalimnion needs to be prevented. This can be achieved by aeration or mixing of selective strata/layers of the lake. Net rates of oxygen depletion depend upon depth and time, and have been determined to be more than  $0.47 \text{ mg.l}^{-1} \text{ day}^{-1}$  in the upper strata of the metalimnion, and the total potential respiration rate has been measured to be  $0.68 \text{ mg.l}^{-1} \text{ day}^{-1}$ . The artificial aeration needs to compensate for these losses. Periods during which aeration is needed can be seen in Figures 44 and 45, which is approximately from late June to mid September (three months), based on the summer of 1999 field measurements. It is recommended that an aeration or mixing system be designed/developed for this purpose. Design criteria can be extracted from this report.

The placement/location and operation of an aeration system for Holland Lake will depend upon the stratification and mixing dynamics that have been illustrated by field measurements in this report and by simulation in another report (Stefanovic and Stefan, 2000). Oxygenation requirements will also depend on dissolved oxygen and feeding requirements of brown trout. Reproduction of brown trout in Holland lake is not anticipated. A potentially strong groundwater flow through Holland Lake must be taken into consideration. Some additional study is needed to characterize that flow.

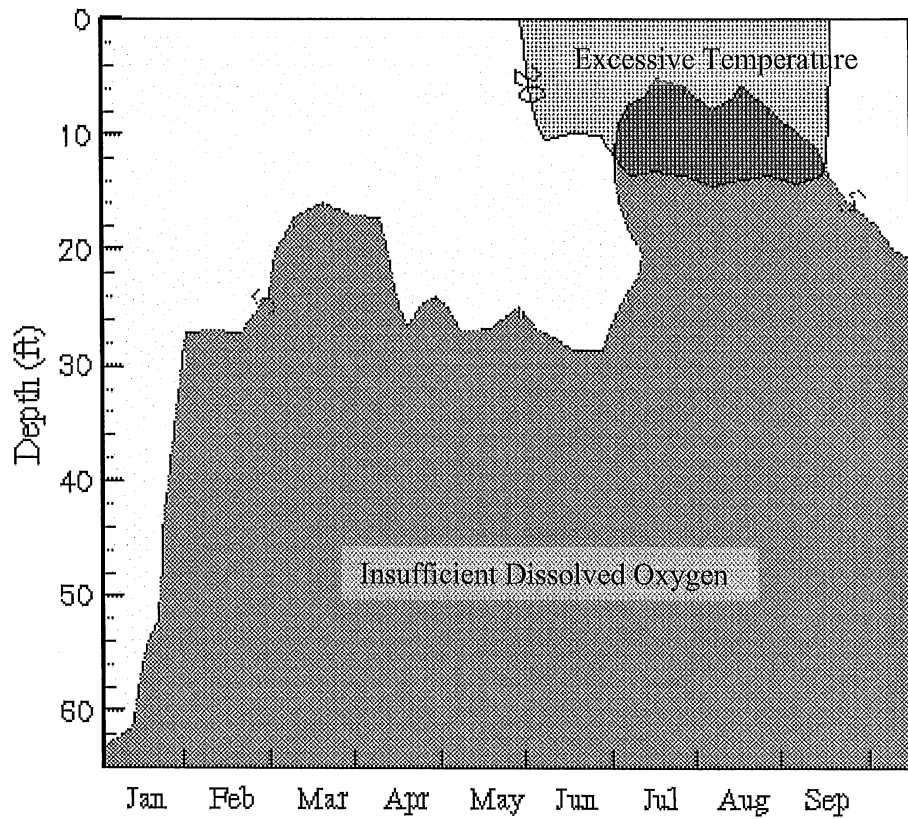


**Figure 44.** Temperature and DO threshold lines (20 °C and 5 mg/l, respectively) for brown trout habitat in Holland Lake. The figure is plotted using the monthly, biweekly and weekly temperature profiles measured by the MNDNR, the Met Council and the St. Anthony Falls Laboratory.

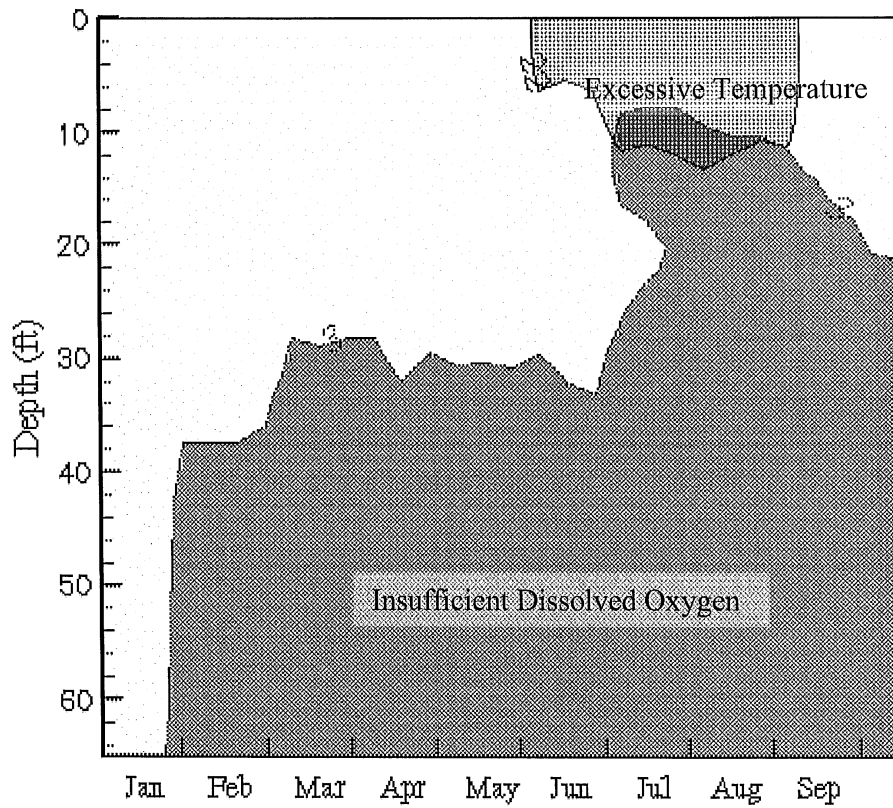


**Figure 45.** Temperature and DO threshold lines (22 °C and 3 mg/l, respectively) for a more severe brown trout habitat in Holland Lake. The figure is plotted using the monthly, biweekly and weekly temperature profiles measured by the MNDNR, the Met Council and the St. Anthony Falls Laboratory.

## References

- Chapra, S. C., 1997, *Surface Water Quality Modeling*. McGraw-Hill, New York, NY.
- Hondzo, M., and Stefan, H. G., 1993, Lake Water Temperature Simulation Model. *Journal of Hydraulic Engineering*, 119 (11):1251-1273.
- Horne, A. J., and Goldman, C. R., 1994. *Limnology*. McGraw-Hill Inc., New York, NY.
- Idso, S. B., and Gilbert, R. G., 1974, On the Universality of the Poole and Atkins Secchi disk-light extinction equation. *J. Appl. Ecology*, 11:399-401.
- Meybeck, M., 1982. Carbon, nitrogen, and phosphorus transport by world rivers. *Amer. J. Sci.*, 282:401-450.
- Minnesota Department of Natural Resources, Division of Fish and Wildlife. Fisheries Lake Survey. 7/22-23/85.
- Minnesota Department of Natural Resources, Section of Fisheries. Lake Survey Report. 02/12/96.
- Minnesota Geological Survey, 1990. Geological Atlas of Dakota County, Minnesota. County Atlas Series, Atlas C-6, Plate 5 of 9, Quaternary hydrogeology.
- Osgood, R. A. Management approaches for the water quality of Holland Lake. *The Metropolitan Council Report to Dakota County Parks and Recreation*, 03/13/1985.
- Osgood, R. A. 1989. An evaluation of the effects of watershed treatment systems on the summertime phosphorus concentration in Metropolitan area lakes: Part 2 of a report to the legislative commission on Minnesota resources. *Metropolitan Council*, Publication Number 590-89-062b.
- Poole, H. H., and Atkins, W. R. G., 1929. Phot-electric measurements of submarine illumination throughout the year. *J. Mar. Biol. Assoc. U.K.*, 16:297-324.
- Thomann, R. V., and Mueller, J. A. 1987. *Principles of Surface Water Quality Modeling and Control*. Harper Collins Publisher Inc., New York, NY.
- Wetzel, R. G., 1983. *Limnology*. 2<sup>nd</sup> edition, Saunders College Publishing.

## **Appendix A. Dissolved Oxygen and Temperature Profiles Measured by the MNDNR**

Water temperature and DO profiles measured by the MNDNR are reformatted and presented in this section. The measurements start in 1975 and end in 1999. There was one measurement per summer in 1975, 1978, 1980, 1985, 1990 and 1995. From December 1997 to May 1999 temperature and DO profiles were measured once a month. In addition to temperature and DO profiles, DO at saturation has been added to the figures.



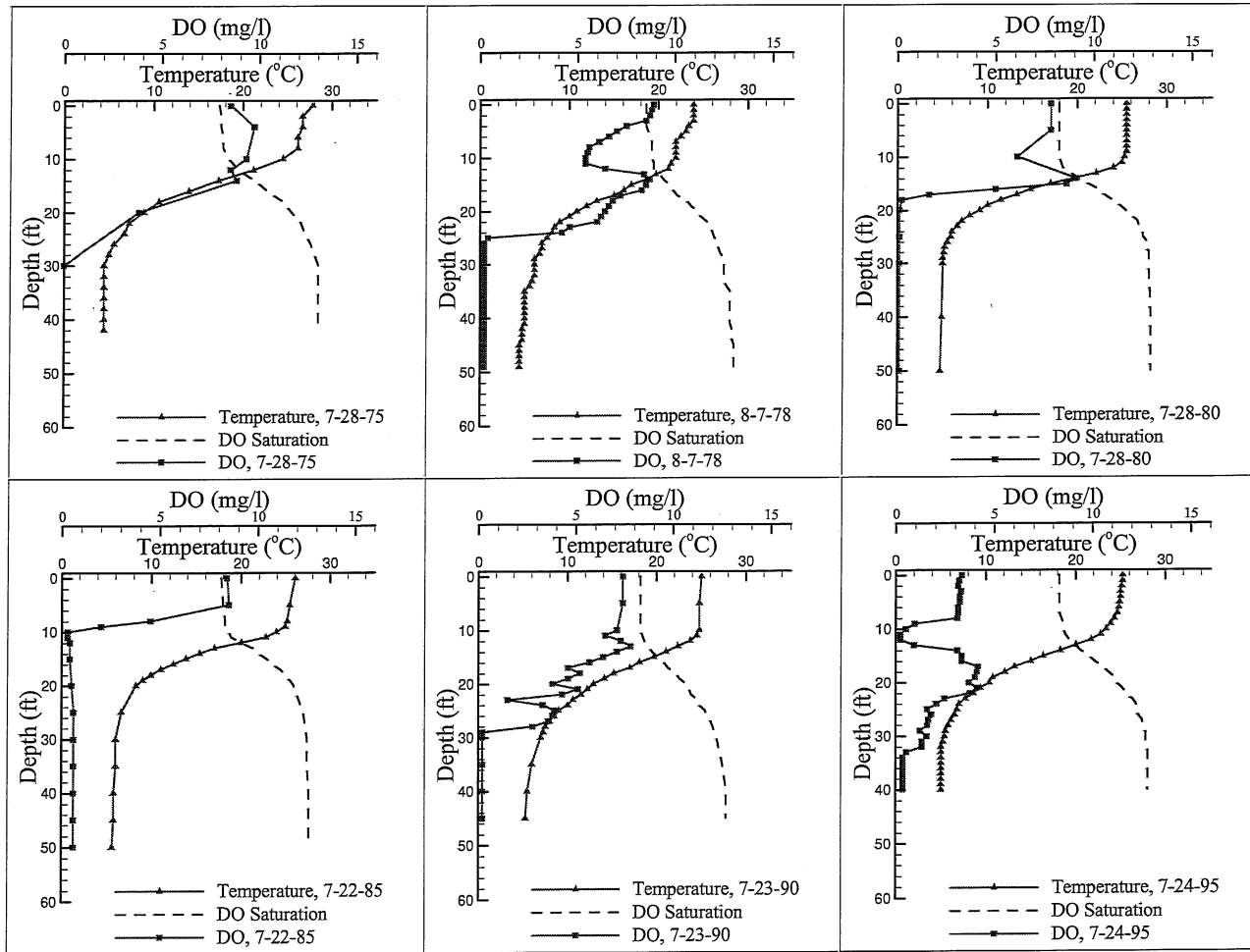
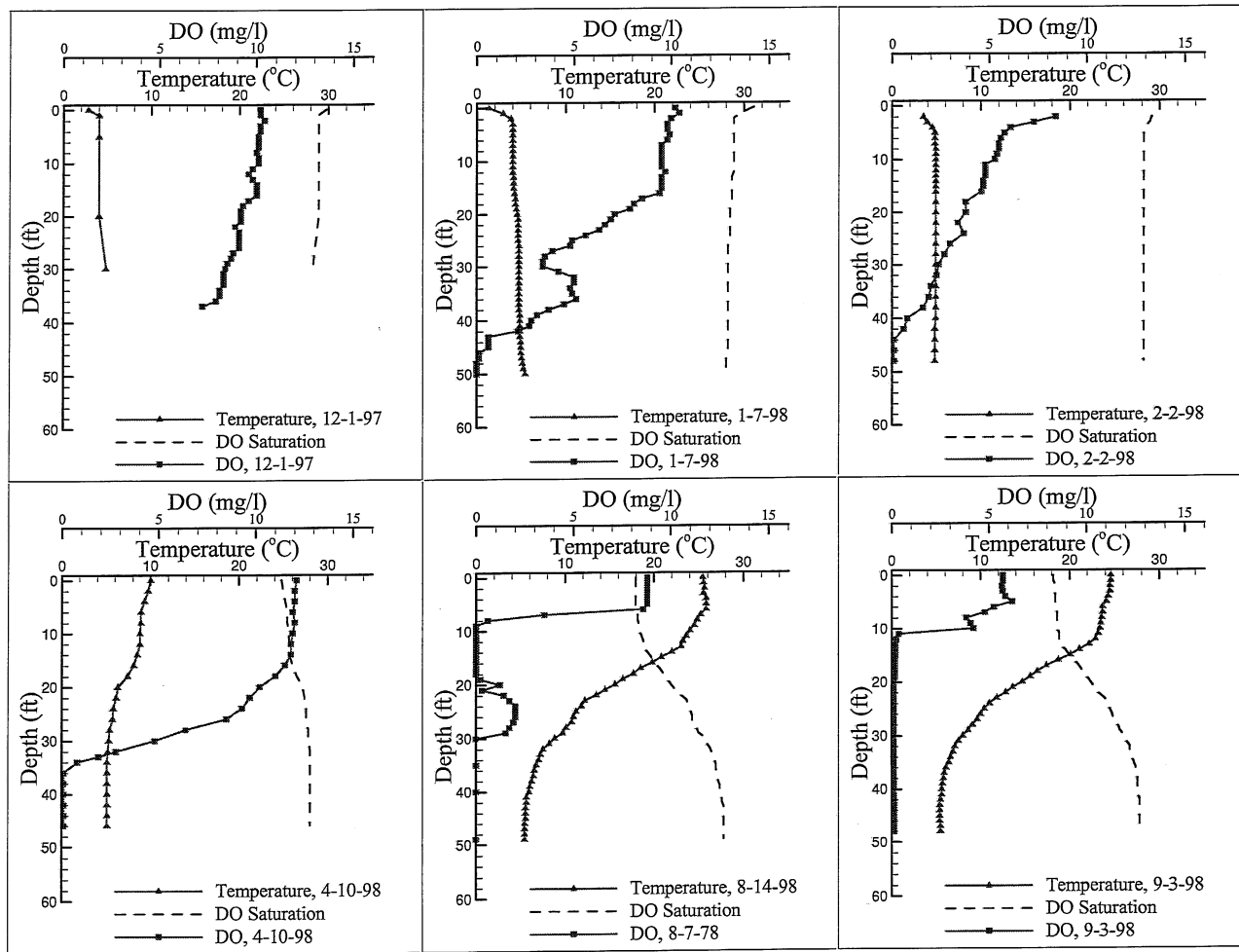
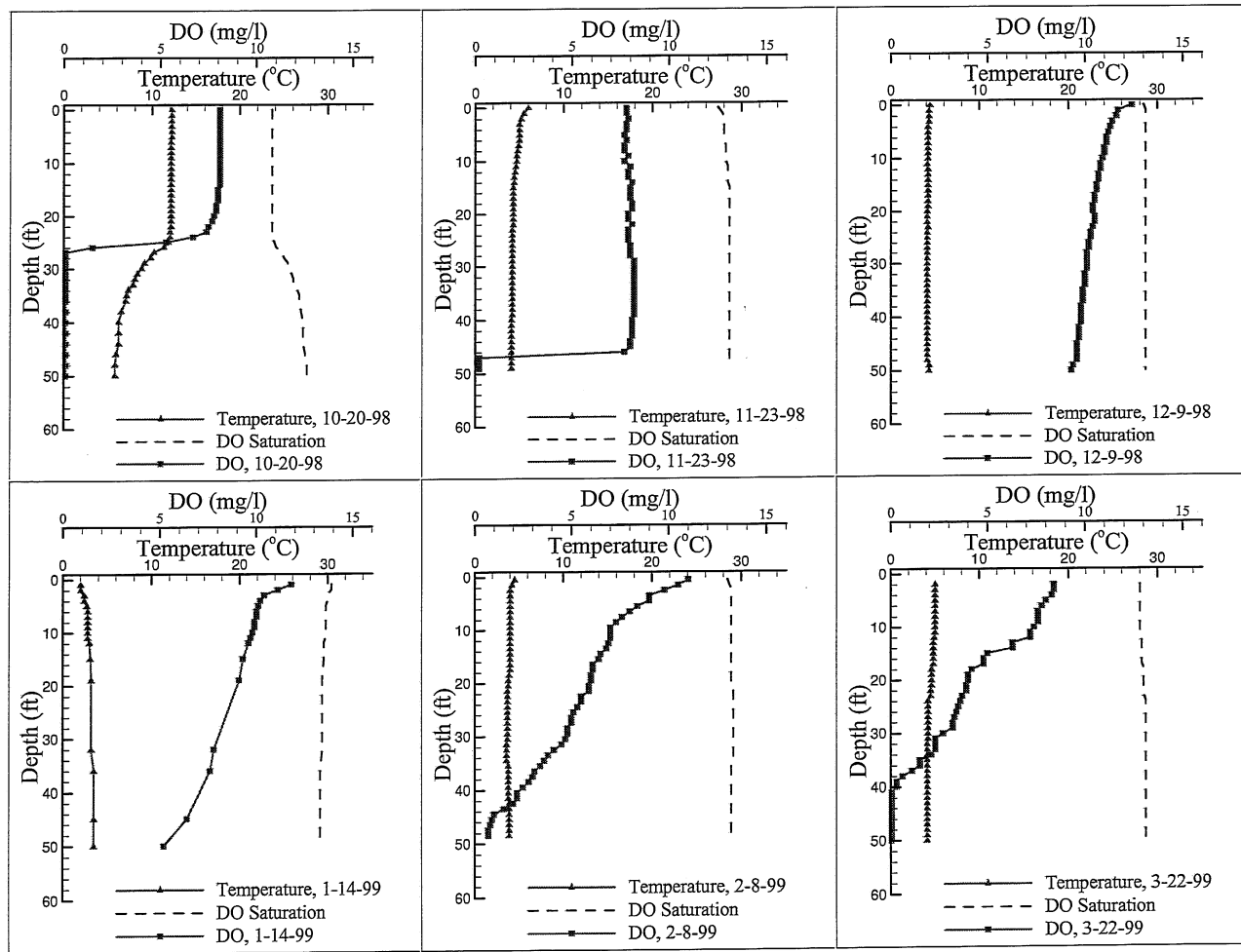


Figure A.1. Temperature and DO profiles in Holland Lake collected by the MNDNR from 1975-1995.



**Figure A.2.** Temperature and DO profiles in Holland Lake collected by the MNDNR from 1997-1998.



**Figure A.3.** Temperature and DO profiles in Holland Lake collected by the MNDNR from 1998-1999.

---

## **Appendix B. Dissolved Oxygen and Temperature Profiles Measured by the Metropolitan Council**

Water temperature and DO profiles measured by the Met Council are reformatted and presented in this section. The measurements are from 1983-1985, 1988 and 1993. The 1984 temperature and DO profiles are presented in Figures 3a and 3b, therefore, they are excluded from this appendix. These measurement have two week intervals. In addition to water temperature and DO profiles, DO at saturation has been added to the figures.

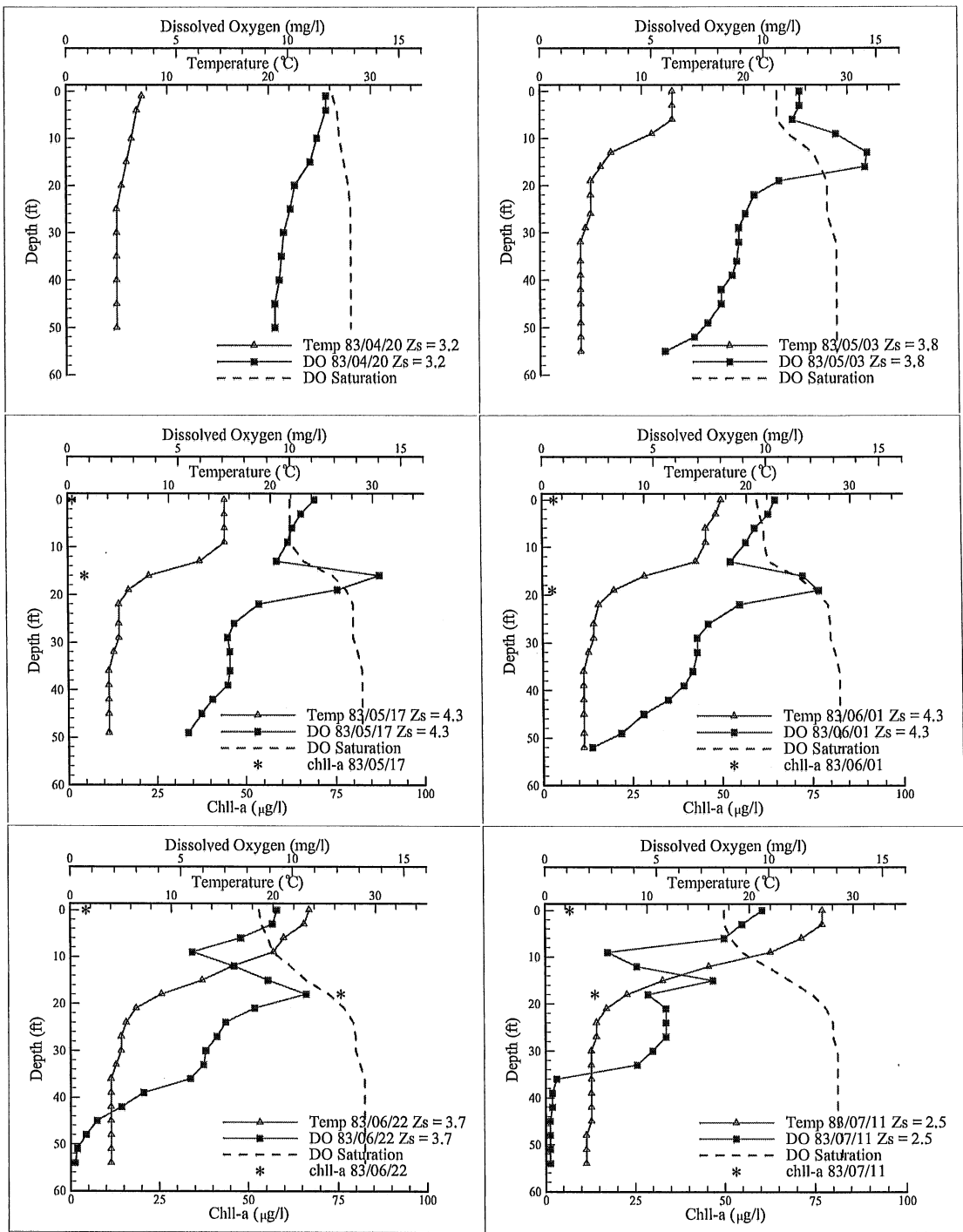


**Figure B.1.** Temperature and DO profiles in Holland Lake collected by the Metropolitan Council in 1983.

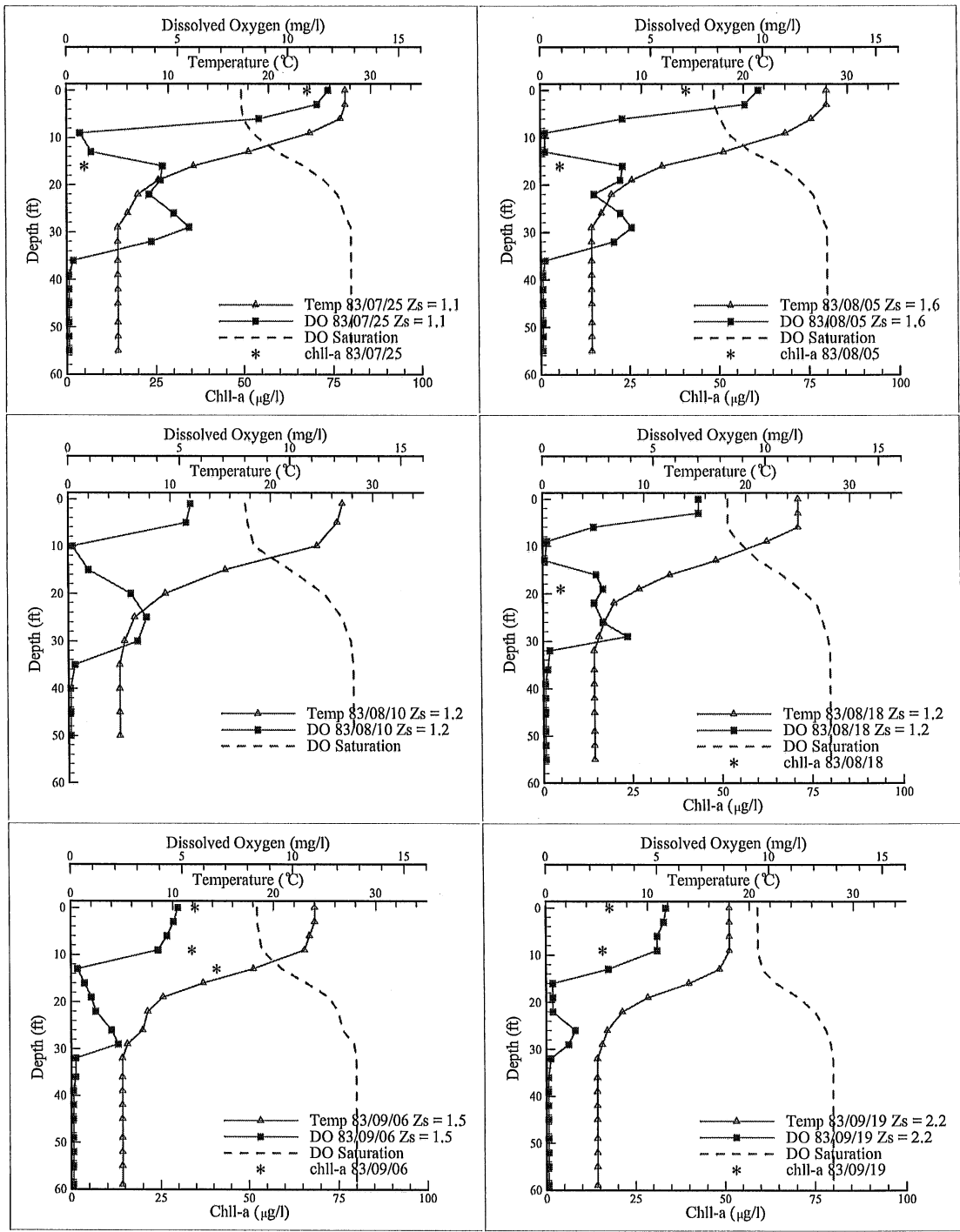


**Figure B.2.** Temperature and DO profiles in Holland Lake collected by the Metropolitan Council in 1983.

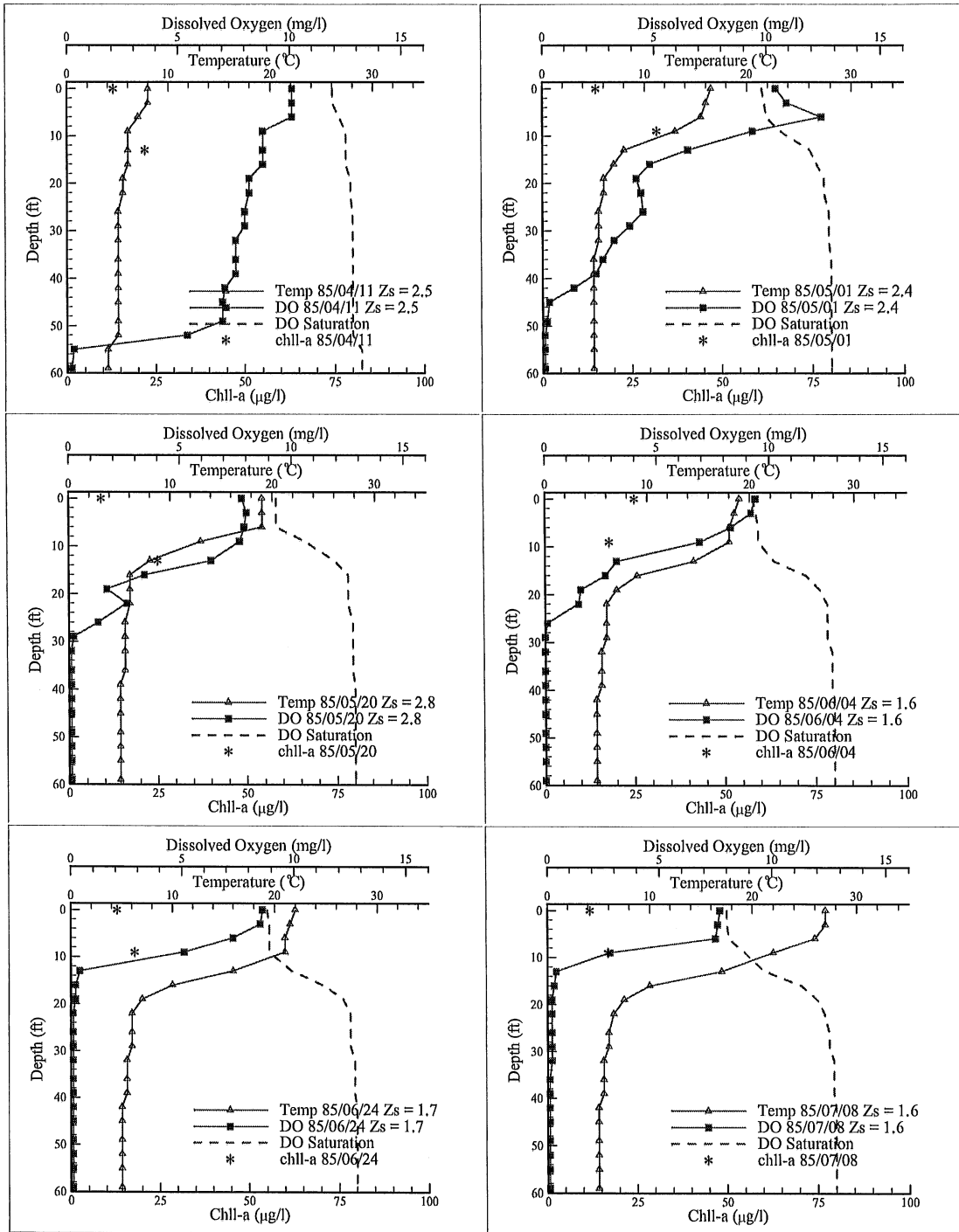


**Figure B.3.** Temperature and DO profiles in Holland Lake collected by the Metropolitan Council in 1985.

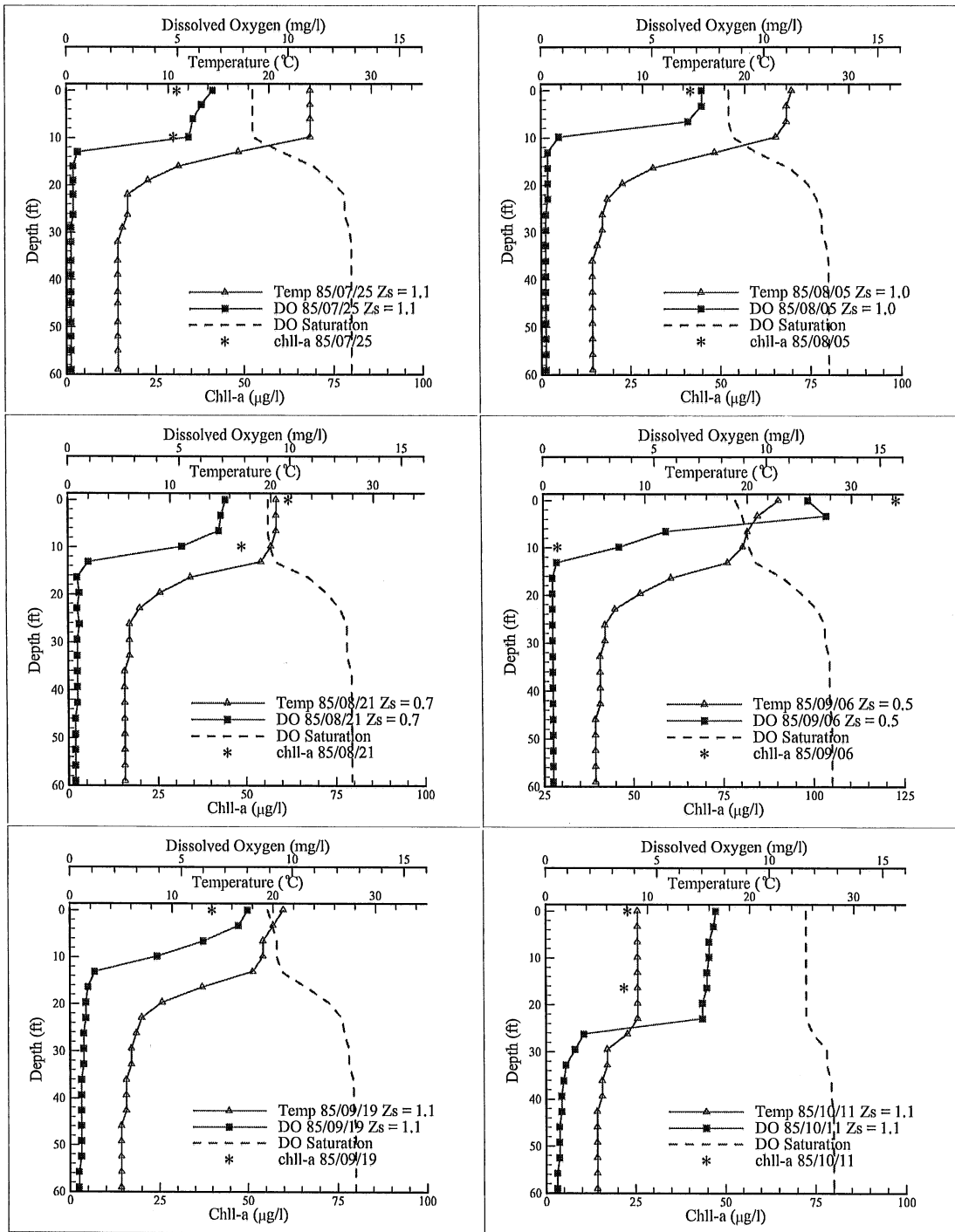


**Figure B.4.** Temperature and DO profiles in Holland Lake collected by the Metropolitan Council in 1985.



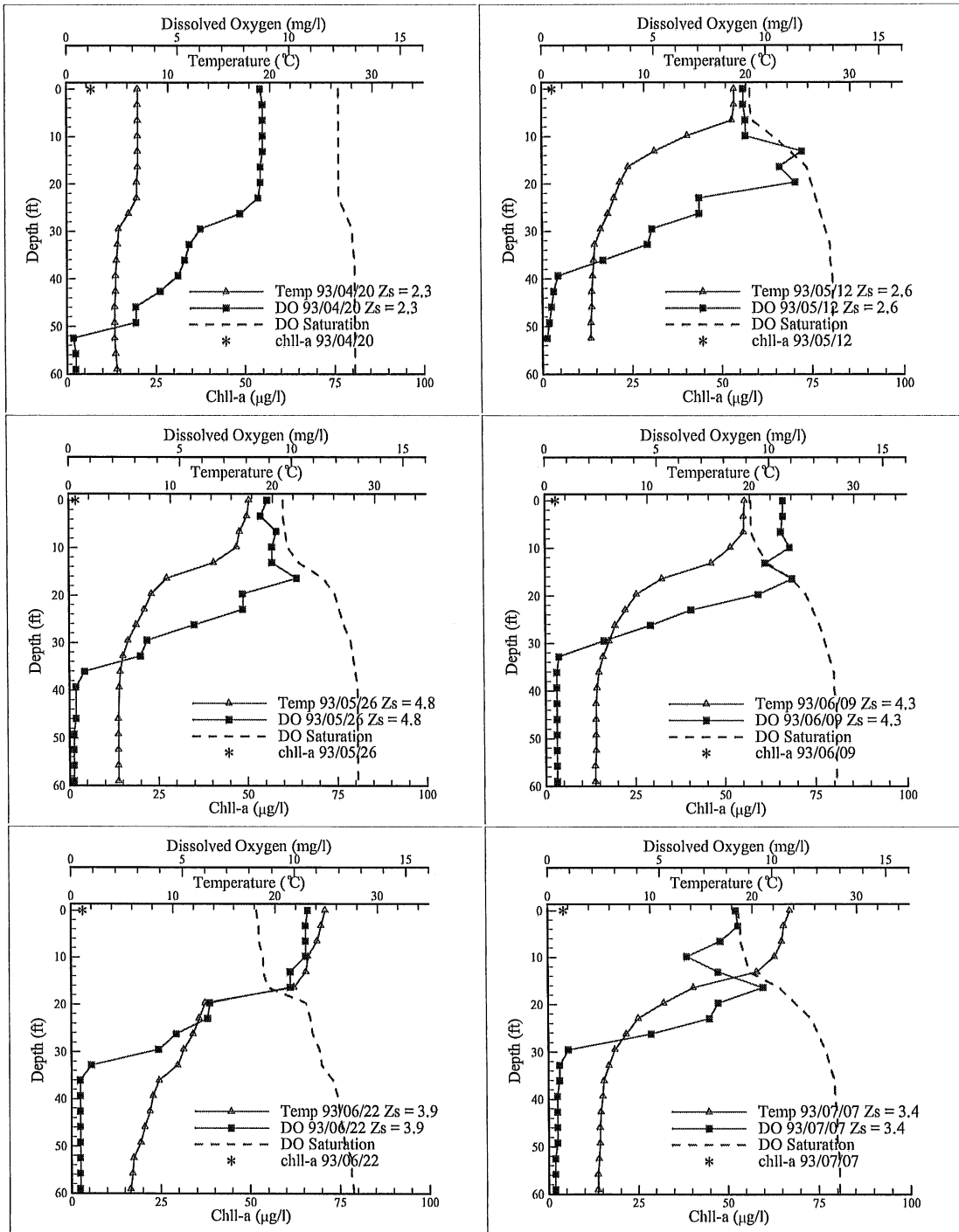


**Figure B.5.** Temperature and DO profiles in Holland Lake collected by the Metropolitan Council in 1993.

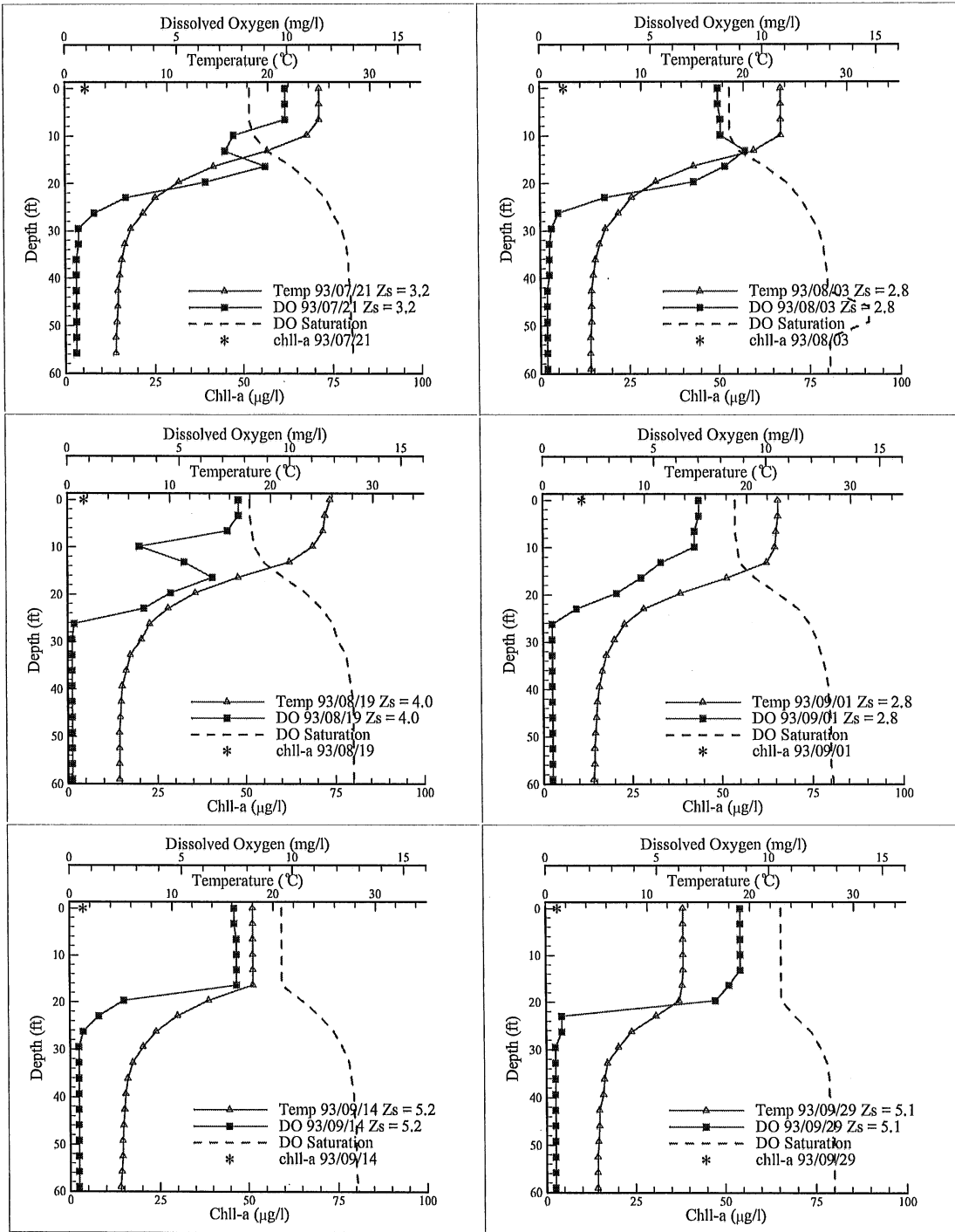


Figure B.6. Temperature and DO profiles in Holland Lake collected by the Metropolitan Council in 1993.

## Appendix C. Calibration of Thermistors Used in Holland Lake

The thermistor probes (Campbell Scientific model 107B) mounted on chains for measuring temperature profiles in Holland Lake had initial and final corrections at room temperatures. The tables below show these corrections and also the probes which and the dates when started malfunctioning.

**Table C-1.** Initial and final corrections applied to the thermistors mounted on Raft # 1.

Depth (ft)	Initial Correction (°C)	Final Correction (°C)	Periods with no or poor data
0.5	-0.021	-0.355	
2	0.071	-0.148	
4	-0.016	-0.470	
6	0.070	-1.120	
8	0.117	-1.152	After 9-30-99, 23:30
10	0.063	-0.652	
12	0.278	-0.347	
14	0.116	-0.284	
16	0.508	-0.284	
18	0.024	-0.051	
20	-0.024	-0.039	
22	-0.086	-0.093	
24	0.002	0.031	
26	0.065	0.000	
28	-0.053	0.007	
30	-0.016	-0.059	
34	-0.018	0.013	
38	0.293	0.000	After 10-8-99, 2:00
42	0.226	-0.040	
46	-0.127	0.046	
50	0.948	0.022	
51	-0.101	-0.049	

**Table C-2.** Initial and final corrections applied to the thermistors mounted on Raft # 2.

Depth (ft)	Initial Correction (°C)	Final Correction (°C)	Periods with no or poor data
0.5	-0.059	-0.355	
2	-0.122	-0.148	
3	0.527	-0.470	After 7-25-99, 14:30
4	0.040	-1.120	
6	-0.097	-1.152	Before 7-15-99, 10:30, and after 8-3-99, 2:00
8	-0.026	-0.652	After 8-14-99, 1:30
10	0.011	-0.347	
12	-0.319	-0.284	After 8-14-99, 99, 18:40
14	0.277	-0.284	
15	-0.010	-0.051	After 9-29-99, 23:50

**Table C-3.** Initial and final corrections applied to the thermistors mounted on Raft # 3.

Depth (ft)	Initial Correction (°C)	Final Correction (°C)	Periods with no or poor data
0.5	-0.211	0.000	After 9-7-99, 22:50
1.3	0.029	-0.023	
3.3	-0.031	-0.330	
5.3	0.019	-2.500	
7.3	-0.011	-1.150	After 8-29-99, 1:20
9.3	-0.021	0.000	After 8-3- 99, 23:50
11.3	-0.001	-0.300	
12.3	-0.001	0.000	After 9-18-99, 15:30

## **Appendix D. Diurnal Dissolved Oxygen and Temperature Profiles**

Water temperature and DO profiles measured by the authors on August 2 and 3, 1999 are presented in this section. There are 7 measurements in a 24-hour period. The measurements were taken at the locations of three rafts: One in the deep subbasin, one in the eastern shallow subbasin, and one at the border of the eastern shallow subbasin and the deep subbasin. In addition to temperature and DO profiles, DO at saturation has been added to the figures. The DO content time series for August 2 and 3, 1999 are presented in Figure D.2.

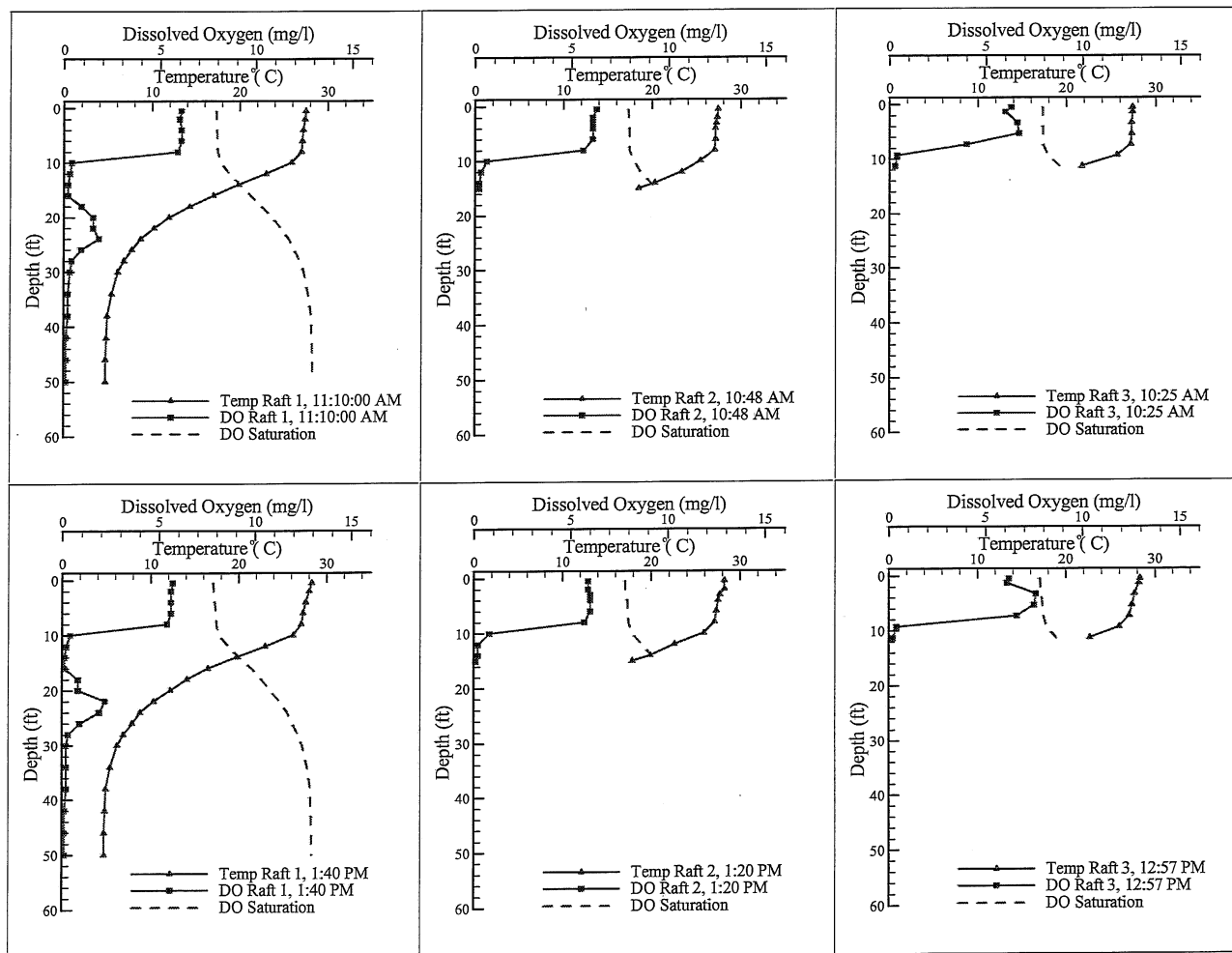


Figure D.1. Diurnal temperature and DO profiles measured in the subbasins of Holland Lake, summer 1999.

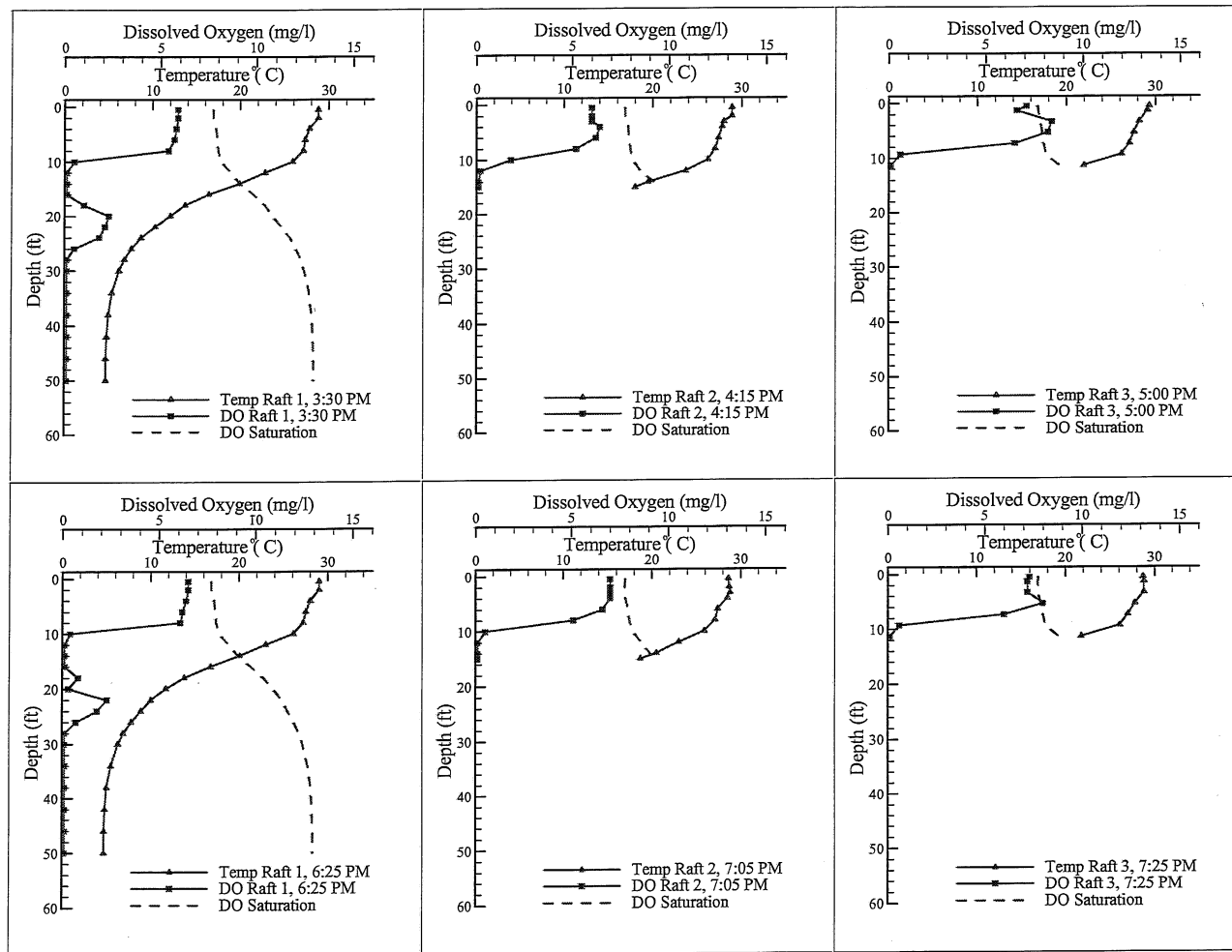


Figure D.1 continued. Diurnal temperature and DO profiles measured in the subbasins of Holland Lake, summer 1999.

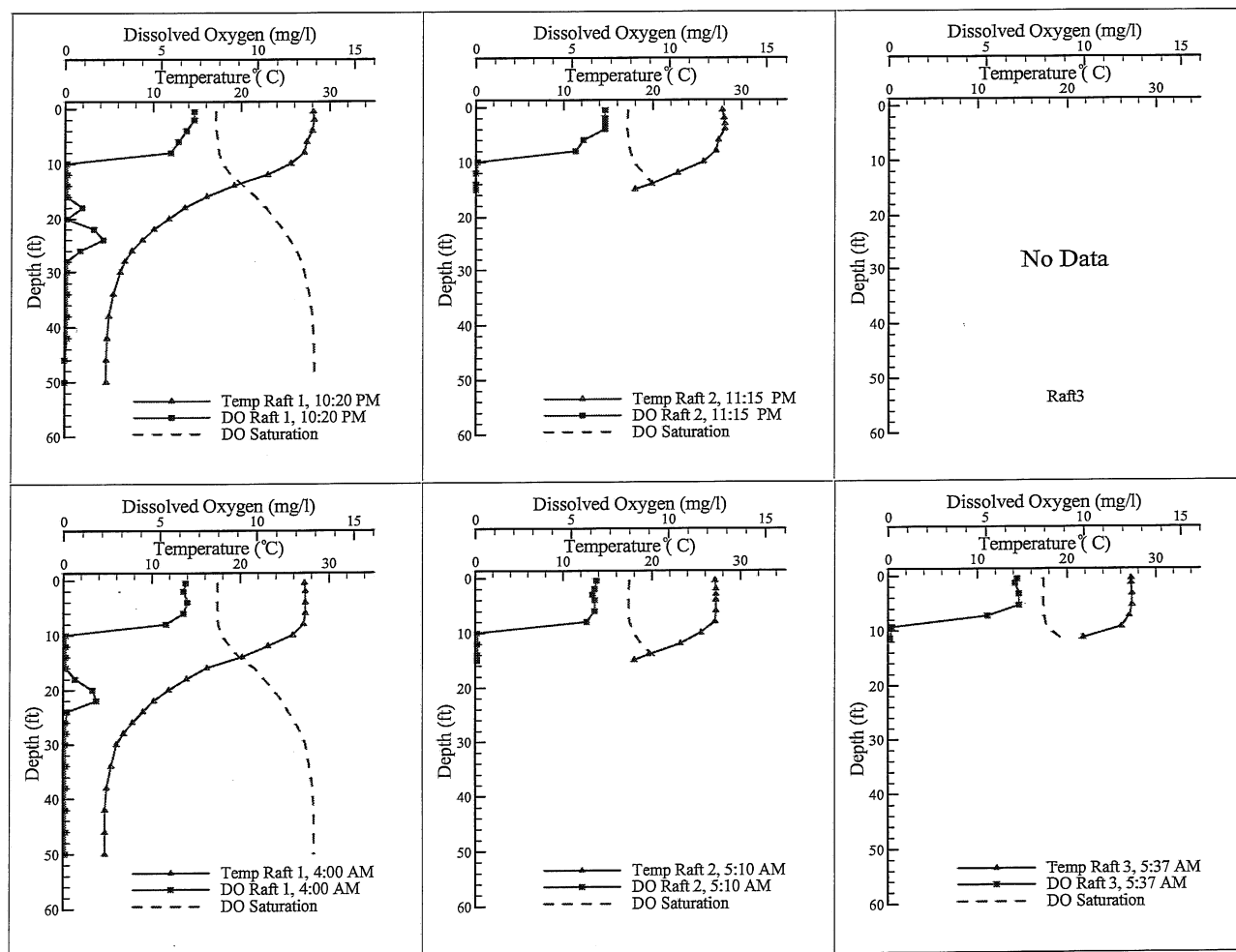
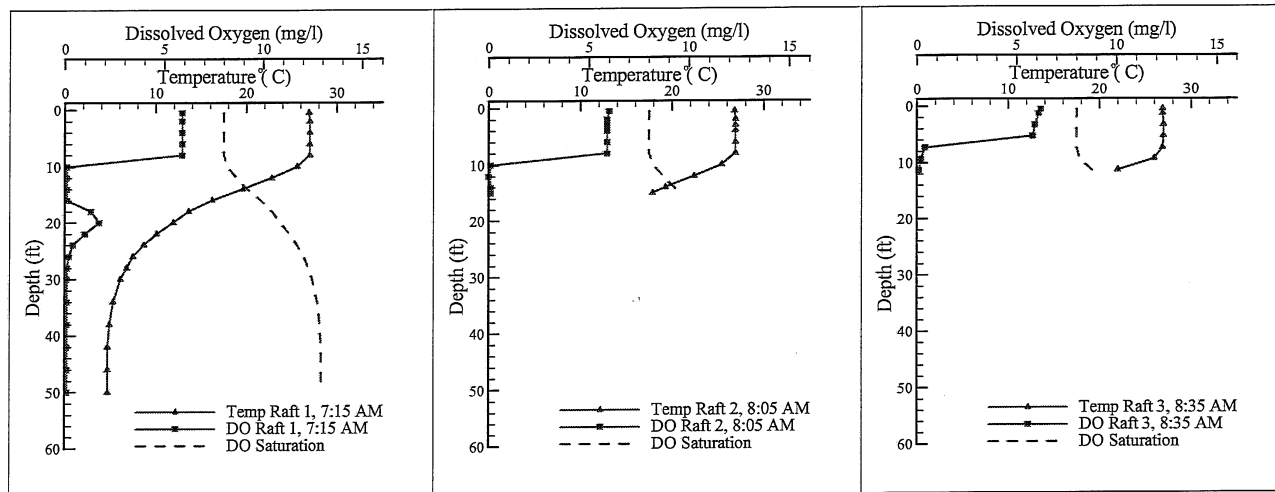
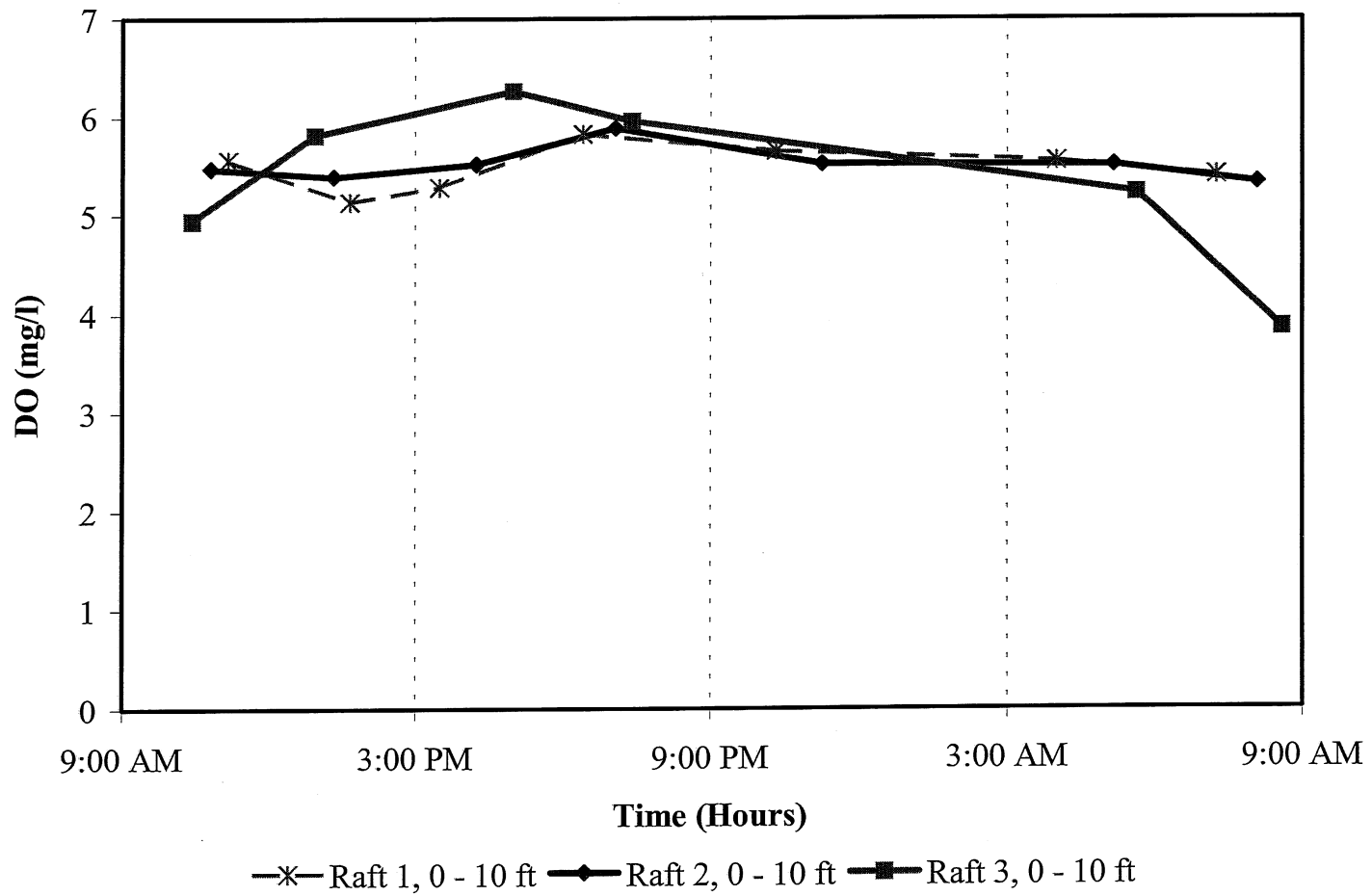


Figure D.1 continued. Diurnal temperature and DO profiles measured in the subbasins of Holland Lake, summer 1999.





**Figure D.1 continued.** Diurnal temperature and DO profiles measured in the subbasins of Holland Lake, summer 1999.



**Figure D.2.** Diurnal dissolved oxygen content in the upper 10 ft of water in Holland Lake, on August 2 and 3, 1999.